UNIVERSITÀ DEGLI STUDI DI ROMA TRE

Facoltà di Scienze Matematiche Fisiche e Naturali

Dottorato in Geodinamica

Ciclo XXI

DEFORMATION PROCESSES ALONG THE CALABRIAN COMPRESSIVE MARGIN

Liliana Minelli

Relatore: Prof. Claudio Faccenna

Coordinatore: Prof. Domenico Cosentino

Correlatore: Dott. Piero Casero

Revisori: Prof. Stefano Mazzoli,

Prof. François Roure

Deformation processes along the Calabrian compressive margin

Preface

CHAPTER 1

Structure and evolution of the Calabrian accretionary prism

CHAPTER 2

Structure and Age of the Alpine Thrusting in the Eastern Sila Massif (Italy)

CHAPTER 3

Processes instability along an active margin from two case-history

Messina Tsunami

Crotone Megalandslide

INTRODUCTION

The Calabrian arc is a fundamental area to understand the tectonic evolution of the Apennine and Maghrebian fold-and-thrust belts within the framework of convergence between African and Eurasian plates in the central Mediterranean. The Calabrian arc has been the subject of several studies since at least the 1950s by geological and geophysical methods. Despite the large amount of collected data, geometry, kinematics, and tectonic evolution of the Calabrian accretionary prism are still poorly defined, particularly in the offshore region. Understanding the structure of the Calabrian accretionary prism bears important implications in the mitigation of hazards connected with the active tectonics of this region, particularly in marine environments.

This thesis addresses the tectonics of the Calabrian convergent margin by using mainly offshore seismic reflection profiles spread over the entire Ionian Sea, in the central Mediterranean. In particular, geometry, kinematics, and time-space evolution of the Calabrian accretionary prism are studied and defined. In one case (Longobucco area, northern Calabria), we integrated structural, geological and thermo-chronological analyses to define the oldest phases of accretion and growth of the Calabrian accretionary prism. Eventually, implications for the mitigation of natural hazards typical of active, or recently-active, convergent margins are considered. In particular, we analyzed two significant case histories: the Crotone megalandslides, which is a presently active margin spreading above a thick Messinian salt layer at very low rates; and the 1908 Messina tsunami possibly triggered by a large landslide which occurred off the Ionian coast of Sicily along the steep Malta Escarpment.

Although several new or old questions remain open, results from this thesis shed new light on the tectonic evolution of the Calabrian accretionary prism and related subduction processes. For the first time, new industrial data have been interpreted and combined with previously published geophysical and geological dataset, to provide a complete view of this tectonically complex region.

1. Introduction

The Neogene tectonics of the Central Mediterranean is connected with the subduction of the Ionian basin under Eurasia and has been mainly dominated by trench rollback, which produced the opening of the Liguro-Provencal and Tyrrhenian back-arc basins and the formation of Calabrian accretionary wedge.

The Calabrian accretionary wedge is a partially submerged south-verging accretionary prism, which extends from South Calabria to the Ionian abyssal plain and, laterally, from the Malta escarpment, to the West, to the Apulia escarpment and Mediterranean Ridge, to the East. The wedge consists of a pile of deformed sediments involved in the convergent setting between Europe and Africa.

Despite the Ionian basin has been investigated in the last forty years by conducting several geological and geophysical surveys, results from these studies are often controversial and, consequently, the structure of the wedge is still poorly defined.

In this thesis, results from a study based on the interpretation of seismic reflection profiles acquired since the end of the 1960's onward in the Ionian offshore by industrial exploration and academic cruises are presented. The main purpose of this thesis is to provide a synthetic outline of the structural setting of the Ionian offshore and, in particular, to define the style and timing of deformations of the Calabrian accretionary complex. To do so, seismic reflection profiles from the Ionian offshore have been collected and interpreted. These data have been combined with other geological and geophysical data from offshore and onshore areas. The huge amount of available data here favors a more complete study with respect to the previous ones. These data allow to identify and to map out the main structures that characterized the Ionian offshore. The aim of this study is then twofold: (1) to describe the structural style of the Calabrian accretionary wedge and (2) to define the evolution of this key-area of the central Mediterranean.

The Calabrian subduction zone represents an anomalous (analogously to the Mediterranean Ridge) low tapered accretionary complex characterized by the absence of trench-like feature and of clear outer deformation front.

The limits of this work arise from the paucity of direct geological constraints for the inner sector of the wedge and for the deeper part of the Ionian offshore. Most conclusions are based on lateral correlations and supported by interpretation provided in previous studies. For this reason, the discussion is mainly based on a key seismic reflection marker, which allows us to describe the structure of the wedge in terms of pre-, syn-, and post-Messinian deformation. All reconstructions of structural and stratigraphic conditions are mainly based on seismic explorations and on a large amount of data available from the oil industry. Further limits derive from the age and quality of the available seismic profiles, and from the lack of high resolution data.

2. Introduction to Mediterranean geodynamic

The evolution of this portion of the Eurasia-Africa plate boundary over Neogene-Quaternary times is generally interpreted in terms of slow relative plate convergence (Argus et al., 1989; De Mets et al., 1994), subduction of the Ionian lithosphere beneath the Calabrian arc, fast slab rollback and associated back-arc spreading in the Tyrrhenian Sea (Malinverno & Ryan, 1986; Patacca et al., 1990; Faccenna et al., 2001 a). The present-day Ionian basin is shaped by the progressive subduction of the deep Ionian basin beneath the Calabrian arc. Subduction of this relic of the Neo-Tethys ocean and the progressive rollback of the slab during Neogene times has produced the opening of two back-arc basins and has resulted in the growth of a large sedimentary Calabrian accretionary wedge (Fig.1). Tomographic images (Selvaggi and Chiarabba, 1995; Mele, 1998; Lucente et al., 1999; Piromallo and Morelli, 2003; Wortel and Spakman, 2000; Montuori et al., 2007) show, under the Calabrian subduction zone, a northwestward dipping slab, which is affected by a 150 km-wide window beneath the southern Apennines. This window opened after a tear occurring within a composite subduction system, formed by the Apulian continental lithosphere and the Ionian oceanic slab (Chiarabba et al., 2008).

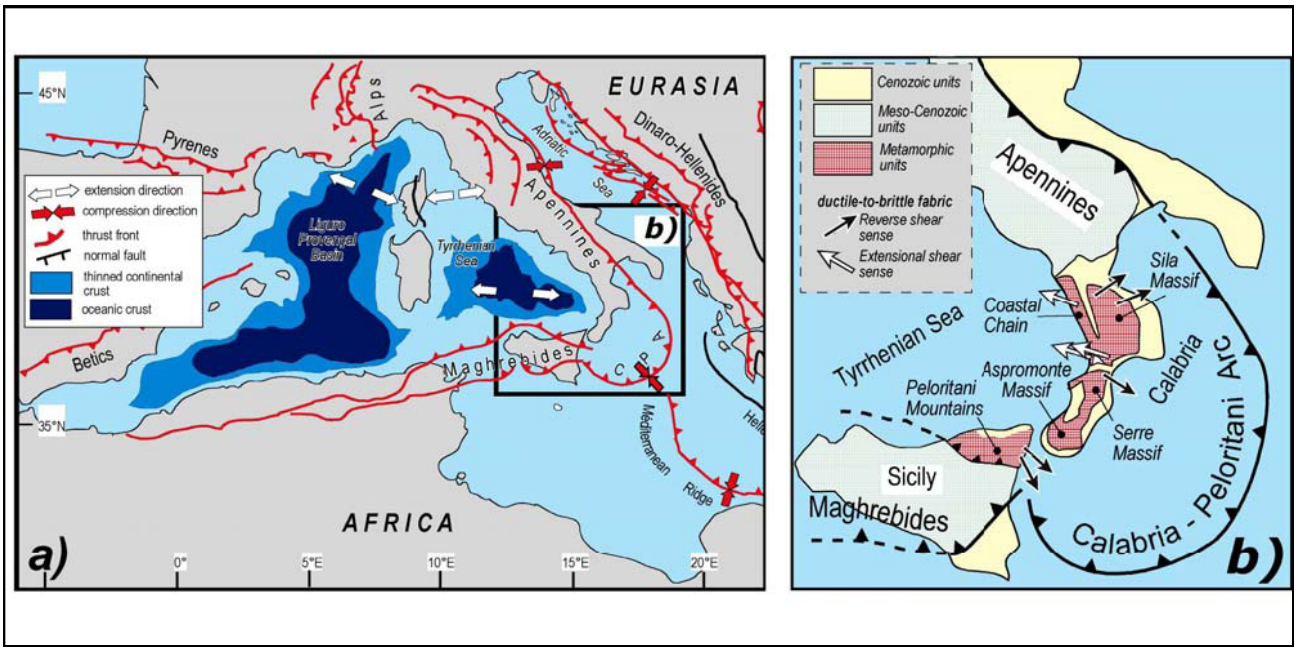

Figure 1 - (a) Synthetic tectonic map of the Tyrrhenian-Apennines system in the framework of the central Mediterranean region (modified after Jolivet *et al.*, 1998). (b) Geological sketch map of the Calabria-Peloritani Arc.

The crustal thickness, reconstructed by refraction OBS (ocean bottom seismometers) and ESP (expanding spread profiles) surveys, shows a progressive thickening from the Ionian abyssal plain to the Calabrian arc, as previously suggested by Hinz et al. (1974). In particular, the crust under the Ionian abyssal plain is between 11

to 17 km in thickness (Makris et al., 1986; de Voogd et al., 1992) and increases to more than 30 km near the Calabrian coast (Ferrucci et al., 1991; Cernobori et al., 1996).

Direct seismological and geological evidence of the present-day subduction activity in terms of shortening in the accretionary wedge and spreading in the Tyrrhenian back-arc basin are lacking. Presently, earthquakes are distributed along the Wadati-Benioff zone well delineating the steeply (70°) dipping Ionian lithosphere beneath the Calabrian Arc (Selvaggi e Chiarabba, 1995).

3. Geological setting of the Calabrian accretionary wedge and Ionian offshore: previous works

The Calabrian accretionary prism is a curved submerged fold and thrust belt originated by the northwestward subduction of the Ionian lithosphere beneath the Calabrian arc and by the southeastward retreat of the slab since late Oligocene to present times (Réhault et alii, 1986; Malinverno & Ryan, 1986; Ricci Lucchi, 1986; Patacca & Scandone, 1989; Boccaletti et alii, 1990; Gueguen et alii, 1998). The prism, located in the Ionian offshore, is bounded to the East by the Apulia Escarpment and by the advancing Mediterranean Ridge, and, to the West by the Malta Escarpment. Towards the South, the Ionian abyssal plain, a flat deep basin of triangular shape, represents the present foreland basin.

Several geophysical surveys have been performed in the Ionian offshore. Seismic reflection (Rossi and Borsetti, 1974; Finetti 1982, 1985; Cernobori et al., 1996; Catalano et al., 2000, 2001; Hirn et al., 1997) and refraction surveys (Makris et al., 1986; Ferrucci et al., 1991; de Voogd et al., 1992; Truffert et al., 1993), dredging and sampling (Rossi and Borsetti, 1974; Scandone et al., 1981; Fabbri et al., 1982; Barbieri et al., 1982; Casero et al., 1984), heat flow measurements (Della Vedova & Pellis, 1992), magnetic (Aris Rota & Fichera, 1985) and gravimetric (Morelli et al., 1975) surveys produced a wealth of data for the interpretation of this area. However, the seismic grid of the previously published works on the Ionian offshore is still loosely spaced and, therefore, both attitude and extent of faults are still poorly constrained.

Main open questions on the tectonics of the Ionian region concern the nature of the Ionian lithosphere, the recent tectonic evolution of the prism, the extent and structure of the Calabrian accretionary wedge, the timing of deformations, and the modalities of interference with the other tectonic elements (Mediterranean Ridge and Southern Apennines) are still debated.

The Ionian subducting lithosphere has been considered as entirely oceanic with the exception of the Ionian abyssal plain, which is interpreted either as an oceanic relict of the Tethys (BijuDuval et al., 1977; Finetti, 1982; Makris et al., 1986; De Voogd et al., 1992; Truffert et al., 1993; Finetti et al., 1996; Finetti and Del Ben, 2000; Catalano et al., 2001) or as a foundered stretching continental crust connecting the African margin with Apulia and southern Sicily (Hinz 1974; Boccaletti et al., 1984; Cernobori et al., 1986; Ismail-Zadeh et al., 1998; Nicolich

et al., 2000; Hieke et al., 2003). Seismic data reveals that the sedimentary cover of the Ionian basin is about 6 - 8 km thick and consists of Mesozoic-Cenozoic pelagic sediments, deep-sea siliciclastic turbidites, and a thick Messinian evaporitic layer (Finetti, 1982; Makris et al., 1986; Ferrucci et al., 1991; de Voogd et al., 1992; Truffert et al., 1993).

Moreover, the Ionian basin is characterized by a positive Bouguer anomaly (310 mGal), which is probably related to mantle density anomalies, by the absence of magnetic anomalies typical of oceanic crust, and by a low heat flux (40 mW/m2). Any geological solution for the Ionian region should then consider that: a) the abyssal plain is 4 km deep, thus requiring a density profile closer to oceanic lithosphere, and b) the crustal thickness is about 12 km.

Previous authors describe the structural setting of the Calabrian accretionary wedge by using seismic reflection profiles (Rossi and Sartori, 1981; Barone et al., 1982; Finetti, 1982; Cernobori et al., 1996; Sioni, 1996). Rossi and Sartori (1981) first divided the accretionary prism in several sectors: i) the Crotone-Spartivento basin, ii) the inner transition zone, iii) the ECA (External Calabrian Arc) and an outer zone (Calabria Ridge s.l.) where gravity and salt are considered as mainly driving deformation process (Rossi and Sartori, 1981; Chamot-Rooke et al., 2005). Similarly, Sioni (1996) (Prismed multichannel survey PM01), moving from NW to SE, recognised the following domains: the Crotone-Spartivento basin, the Calabrian arc, the Messina cone, the Ionian abyssal plain, and the Syrte basin (Fig. 2).

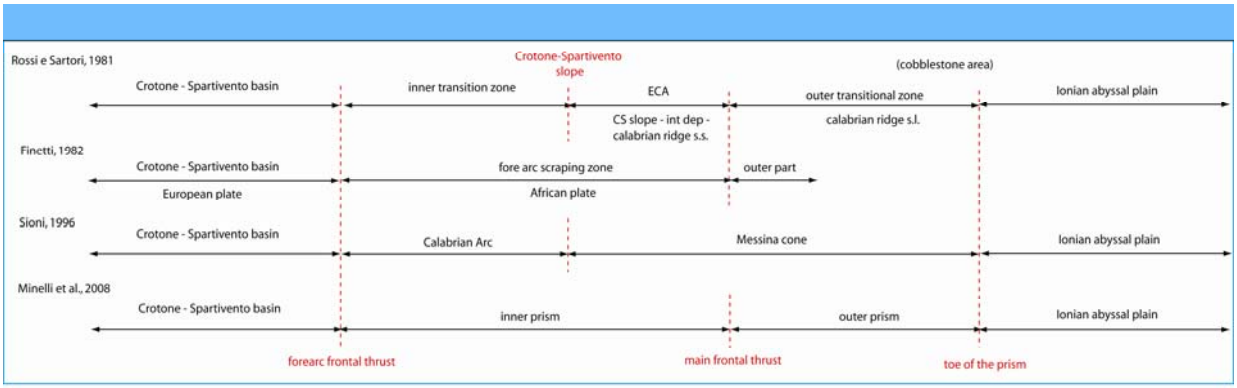

Figure 2 – Summary of nomenclature used for describe the main structure of the Calabrian accretionary prism in the previous works (Rossi and Sartori, 1981; Finetti, 1982; Sioni, 1996) and that proposed in this work (Minelli, 2008).

Cernobori et al. (1996) show (1) progressive landward thickening of deformed sedimentary piles resting upon less deformed sediments, (2) the presence of a décollement level detected at the interface between accreted and subducting sequences, and (3) important shortening expressed by reverse faulting, folding and thrusting. They show also the contact between the Sila crystalline backstop and the Calabrian accretionary wedge (Fig. 3). Finetti (1982) outlines a complete section of the Calabrian Arc from the undeformed area of the Ionian abyssal

plain up to the area deformed by Neogene-Quaternary compressional structure. In the outer domain of the Calabrian Arc, the basal décollement corresponds to the base of Messinian evaporite and progressively deepens by involving the entire sedimentary succession (i.e., Tertiary and Upper Mesozoic). Moreover the outer part of the arc is characterized by frontal sliding allochthonous or mélange complexes. Main questions about the prism thus concern the nature of the outer wedge zone and the recent-Neogene activity of the accretionary prism.

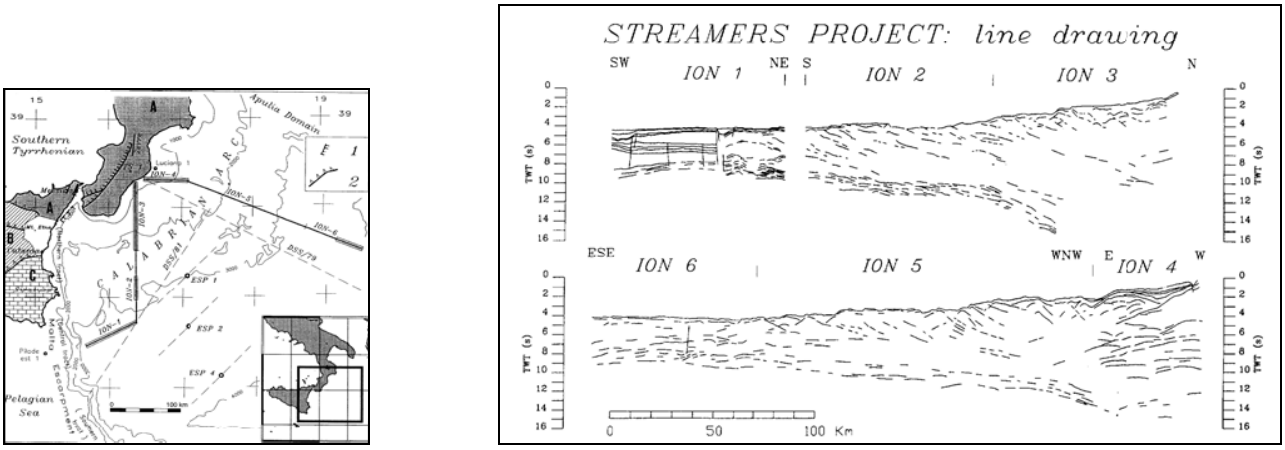

Figure 3 – (a) Location map of the STREAMERS profiles in western Ionian Sea and (b) linedrawing of the Calabrian accretionary prism, by Cernobori et al. (1996)

The **western boundary** of the Calabrian accretionary wedge has been extensively surveyed during several cruises. The main feature of the area is represented by the Malta Escarpment, a NNW-SSE trending, 250 km long structure extending from the eastern margin of Sicily to the Medina Mounts in the Ionian abyssal plain. The Malta Escarpment links the Hyblean continental plateau, to the West, to the Ionian abyssal plain and Calabrian accretionary prism, to the East. Despite its prominent structure, it cannot be considered as an oceanic-continental boundary. Indeed, the age of the escarpment is probably Tortonian (Makris et al., 1986) to post-Tortonian (Scandone et al., 1981; Casero et al., 1984; Sartori et al., 1991) and developed by re-activating a Mesozoic crustal-scale structure.

The stratigraphic succession that forms the substratum of the escarpment probably extends from late Triassic to Miocene as attested by sampling along the escarpment (Biju-Duval et al., 1982; Casero et al., 1984) and on the Alfeo seamount (Rossi and Borsetti, 1974). Along the escarpment, magmatic activity has been registered by magnetic anomalies (Morelli et al., 1975) and basalts samples (Scandone et al., 1981; Biju-Duval et al., 1982). Several NNW-SSE striking, east dipping, extensional/strike slip faults have been described along the northern offshore of Sicily, with evidences of recent activity as testified by Plio-Quaternary synrift deposits (Rossi and Borsetti, 1974; Cernobori et al., 1996; Hirn et al., 1997; Bianca et al., 1999; Adam et al., 2000; Nicolich et al., 2000; Argnani et al. 2002; Argnani and Bonazzi, 2005) (Fig.4). Argnani et al. (2002) also describe compressional

deformation inverting some recent normal faults. Toward the south the Malta Escarpment is not affected by recent faulting but flattens out toward the Ionian basin (Argnani et al., 2002).

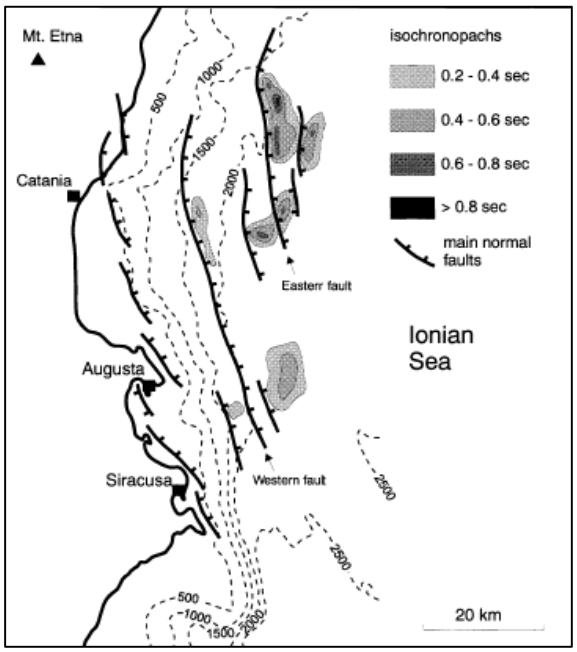

Figure 4 – Structural sketch map of the Ionian offshore zone of eastern Sicily derived from the analysis of seismic reflection profiles. Isochronopachs of the synrift basins developed along the hanging wall of the major normal fault segments (Bianca et al., 1999).

The **eastern margin** of the Calabrian accretionary wedge is located between the Italian coasts of Calabria and Puglia and extends toward the southeast as far as the Cephalonia Island. This area is characterized by the presence of the Apulian platform that extends over the Apulian region and, probably, over the Straits of Otranto up to the Greek islands of Zante and Cephalonia, where the platform abruptly terminates against the Cephalonia transform fault. The southward extension of the platform is not obvious. According to geophysical data, industrial wells, and submersible observations, the platform reaches the Cephalonia Fault and is abruptly truncated and displaced to the southwest. The Apulian Escarpment, the southwestern boundary of the Apulian platform is a recessive erosional boundary which developed during the Messinian lowstand (Bosellini, 2002). It separates the Apulian ridge to the East from the Ionian abyssal plain to the West. The Apulian platform bent and flexed both beneath the Hellenides, to the East, and beneath the Southern Apennines thrust belts, to the West. The Apulian ridge, which is the submerged offshore prolongation of the Apulian platform, represents the weakly deformed foreland basin and is presently buried below the Pliocene Apenninic foredeep (Central Adriatic basin, Bradanic Valley basin, Taranto Valley) related to the east-verging Apenninic thrust belt and under the Mio-Pliocene foredeep to the East (South Adriatic basin) which are related to the Hellenic and Dinaric thrusts belt.

Several geophysical (seismic reflection survey) and geological data (industrial wells, and sample, and dredge) have been collected in this area (Finetti and Morelli, 1973; Rossi and Borsetti, 1974; Finetti, 1976; Rossi et al.,

1983; Doglioni, 1999). The Apulian carbonate platform consists of a continental crust with Mesozoic (Jurassic-Cretaceous) shallow water carbonates, which are about 7000 m thick (2 s TWT) (Mostardini and Merlini, 1986) and a thin sequence of Tertiary calcarenites and limestone. The lithology is confirmed by the onshore drilling and dredge offshore along the main escarpment. In places, the Messinian horizon lies on top of the carbonatic basement or on a sequence of Miocene age (Rossi and Borsetti, 1974). On top of these units, also a sequence of marls and clay of Pliocene-Pleistocene age has been recovered by dredges along the Apulia escarpment.

4. Seismic dataset

Fig. 5 shows the location of the principal data used in this work. Data include multichannel seismic reflection profiles acquired in the Ionian Sea since the end of 1960's (i.e., Italian Commercial Zone "F" and Zone "D" lines, Mediterranean Sea "MS" lines by OGS, Calabrian Arc data supplied courtesy of Fugro, ION Streamers profiles, CROP seismic reflection profiles of the Italian crust sponsored by ENEL, ENI and CNR, PM01 of MCS Prismed survey and ARC of Archimede academic cruise managed by Ecole Normale Supérieure team).

The resolution and the quality of the seismic profiles remarkably vary due to different acquisition parameters and energy systems used during different surveys. Data from some hydrocarbon boreholes are also available near the Calabrian and Sicily coasts and have been used to calibrate the seismic data. We have also used all geophysical and geological data (ESP refraction data, dredged and gravity or piston core, Ocean Drilling Program (ODP) and Deep Sea Drilling Project (DSDP)) available for the Ionian offshore to better define the stratigraphic succession of the incoming subducting sediments.

The recognition along several seismic profiles of the main reflection horizons and of their geological attributes allowed us to date the activity of the main thrust systems in the Calabrian accretionary prism.

Furthermore, the high-density grid of the seismic lines allowed us to map out the main structural features and to reconstruct the evolution of the accretionary processes in the Ionian offshore.

In this thesis, seismic profiles are presented as line-drawing distance against reflection time (TWT = two-way travel time), and thickness variations are expressed in millisecond (ms) TWT.

5. Seismic stratigraphy

For the seismic interpretation of the entire dataset in the Ionian offshore, starting from the reliable data on the less deformed foreland basin, the Ionian abyssal plain, it is possible to extend the interpretation of the main reflectors to the complex internal parts of the wedge. Fig. 6 shows the acoustic stratigraphy of four

sedimentary sections along a NW-SE profile crossing the Calabrian accretionary wedge from the Crotone-Spartivento basin to the foreland basin.

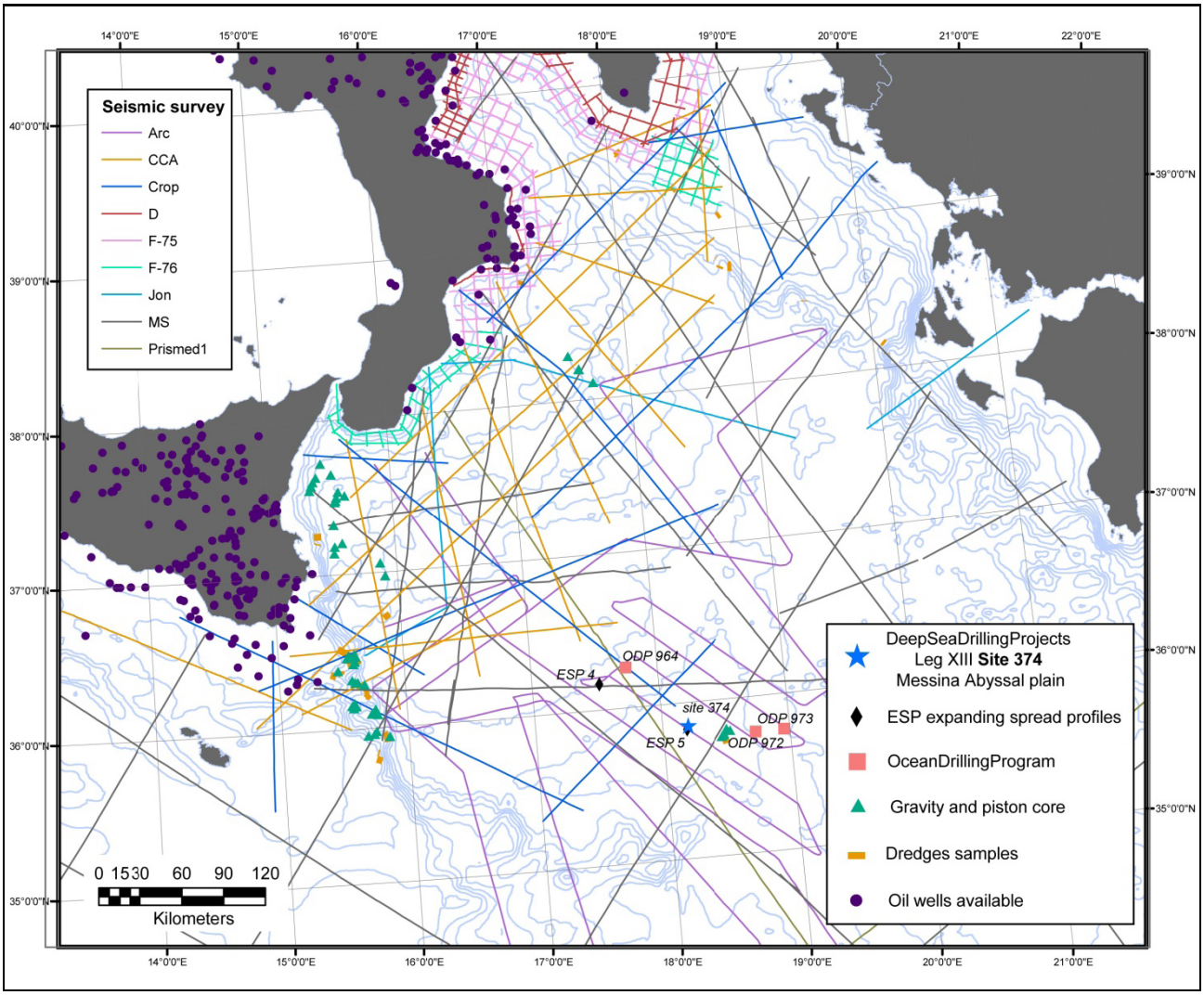

Figure 5 - Location map of seismic reflection profiles across the Calabrian accretionary prism in the Ionian offshore (Eastern Mediterranean Sea), wells and geophysical data. Solid lines, with a color-coded according to their source, indicate the multichannel seismic profiles using in this work. The stars indicate the position of DSDP (Hsu et al., 1978) and squares of the ODP drilling (Emeis et al., 1996). Violet dots indicate the locations of the wells available by oil industry. Diamond indicate the location of the ESPs profile (de Voogd et al., 1992). Triangles and yellow lines indicate dredge samples and gravity or piston core (Rossi e Borsetti, 1974; Scandone et al., 1981; Morlotti et al., 1982; Bizon et al., 1983; Casero et al., 1984; Sartori et al., 1991; Hieke et al., 2006).

In the Ionian basin, a few main reflectors are recognized. For their marked continuity and strong signal, these reflectors are already known in the entire Mediterranean region (Ryan et al., 1978; Finetti and Morelli, 1973; Casero et al., 1984; Reston et al., 2002; Polonia et al., 2002; Hieke et al., 2003). These data were used in the

calibration together with existing data produced by the oil exploration activity near the Calabria and Sicily shore.

In the Ionian offshore, a typical example of good reflectivity of the sequence comes from the foreland region, where these reflectors are undisturbed and has been also calibrated by ESP refraction data (De Voogd et al., 1992) and by DSDP (site 374 Messina) drilling. Five main seismo-stratigraphic units (PQ, ME, PM, MC and acoustic basement) separated by regional reflectors (A, B, K and S) have been detected in the Ionian abyssal plain.

horizon A: base of Plio-Quaternary sediment (PQ unit) or top of the evaporite (also named as M-reflectors (Ryan, 1969)). The A reflector, a strong high amplitude reflector, is almost continuous in the whole basin and it corresponds to the top of Messinian sequences. it is easily identified because of its typical seismic signature. However, in regions where the evaporites are absent, the hiatus is still marked by a regionally continuous and strong M-reflector that delineates a prominent angular unconformity at the base of the Pliocene-Quaternary succession. Therefore, because the M reflector is time-transgressive and it does not always represent the top of the Messinian, it can be better considered as the base of the PQ unit. This interpretation implies that M–reflector does not indicate the presence or not of Messinian evaporite.

horizon B: base of Messinian (evaporite and terrigenous unit ME) sequence. This horizon is attributed to the base of evaporites because it represents the first flat reflector below the interval, where diapiric structures are evident (Finetti and Morelli, 1973). While the Plio-Quaternary sequences and top of Messinian evaporites were drilled (DSDP site 374), no direct well drill was operated through the pre-Messinian sequences. Geological correlation, previous works in other regions, and seismic velocities have been used so far to interpret these sequences.

horizon K: top of Mesozoic sequences (unit MC) possibly constituted by carbonate series or lower boundary of the Tertiary clastic sequence (unit PM).

horizon S: top of the acoustic basement. In the foreland, this horizon lies at about 8 s (TWT) and it has been interpreted as the upper layer of oceanic crust (layer 2a) in agreement with de Voogd et al., (1992).

PQ unit: consists of sub-parallel, high-frequency, low amplitude reflectors, consistent with terrigenous deposits characterized by an average thickness of 200-400 ms TWT in the entire Ionian offshore except for the Crotone-Spartivento basin, where it reaches the maximum thickness of 2 s TWT. In the Ionian abyssal plain, the sequence is almost undeformed, whereas in the internal sector of the wedge, it is strongly deformed. In the forearc basin, the PQ unit is affected by normal faults (syn- or post-sedimentary) and involved in salt tectonics documented by diapiric structures. The lower boundary of these upper sediments is defined by strong reflectors interpreted as the top of the Messinian evaporitic sequence.

ME unit: consists of evaporitic and clastic sediments of Messinian age. The top is marked by the A (or M) reflectors and the base by the B reflectors, which are planar, continuous and high amplitude reflectors. In the foreland basin, this unit has an average thickness of 0.4 s TWT, this thickness being probably the original thickness formed in the basin. The seismic profiles show a gradual thickening of the Messinian unit toward the prism. The Messinian sediments are, in fact, progressively incorporated in the Calabrian front of deformation. In the internal sector of the prism, salt layers are present in places as attested by diapiric structures and typical deformational features of salt tectonics. In the foreland basin, the ME unit consists of, as documented by ESP refraction data, an upper part identified by high velocity and related to the upper evaporitic layer, and a lower part less reflective related to the Messinian clastic sequence.

PM unit: sequence poorly reflective, well layered, consistent whit deep water clastic and marls Tertiary terrigenous sediments (Ryan et al., 1973; Hsu et al., 1978). This unit is deformed under the Ionian basin and its thickness varies from 1.5 s TWT to 0.4 s TWT. In the frontal part of the wedge, this unit represents the subducting sediment. Moving landward, the sediments are progressively incorporated into the Calabrian prism. The lower boundary, K reflectors, marks the transition to the Mesozoic carbonate series.

MC unit: is characterized by strong, relatively continuous, and low frequency reflections, consistent with the presence of Mesozoic carbonates. The average thickness is 1.5 s TWT. These sequences are subducted beneath the Calabrian prism.

Acoustic basement: in the foreland basin, the acoustic basement is characterized by reflective sequence that shows an increasing velocity with depth.

Fig. 6 shows also as in the inner sector of the prism the internal deformation obscures the main horizons.

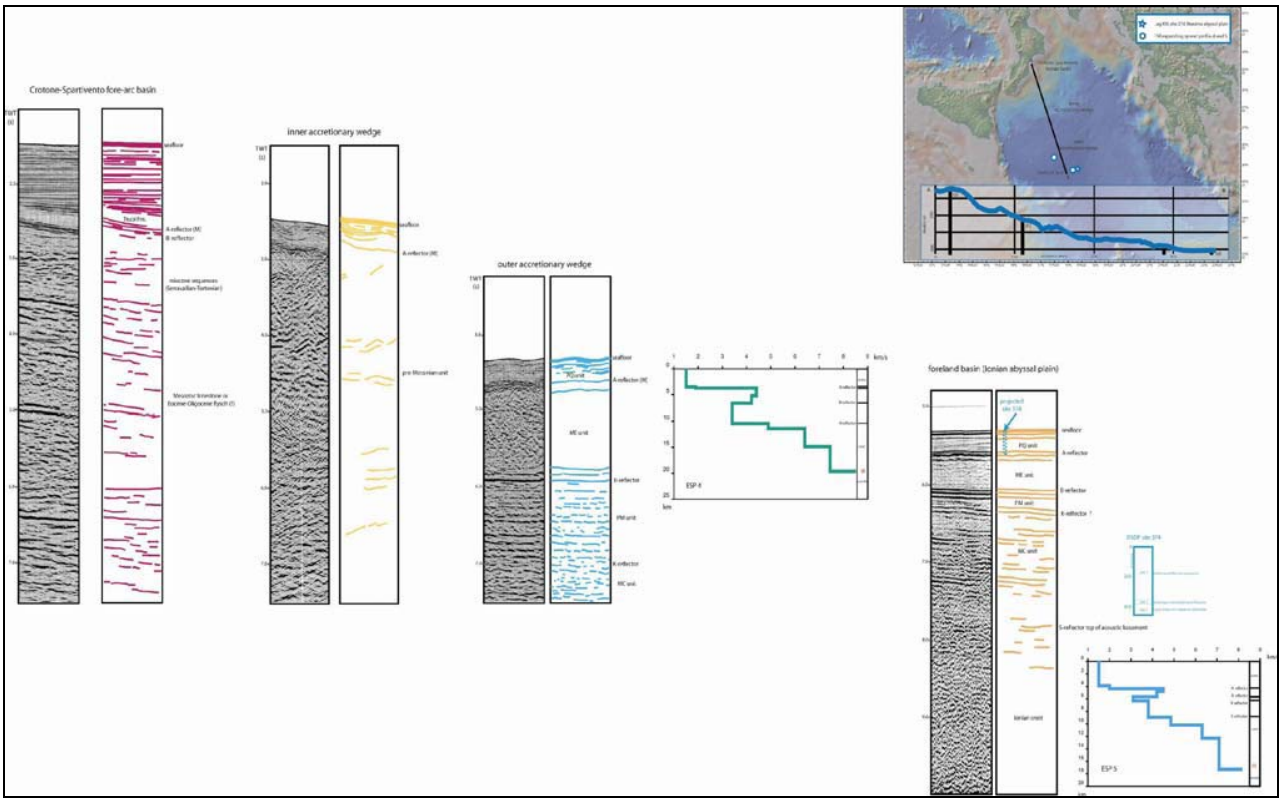

Figure 6 - Seismic stratigraphy and line drawing of the incoming sedimentary section in the Ionian offshore. The four column are aligned along a general NW-SE cross section through the Calabrian accretionary prism from the Crotone-Spartivento basin (a), to the foreland basin, Ionian abyssal plain (d). Vertical scale in two-way traveltime, TWT (s). The main reflector labels A, B, K and S, as defined by Finetti and Morelli (1973), have been used to distinguish the different seismic unit. According to Finetti and Morelli (1973), these reflections may represent: A base of Plio-Quaternary sequences (A reflector also identified as the M reflector), B base of Messinian evaporitic sequences, K transition between Cenozoic and Mesozoic sediment, probably top of carbonate series, S top of the acoustic basement . The seismic lines, where it was possible, has been calibrated using velocity data ESP (de Voogd et al., 1992) and hole (site 374) drilled during Leg 13 of DSDP (Hsü et al., 1978).

a) Example of seismic reflection line acquired in the Crotone-Spartivento forearc basin. Here it is possible to observe a thick infilling of Pliocene-Pleistocene age, onlapping the older sequences, the middle-upper Miocene sequence. The main horizons have been calibrated using the oil well data available for the Calabrian continental margin.

b) Example of seismic reflection line acquired in the inner accretionary wedge. It is possible to recognize only the Plio-Quaternary sequence and the M reflector (know as a depositional or erosional surface of Messinian age). Below that horizon, the sequences are more deformed.

c) Example of seismic reflection line acquired in the outer accretionary wedge. The main reflector has been calibrated by seismic refraction data (ESP 4). The PQ sequence is more deformed than in the foreland basin because it is involved in the convergence process. The thickening, northwestward, of the ME unit is indeed related to the growth of the accretionary wedge in its frontal part. Below the PQ and ME units, a sub-horizontal sequence of clastic Tertiary sediments is present.

d) Example of seismic reflection line acquired in the Ionian abyssal plain. This part of the line is located in the foreland basin and the related interpretation was constrained by drilling exploration DSDP, leg XIII, site 374 (Hsü et al., 1978) and by ESP 5 (de Voogd et al., 1992).

The line shows five major acoustic units within the flat undeformed foreland basin: PQ and ME (drilled by DSDP), PM, MC and Ionian crust (inferred from velocity data), for a total thickness of about 12 km.

6. Structure of the Calabrian accretionary wedge

The Calabrian Arc is a 400 km long and 300 km wide accretionary complex extending from the southern coast of Calabria region to the Ionian abyssal plain and from the Malta Escarpment to the Apulian Escarpment. In the eastern sector, the Calabrian Arc collided with the advancing Mediterranean Ridge (Fig. 7), another accretionary complex of Messinian age related to the Hellenic subduction zone (Le Pichon et al., 1982). The eastern (Apulian plateau) and western (Hyblean plateau-Alfeo Seamount- Malta and Medina platform and Medina Mounts) edges of the prism and, toward the south, the Sirte basin are characterized by continental crust overlain by thick Mesozoic to Quaternary carbonates and terrigenous sediments. Crossing the wedge along a NW to SE section, we distinguished the crystalline backstop (Calabro-Peloritano arc) thrust on a pre-Messinian accretionary complex, both partly covered by the forearc basin, the outer wedge and the foreland basin.

In the following, I will present the result of the seismic lines interpretation describing the western, the eastern edge and the different portions of the prism.

6.1 Western margin

The western margin of the Calabrian accretionary wedge is located east of the Malta Escarpment. Fig. 8 displays a seismic profile perpendicular to the Malta escarpment that extend from the Hyblean plateau to the Calabrian accretionary prism. The line-drawin shows the contact of the Calabrian accretionary wedge, a severely mobilised domain in the east of the profiles, with the foreland basin constituted by the Hyblean plateau downfaulted toward the Ionian Sea. This important crustal structure, interpreted as a strike-slip fault (CNR, 1983), is an important feature representing the lateral ramp of the wedge. As suggested by the presence of a syn-rift basin infilled with Plio-Pleistocene deposits with growth structure, the lateral ramp reveals a recent extensional re-activation (Cernobori et al., 1996). This crustal feature displaces the deeper horizons suggesting that this fault probably acted as transform or strike-slip faults also during pre-Messinian time. This extensional basin, which marks the contact with the Calabrian accretionary prism, is roughly parallel to the Malta Escarpment, turning then to an E-W direction south of the SE corner of Sicily. Further to the North, this fault shows a main extensional behaviour and is connected with the extensional system affecting the eastern boundary of the Hyblean plateau (Bianca et al., 1999; Argnani e Bonazzi, 2005). The foreland units are represented by a differently tilted and stretched continental or oceanic crust overlain by a well layered sequence probably of Mesozoic-Tertiary age.

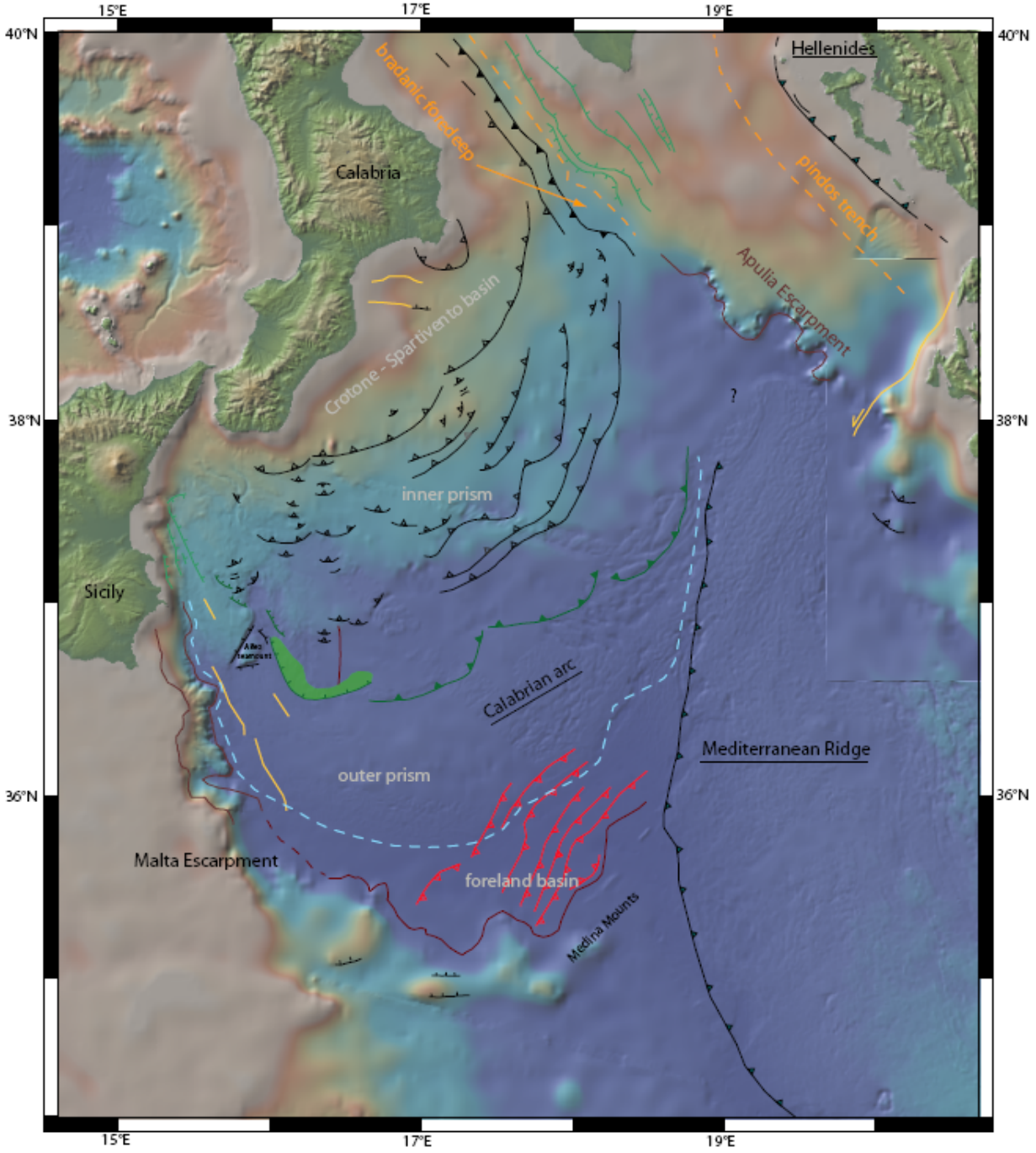

Figure. 7 - Structural map of the Ionian offshore drawn mainly from seismic lines data and other geophysical constraints when available (ESP, well data). Emphasis has been put to distinguished the thrust system using different colour referring to their age of activity, the post-Messinian (shown in black), Messinian (shown in green) and pre-Messinian (shown in red) structure. Normal fault is in green. The dotted orange lines are the borders of the foredeep basins. In yellow probable strike-slip faults. From north to south the four structural domain (Crotone- Spartivento basin, Inner prism, Outer prism, and foreland basin. The dotted light blue line represent the outer front and the onset of the undeformed Plio-Quaternary unit (foreland basin). The green transparency area is the basin that marks the extensional reactivation of the lateral ramp of the wedge.

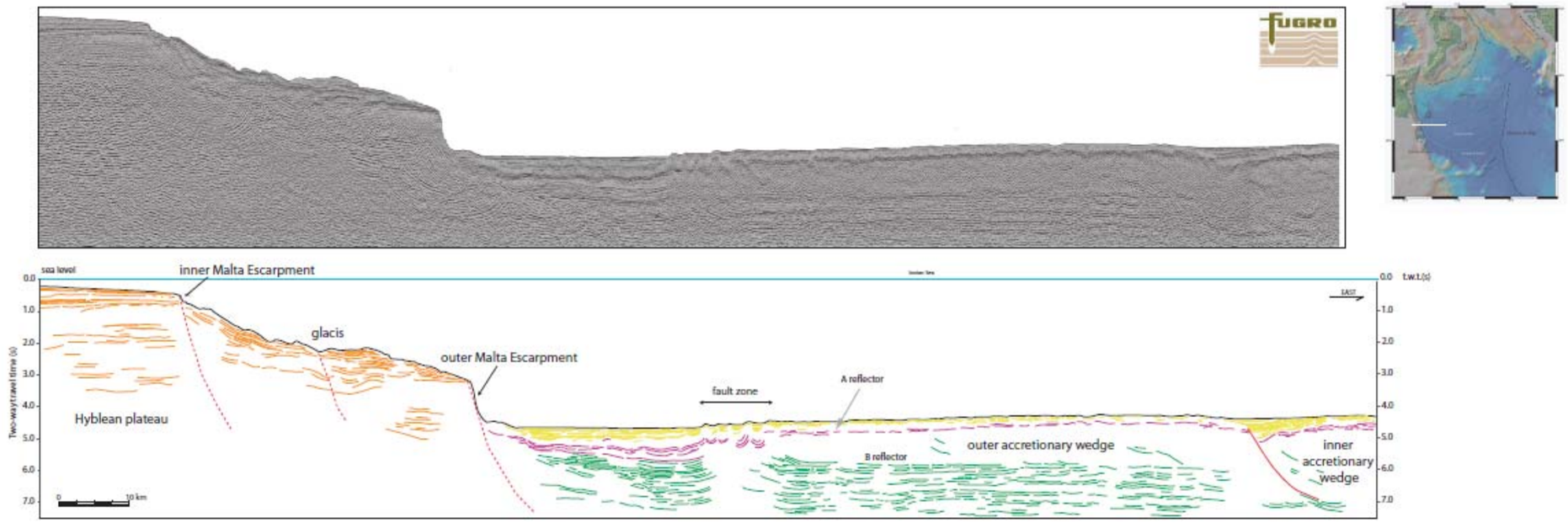

Figure 8 – Seismic reflection profile, data supplied courtesy of Fugro, and line drawing from the western boundary of the Calabrian accretionary prism. See inset for location of the section displayed in this figure.
In yellow Plio-Quaternary sediments, in pink A (M) horizon and Messinian reflectors, in green Mesozoic (?) till to Tortonian reflectors, and in orange undefined reflectors of Hyblean plateau.
The profile shows the recent activity of the Malta escarpment, the extensional re-activation of the lateral ramp that divides the inner from the outer accretionary prism

.

Above this basement, a terrigenous sequence is present, showing well-layered shales and marls, which are Tortonian-Serravallian in age (Casero et al., 1984; Cernobori et al., 1996). These sediments thicken toward the Calabrian prism. On top of these sediments, there is a clastic wedge of Messinian age draped by the Early Pliocene Trubi Fm and Late Pliocene-Quaternary clays (Sartori et al., 1991; Bianca et al., 1999).

The Messinian wedge is a quasitrasparent layer without outstanding reflection inside. The upper and lower boundary of this clastic wedge are the M and B reflectors, respectively. The age of this wedge is, therefore, Messinian. The M and B reflectors are affected by the movement of the Malta Escarpment fault system indicating its recent activity. Its thickness varies from 1.2 s (t.w.t.) near the contact with the Calabrian accretionary wedge, to 0.2-0.3 s (t.w.t.) towards the Malta Escarpment. Moving further toward the west, its thickness abruptly reduces along a fault zone with probable strike-slip movements. In correspondence of this fault, there are salt diapiric ascents. In map view, this fault run parallel to the Malta escarpment. The Plio-Quaternary sediments are undeformed except along the lateral ramp of the wedge and in correspondence of the faulted zone. The sequences up to Tortonian age show a progressively pinching-out from East toward the Malta Escarpment on a differently tilted substratum.

6.2 Eastern margin

The eastern margin of the Calabrian accretionary prism is defined by the southern Apennines frontal thrust, by the Apulian escarpment and, toward the south, by the contact with the advancing Mediterranean Ridge. Fig 9 shows the eastern margin of the prism along the Taranto valley, the north-western extremity of the Ionian sea between Calabria and Apulia, and the eastern Ionian sea in front of Lefkada Island. In Fig 9, four seismic sections running perpendicular to the main feature are located. The profiles cut across the southern Apennines frontal thrust, the Bradanic foredeep (or its offshore prolongation, i.e., Taranto Valley), the Apulian ridge, and the Hellenic foredeep (South Adriatic basin). The seismic sections through this sector of Ionian sea show the flexure of the Apulian plateau below the Southern Apennines to the west and below the Hellenides to the east. The Apulian foreland divided the two foredeep basins related to these fold and thrust belts. The sections show clearly a restraining of the Bradanic foredeep basin toward the south where the Apulian foreland is abruptly truncated by the erosional escarpment. The seismic sections (a) and (b) of Fig. 9 show the allochthonous units that constitute the southern Apennines emplaced toward the foreland, i.e., the Apulian platform. The accretionary wedge is composed of two units: the upper one includes the sedimentary sequence of Plio-Pleistocene age, whereas the lower one is more chaotic and has been attributed to the allochtonous Apenninic terranes emplaced along the margin during Neogene time (Finetti e Morelli, 1973).

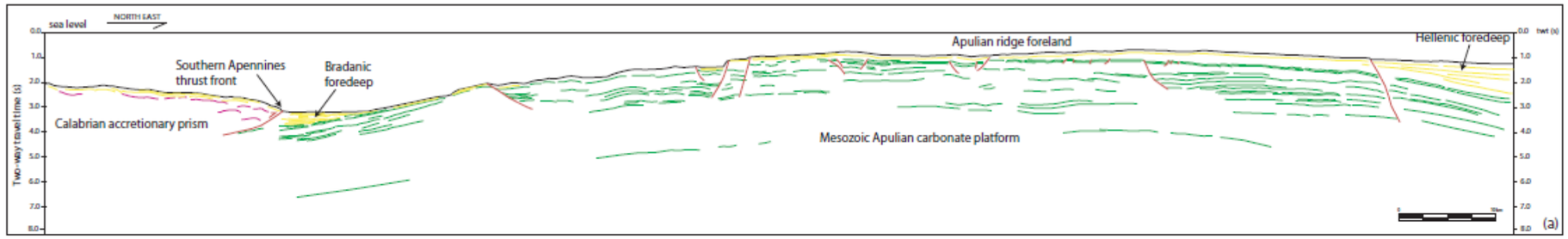

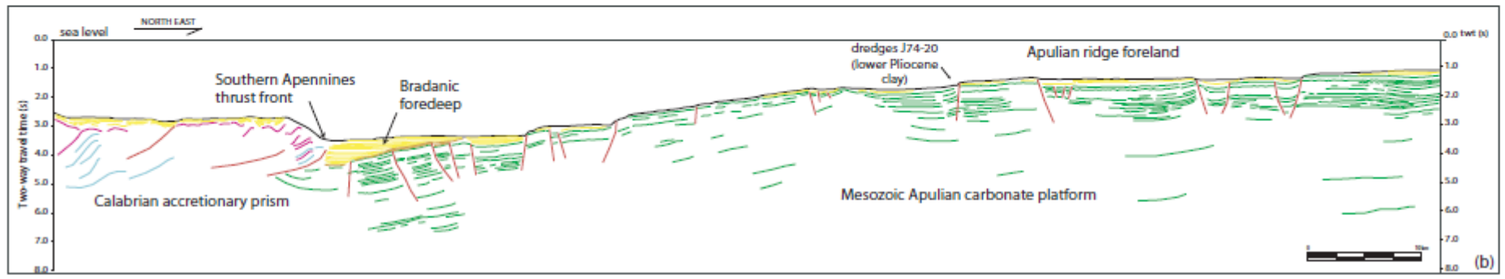

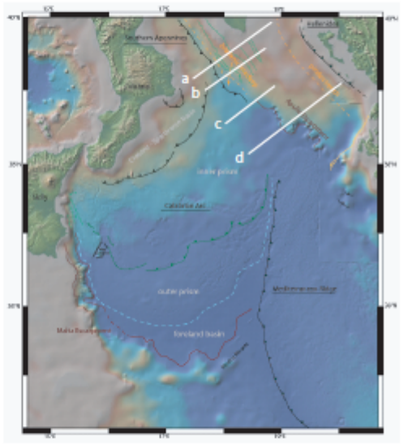

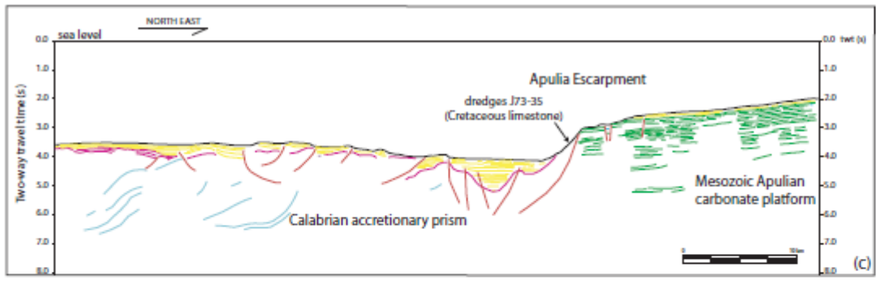

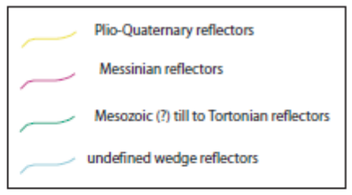

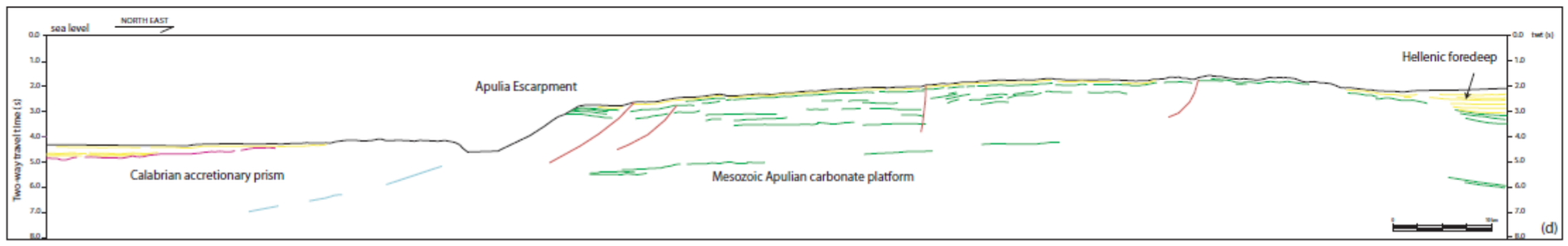

Figure 9 – Four line drawing from the eastern boundary of the Calabrian accretionary prism. See inset for location of the sections displayed in this figure.

In the accretionary prism, a back-thrust system deforms the Miocene sequences below the Messinian unconformity. The front of the accretionary wedge is marked by an eastward verging thrust overriding the narrow foredeep deposits of the Taranto Trench.

The trench-like feature of the Taranto Valley represents the offshore prosecution of the Bradanic foredeep resting on top of the Apulian downfaulted platform. The sections display a thick, well stratified sedimentary squence made up of Pliocene to Pleistocene sediments progressively onlapping, toward the east, the upper Miocene deposits and the Apulian upper Mesozoic strata.

To the east, during Upper Pliocene-Lower Pleistocene, the flexed border of the Apulian platform was downfaulted beneath the Southern Apennines thrust belt in response to the east rollback of Apennines slab. The platform is affected by normal faulting. The fault system, observed and defined by the analysis and interpretation of seismic sections, is represented by NW-SE trending segments, dipping SW or NE. This system generated horst and graben structures and extends along the Ionian offshore side of the Apulian platform, mainly following the present seashore. These faults bound a series of little sedimentary basins infilled by syn-rift clastic wedge of Plio-Pleistocene age. Some of these faults are presently active and disrupt the seafloor producing big scarps. Along some of these scarps several campaigns have dredged Cretaceous series overlain by unconsolidates sediments. Moving toward the Hellenides chain, the Apulian platform is flexed continuing below the South Adriatic foredeep where Mesozoic strata are deeply buried, indicating the continuation of the down-faulted Apulian platform beneath the recent sedimentary fill.

The Apulian margin shows two main acoustic sequences: the lower one, which locally exhibits a few parallel internal reflectors with an upper boundary which is a truncated surface and an upper unit showing internal reflectors. Rossi and Borsetti (74-77) proposed a stratigraphic correlations between acoustic sequence in seismic profiles and age and nature of the exposed Apulian platform based on dredge results. The acoustic basement represents the calcareous and dolomitic series of Apulia region and the upper unit corresponds to sediment up to Messinian (Lower Pliocene marls, Trubi fm., Upper Pliocene-Pleistocene strata). Rossi et al. (1983) suggest that the basement is not represented only by massive limestone (Finetti, 1976) but includes also Oligo-Miocene calcareous marls.

South of the lines (a) and (b) the linedrawing (c) and (d) of Fig.9 show a different setting showing the sharp erosional termination of the Apulian platform along the Apulian escarpment. This NW-SE geomorphic feature trending put in contact the Apulian platform with the more chaotic sequence of the Calabrian accretionary wedge. This sector represents an undeformed foreland basin where no collision took place. The Apulia escarpment is probably one of the two conjugate passive margins (the other one is the Malta Escarpment), which bound the oceanic Ionian basin (Catalano et al., 2001).

6.3 Calabrian accretionary wedge

The stratigraphy, style of deformations and internal seismic characters of the Calabrian accretionary wedge suggest the division of the CA into four major structural zones, from the backstop to the foreland basin (Fig. 10):

1. Crotone - Spartivento forearc basin: is a subsiding, poorly deformed, segment of the wedge filled up by Plio-Quaternary sediments. The basin lies on top of the crystalline basement and of the inner prism. The southern boundary of the basin is represented by a thrust named forearc outer thrust.

2. Inner accretionary wedge: is the inner portion of the accretionary wedge, which is constituted by pre-Messinian sediments, mainly accreted during pre-Messinian time; minor post-Messinian thrusts and backthrusts are, however, present. It is separated from the outer accretionary wedge by a main frontal thrust.

3. Outer accretionary wedge: is the frontal part of the wedge and is separated from the inner wedge by the main frontal thrust. In this outer sector, we observe the deformation of the Messinian to Quaternary sedimentary section.

4. Foreland basin and intra-plate deformation zone: is the poorly deformed foreland basin of the Calabrian Arc and the Mediterranean Ridge. The foreland basin shows a compressive deformation probably of Tortonian age.

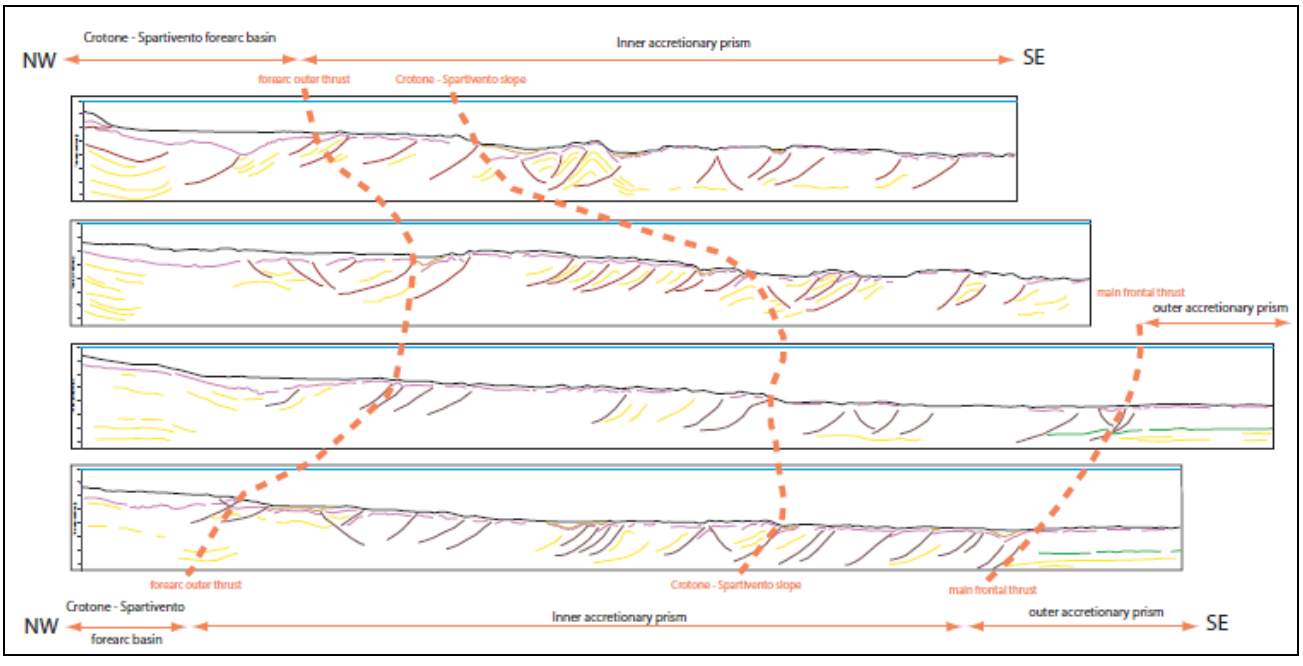

Figure 10 - View of four line-drawings of the Calabrian accretionary wedge running NW-SE. In pink the M reflector, in green the B reflector and in yellow reflections not constrained.

6.3.1 Crotone - Spartivento forearc basin

The Crotone-Spartivento basin is a forearc basin (Rossi and Sartori, 1981) with a mean length of 220 km and a width of 40 km. The basin is filled by Tortonian to Quaternary sediments. The forearc basin extends in the Calabrian offshore area from Crotone to Spartivento and is partly exposed on land in the Ionian side of Calabria, where post-orogenic, middle-upper Miocene (Serravallian (?)-Tortonian or slightly older) basal deposits rest on top of the crystalline complex and sedimentary nappes of the Calabria-Peloritani Arc (Amodio-Morelli, 1976; Cavazza and De Celles, 1998). The basin rests on top of both the crystalline Sila massif and the inner accretionary prism. This wide NE-SW oriented basin is bounded northward by the Calabrian slope (continental margin of Calabria region), and seaward by a post-Messinian landward dipping reverse fault (forearc outer thrust) that overthrust the basin over the inner accretionary complex. This reverse fault represents a relatively continuous element across the mapped area and, according to Rossi and Sartori (1981) and Barbieri et al. (1982), seems to be reactivated by an extensional tectonics.

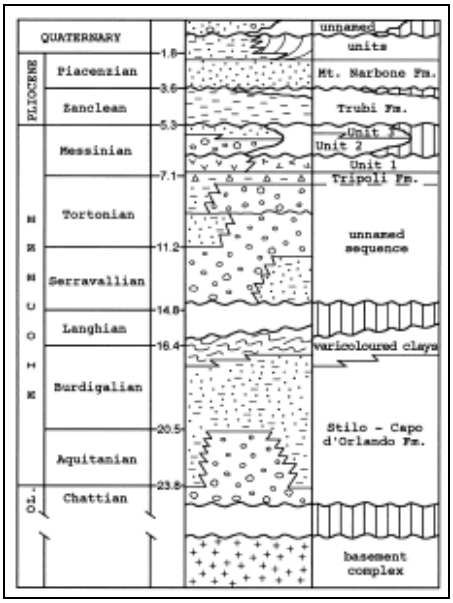

Figure 11 – (a) Lithostratigraphic chart of the proximal portion of the Calabrian forearc basin fill;
(b) Generalised stratigraphic relationships in the same area. No scale implied (Cavazza and De Celles, 1998)

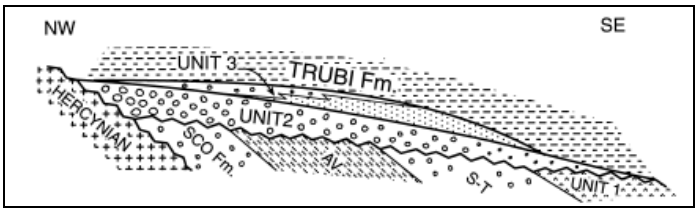

The subsidence of the basin in the offshore region is mainly Pliocene-Pleistocene in age. The Crotone-Spartivento basin is divided by a structural high located off Punta Stilo, immediately to the south of the Catanzaro isthmus (Fig. 12). The two sub-basins present some differences (Barone et al., 1982; Barbieri et al., 1982). The northeastern one, comprising the graben of the Squillace Gulf, is wider, has a maximum depth of 1700-1800 m, and is characterized by a diapiric structure, while the southwestern one is narrower. The basin

filling starts earlier in the Aquitanian (on-shore outcrop of Stilo–Capo d'Orlando Fm., Cavazza & De Celles, 1998) and reaches a depth of about 2000 m (Fig. 11).

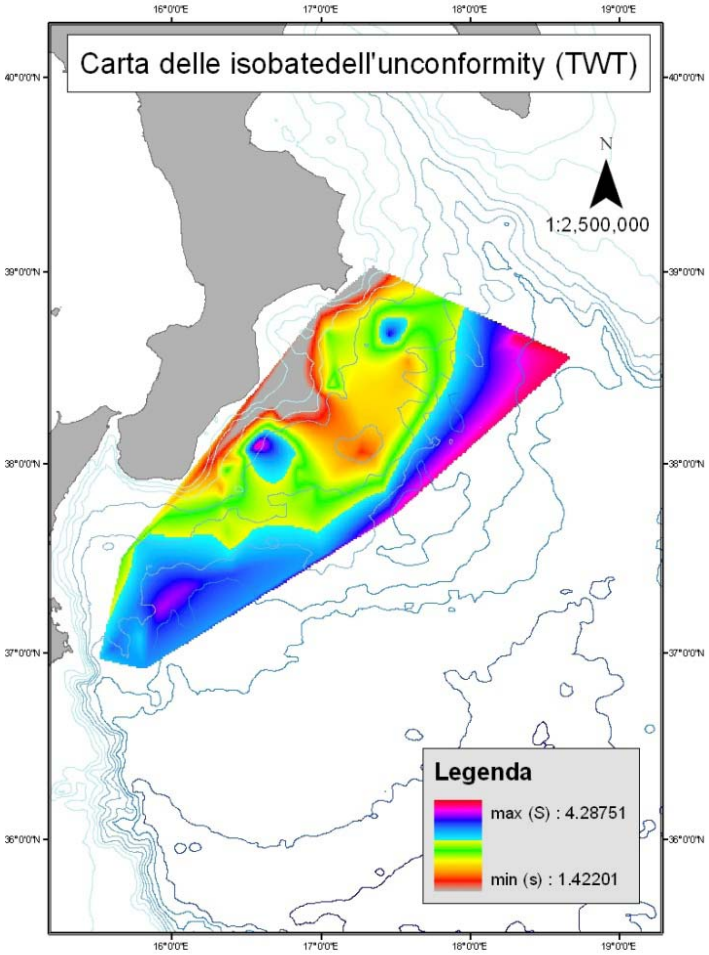

Figure 12 – Map of the isobaths of the M reflector below the offshore forearc basin. The coloured scale is in sec TWT. The map shows the two sub basin, divided by structural high of P.ta Stilo, of the forearc basin, where there is the maximum thickness of the inflling sequence.

The basin is characterized by an extensional tectonics with synsedimentary faults and typical features related to the Messinian salt tectonics (M/A reflector). The basin is also affected by sliding and slumping, as suggested by the dredge and cores recovered in the basin by Barbieri et al. (1982).

The stratigraphy of the basin consists of:

- the Upper Miocene unit, which is exposed onshore in the Crotone basin and is probably correlated with the transgressive Serravallian to Tortonian sandstone and mudstone of the S. Nicola Fm. and Ponda Fm. Estimating the thickness of this unit is very difficult in seismic profiles; however, by considering the well stratigraphy in shallow water areas, the average thickness should be about 1000-2000 m. These post-orogenic sediments disconformably cover the stacking of Calabria-Peloritani Arc, which is made up of crystalline and carbonate thrust sheets. These sheets were deformed during

the lower Miocene time (see chapter 2) and were reached by onshore and offshore wells. On top of this sequence, an infra-Messinian angular unconformity, tied with near coastal industrial wells, cross-cuts all the previous structured Miocene sequence. On top of the Messinian unconformity, in spite of its limited thickness and high seismic velocity, fig. 10 (a) shows thin layer of Messinian salt.

- a thick, Plio-Quaternary, subhorizontal and well-stratified sequence infilling the basin. The wells stratigraphy onshore and in shallow water area show conglomerates and sandstones fining upward to marine shales related to an increasing widespread subsidence. The thickness of the infilled sequence varies from 0.4 s TWT up to more than 2 s TWT. This slive is often deformed by diapiric structure. In the sedimentary filling we can recognize several unconformity related to the complex tectono-stratigraphic history of the basin. The most clear is the infra-Pliocene angular unconformity evident near the Calabrian slope. This unconformity bounds the lower Pliocene Trubi Fm, which is a quasi-transparent layer.

Near Crotone, also the middle-upper Miocene sequences are involved in compressive deformations related to the growing and accretionary history of the prism. The Pliocene-Quaternary sediments, conversely, are affected by synsedimentary normal faulting, tilted blocks, rollovers and extensional diapirs in the landward inner sector of the basin, and by compressive tectonics (folds and thrusts) in the outer sector, probably in relation with a gravity sliding processabove a salt layer. The landward boundary of the Crotone-Spartivento basin (Calabrian slope), near the Crotone peninsula, is instead affected by huge complex gravity sliding and slumping involving the sedimentary cover, made up of Pliocene and Pleistocene clays, dredged along the slope (Rossi e Borsetti, 1974), above the salt layer (M reflector). This matter will be discuss in Chapter 3.

Fig 13 shows, below the present forearc basin, the southward dipping reflectors of the Calabrian block consisting of the Sila crystalline unit, which is exposed onland and partly overthrust onto the carbonate formations of Mesozoic age. The Plio-Quaternary offshore tectonics of the basin is characterized by a regional subsidence, interrupted in several moments by compressive deformations (thrusts and backthrusts with Pliocene piggy back basins) as shown in Fig. 13 (a) and (b) and extensional reactivation of the previous compressive structures.

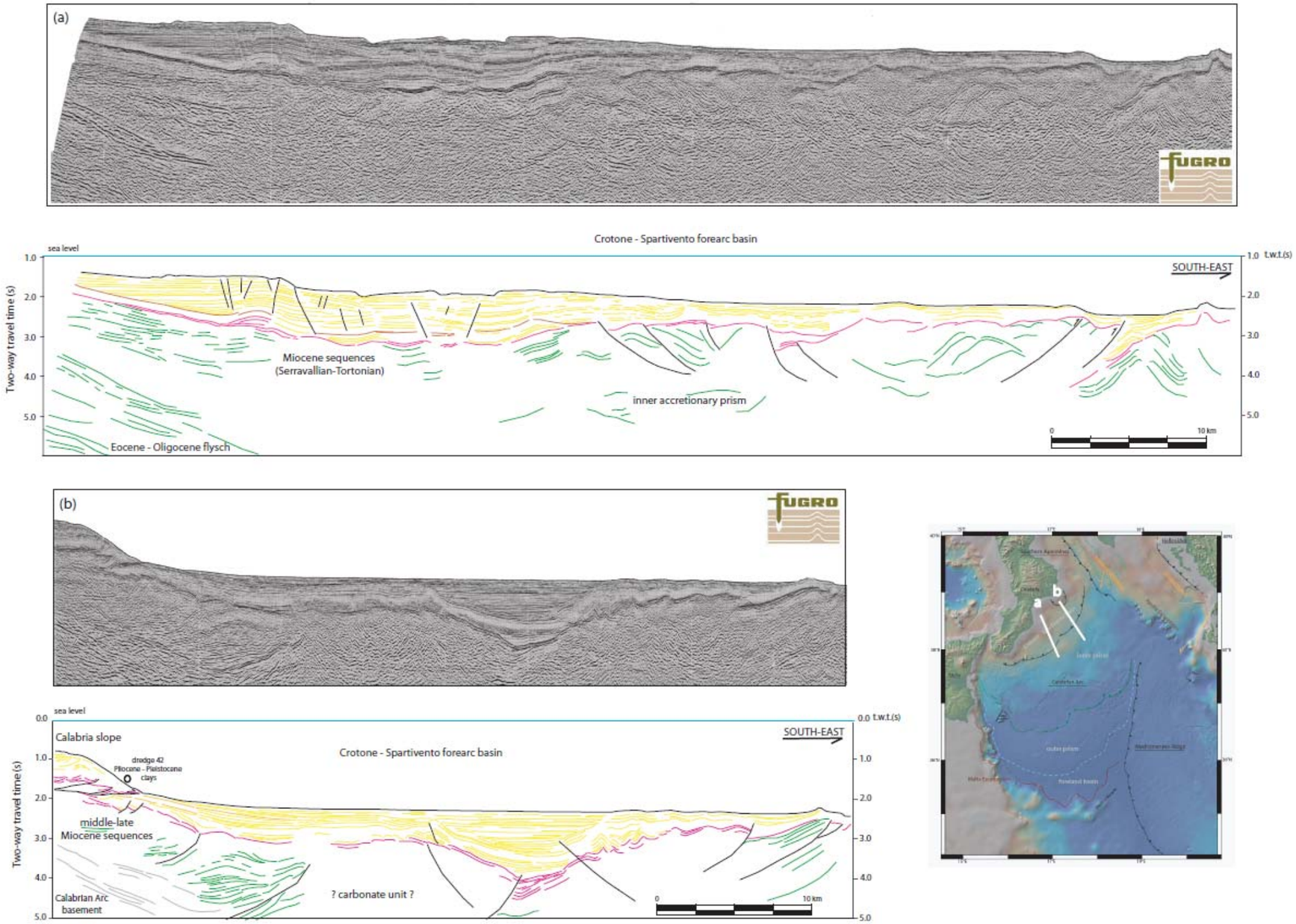

Figure 13 – Two seismic reflection profiles, data supplied courtesy of Fugro, and line-drawing related from the Crotone-Spartivento forearc basin. See inset for location of the sections displayed in this figure. In yellow the Plio-Quaternary sediments, in pink the A (M) reflectors, and in green undefined pre-Messinian reflectors. Near the Calabrian coast, where calibrated, below the Messinian unconformity Tortonian to Serravallian unit, outcropping in the eastern side of the Sila Massif (S. Nicola and Ponda formations) are present. In profile (b) in grey are represented the reflectors of the Sila crystalline unit, tied with wells.

6.3.2 Inner accretionary wedge

The inner accretionary prism extends from the southern boundary of the forearc basin, the forearc outer thrust, to the main frontal thrust. This ramp represents the locus where the basement unit of the Ionian plate is involved in the accretionary structure. In the western sector, the ramp is extensionally re-activated.

The extreme tectonization of the accretionary complex and the lack of stratigraphic constraints make very difficult the geological interpretation of the seismic profiles.

This sector of the accretionary complex is an arcuate belt, 130-140 km long and 280-300 km wide on average. It consists of a nappe stack of pre-Messinian units scraped-off from the downgoing plate. It is characterized by several NE-SW oriented and southeast verging thrusts, deforming in same cases the M reflectors. On top of the M reflector, a thin layer of Plio-Quaternary sediments is present and locally deformed by a post-Messinian reactivation of the previous structure.

The inner wedge can be divided into two domains with different topographic slope by the Crotone-Spartivento slope (Rossi and Sartori, 1981) which is a morphological element of the Ionian offshore. This structure has been previously interpreted either as the superficial expression of the subduction zone (Sioni, 1996) or considered as one of the main thrusts of the Calabrian Arc (Rossi and Sartori, 1981). The inner portion of the inner wedge is 60 km long and has a topographic slope of 0.6° whereas the outer portion, having the same length, has a 0.14° of slope. The slope have a vertical displacement of 0.6 s (TWT).

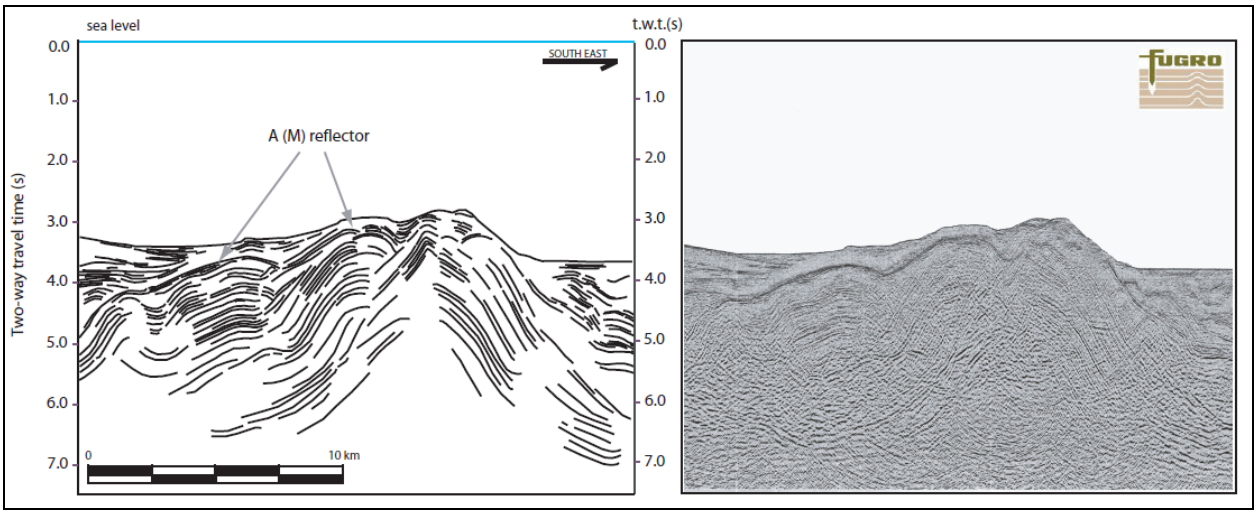

Figure 14 – Line drawing (a) and seismic reflection profiles (b), data supplied courtesy of Fugro, of the structure of the inner accretionary wedge. The reactivation of this structure is clearly post-Messinian in time.

In the southeast sector of the inner prism, we observe a spectacular inversion structure (Fig. 14) that involves basinal sequence, with reflectors of high amplitude and lateral continuity. This structure has not so far been depicted. The age of such inversion is not clear, but we suggest a post-Messinian reactivation, by analogy with other structures. In map view, the inverted structure closes toward the southwest.

6.3.3 Frontal ramp and outer accretionary wedge

The outer wedge extends from the main frontal thrust to the foreland basin, to the south, and pinches out against the Malta Escarpment, in the western side. Toward the east, the wedge tapers until it disappears in the contact zone with the Mediterranean Ridge. The total length of the outer wedge is about one hundred kilometers toward the abyssal plain, and forty kilometers toward the Malta Escarpment (Fig. 15).

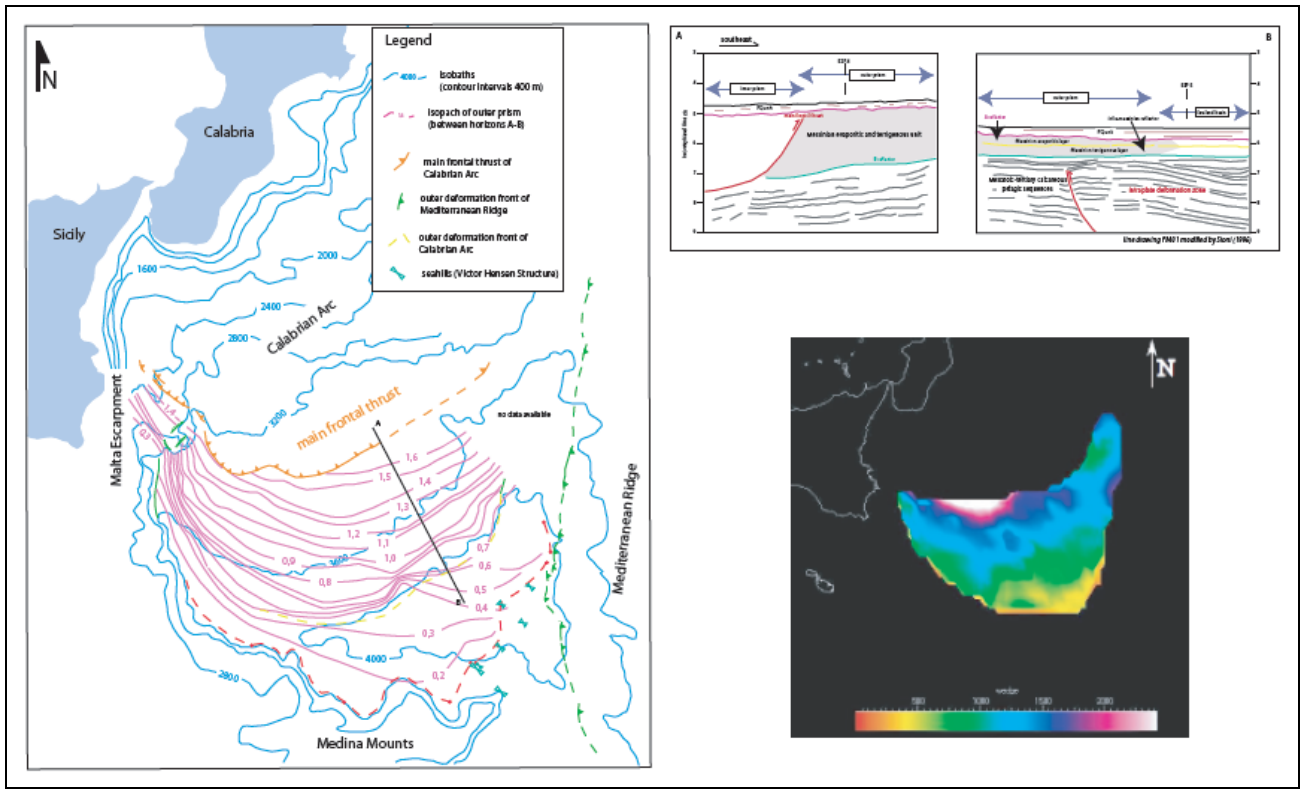

Figure 15 – (a) Isopach map of the outer accretionary wedge from the main frontal thrust to the foreland basin. Has been considered the thickness between A and B reflectors as shown in profile AB, a synthetic line drawing crossing the outer accretionary prism (b). The thickness is expressed in TWT - two way traveltime (s) (c) computed isopach map from seismic reflection profiles using Gocad; the color coded bar show the thickness expressed in TWT (s), in pink the maximum thickness.

Toward the south the Calabrian accretionary wedge is thrust onto the wedge shaped subducting Ionian sediments. The frontal ramp, thus, divides the mobilized domain of the Calabrian accretionary complex from

the foreland basin. In map view, this element has a convex shape running from the eastern margin of the Hyblean plateau, as previously described, towards the Apulian plateau, where the seismic grid is less dense.
Along this ramp the basal décollement rumps into the top shallow part of the subducting sequences. We thus consider this ramp as the main frontal thrust of the wedge.
The outer accretionary wedge, at the front of the main frontal thrust, displays a thickness varying from 1.8 s TWT to 0.3 s TWT. This wedge is bounded by the A and B reflectors, which represent the base and top of the Messinian unit (ME), respectively. Direct information constraining the A reflector comes from some piston core and Deep Sea Drilling Project Site 374, which penetrated the Plio-Quaternary sequence and over 80 m into the Messinian evaporite formation (Hsu et al., 1978). The B reflector is taken from Finetti and Morelli (1973). The presence of the evaporitic layer on top of the outer wedge is also confirmed by the ESP 4-5 (de Voogd et al., 1992) running seaward of the Calabrian wedge (foreland basin) and further upslope onto the Calabrian prism. This sedimentary wedge is a quasi-transparent layer without internal reflection and follows the sedimentary wedge as observed at the foot of the Malta Escarpment. This body extends from the eastern side of the Hyblean plateau, where it pinches out toward the Malta Escarpment, to the Messina abyssal plain, where, toward the east, it is restrained by the frontal thrust of Mediterranean ridge. The origin and nature of this body will be discussed later. On top of the wedge, a thin sequence of Plio- Quaternary turbidite deposits occurs (Muller et al., 1978; Hieke, 2000). The PQ unit gets thicker towards the Ionian abyssal plain (i.e., 450 m in ESP 5). The Plio-Quaternary unit shows small folds, which creates the cobblestone topography (Hersey, 1965), well know in the Ionian abyssal plain. Three different hypotheses have been put forward: they might be megaripples (Emery et al., 1966), collapse structures caused by karst processes (Hinz, 1974; Ryan et al., 1973), gravitative, plastic and viscous flows in the frontal thrust area (Rossi and Sartori, 1981), or compressive deformation related to the advancing basal décollement. Below the outer wedge, it is possible to observe the subducting sediments characterized by subhorizontal parallel reflectors mainly consisting of Mesozoic and Tertiary clastic sequences, and Ionian crust, as suggested by the related refraction velocity.
Several authors (Rossi and Sartori, 1981; Finetti, 1982) deemed the outer wedge as an allochthonous gravitative slide or melange without real compressive deformations inside.

6.3.4 Foreland basin and intra-plate deformation zones

The foreland basin is represented by a triangular shape flat basin coincident with the Ionian abyssal plain. It ends against the Medina Mount, a complex horst structure affected by volcanism (Finetti, 1982). Here the seismic stratigraphy has been calibrated using a drill site 374 and a refraction data of ESP 5. The Ionian basin is the foreland for both the Calabrian Arc and for the Mediterranean Ridge. The toe of the accretionary complex

is not clear in the seismic profiles. We take, as beginning of the foreland basin, the point where the PQ unit lies subhorizontally (Fig. 16). The seismic sections reveal intense compressive deformation of the basement unit during Tortonian time. Deformation consists of numerous reverse faults down to crustal level. The reverse faults are mainly oriented NE-SW and the total amount of shortening is 5-6 km (Chamot-Rooke et al., 2005). This event was probably responsible of the rise of Medina Mounts, even though, at some places, the faulting along the escarpment seems still active (Hieke et al., 2003).

In the foreland basin, the PQ unit is undeformed and lies horizontally above the evaporitic layer (ME unit), which is mainly composed of an upper evaporitic layer and a lower more clastic one. Moving toward the prism, the PQ shows little deformation with small wavelength folds (cobblestone topography).

The Medina Mount (including its prolongation as VHStr, named Marconi seamount by Finetti (1982), NStr (Hieke & Vwanninger, 1985) and VaStr (Hieke et al., 2003)), which is located between the Sirte margin and the Ionian abyssal plain, shows sharp NE-SW escarpments. In places, the Medina Mount structures rise the seafloor, thus suggesting a recent extensional tectonics. A vertical displacement of about 0.1 s TWT of the M reflector above NStr indicates post-Messinian movements (Hieke et al., 2003). Below the B reflector, a well-stratified sequence up to Mesozoic is present. In the central abyssal plain, this sequence is affected by compressive deformation expressed by numerous reverse faults and backthrusts dipping toward the southeast and the northwest, respectively, with synkinematic strata on top of the pre-Messinian reflectors, which are southeastward-dipping. These faults are crustal features, which could be related to a basin inversion re-activating previous extensional faults. The Messinian evaporites do not seem affected by the compressive deformation and the timing of this intraplate event is probably Tortonian in age (Chamot-Rooke et al., 2005; Sioni, 1996). The total thickness of this unit, depending on the chosen interpretation for the top of the crust, is about 3-4 km as suggested by geophysical data (de Voogd et al., 1992). The unit is mainly composed of thick Mesozoic carbonates and tertiary clastic sediments. According to Hieke et al. (2003), the deformation pattern of the pre-Messinian reflectors indicate a tilted block and horst-like feature created by extensional tectonics.

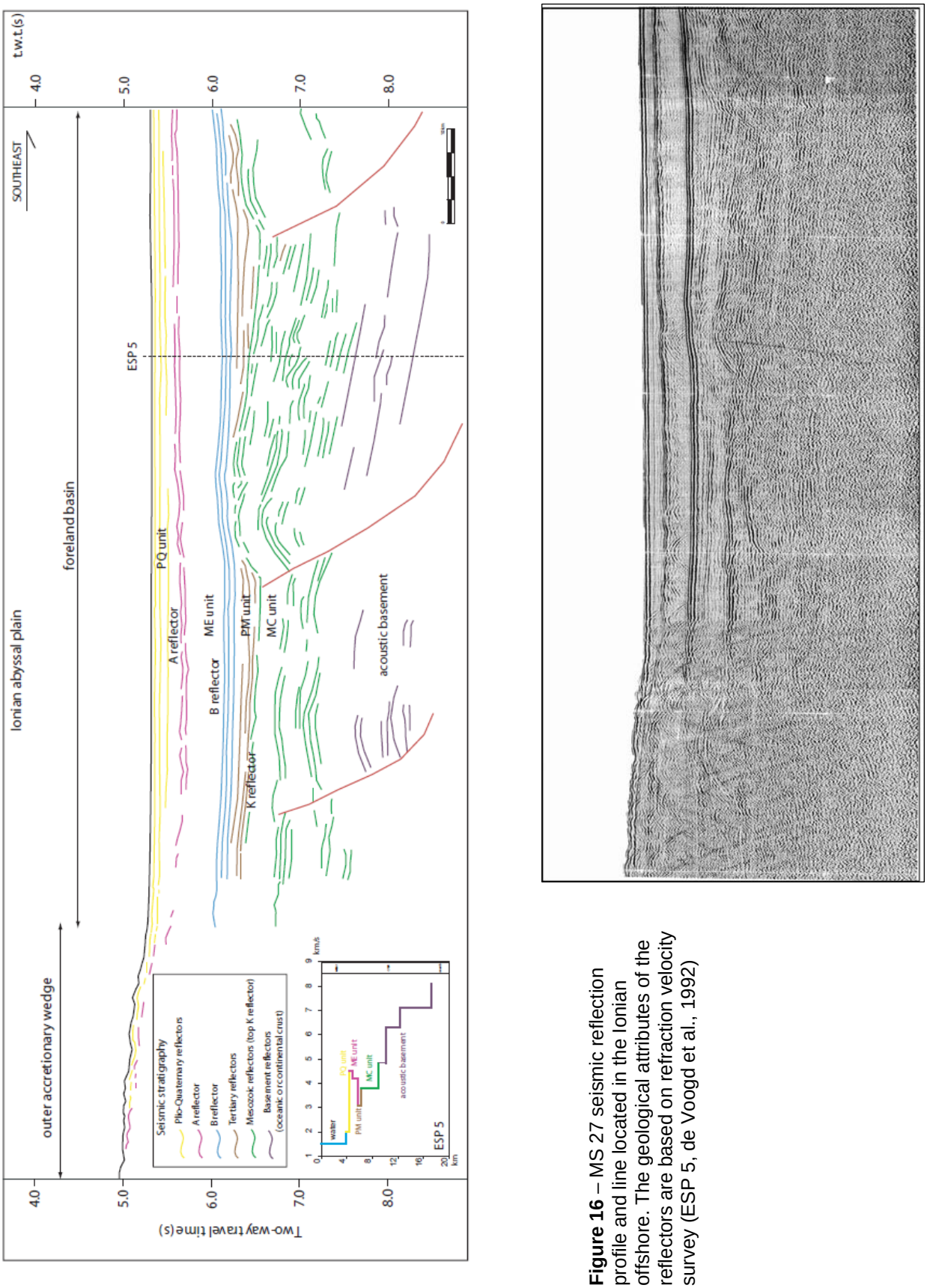

Figure 16 – MS 27 seismic reflection profile and line located in the Ionian offshore. The geological attributes of the reflectors are based on refraction velocity survey (ESP 5, de Voogd et al., 1992)

7. Discussion

The main open questions rised from the geological interpretation of the seismic reflection profiles are:

i. Age and deformation in the Ionian abyssal plain basin.

ii. Present boundary of the Calabrian accretionary prism and its connection with the Southern Apennines thrust front and Mediterranean Ridge.

iii. The nature of the outer accretionary prism.

7.1 Discussion on intraplate deformation (Ionian abyssal plain)

The present foreland basin of the Calabrian accretionary prism is located in the Ionian abyssal plain, a triangular shape basin with an average depth of 4000 m. The seismic stratigraphy of the basin has been reconstructed using the refraction velocity (de Voogd et al., 1992) and the drill 374 of Leg XIII of DSDP project. In summary above an oceanic or stretched continental crust, covered by Mesozoic carbonate and Tertiary clastic unit, a Messinian (evaporitic and terrigenous) sequence and a thin level of Plio-Quaternary sediments mainly composed of turbiditic layer are present (Hieke et al., 2003). The total thickness is about 12 km. This central area of the Ionian Sea comprises between the outer deformation fronts of the Mediterranean Ridge and Calabrian Arc and, southeastward, the Medina Mount, which has been affected in pre- Messinian time, as revealed by reflection seismic profiles by compressive deformation. The recognized structures, expressed as numerous reverse faults, all involve the crustal section up to the upper Miocene (B reflector). The Messinian and Plio-Quaternary units, lying above a flat B reflector and forming the outer wedge of the accretionary prism, are not affected by the deformation. The age of Mesozoic basin inversion (shortening of a former extensional basin) is probably Miocene, and should be bracketed between 13 Ma and 8 Ma (Serravallian –Tortonian) as suggest by Sioni (1996) and Chamot-Rooke (2005), suggesting also that this compressive deformation causes the rise of the Medina Mount. According to Hieke et al. (2003), this deformation is instead related to an extensional setting. The main structures are 10 km spaced thrust and back-thrust, southeast and northwest dipping, respectively, and N30°- 40° striking, with a total amount of displacement of about 10 km. Thrust and backthrusts are characterized by syn-kinematic basins with growth-structure, typical of compressive tectonic settings.

According to velocity refraction data by de Voogd et al. (1992) these faults should involve the levels 2a-2b-3 of the hypothetical oceanic crust. This kind of intraplate compressive deformations is not exclusive of the continental crust, as previous cases of diffuse oceanic compressional deformation have been described in the central Indian Ocean (Chamot- Rooke et al., 1993).

In any cases, the presence of intraplate deformations demonstrates that the subduction zone at that time was locked. This event could have happened in fact after the opening of the Liguro-Provencal basin and shortly before the opening of the Tyrrhenian basin, and could be correlated with the quiescent phase of backarc spreading. Similar cases of inversion tectonics have been described also in other cases as in the NW European Alpine foreland in response to compression generated by European-Afriacan plate collision in the Cenozoic (Ziegler, 1987). In some cases the inversion occurred some 1600 km far away from the plate boundary (Ziegler et al., 1998). Orogenic forelands often comprise previously stretched and rifted passive continental margins and they are characteristically highly anisotropic and represent a weakness zone where deformation could be localized due to variation in basin geometry or sedimentary fill, or due to the presence of pre-existing fault zones (Turner and Williams, 2004). This phase predated the forward propagation of the outer accretionary prism above a Messinian décollement.

7.2 Discussion on the boundary of the Calabrian accretionary prism

7.2.1 Western boundary of the Calabrian accretionary prism

The offshore western boundary of the Calabrian accretionary prism is characterized by the presence of two main important crustal features: the Malta Escarpment and a lateral ramp of the wedge. Both structures show a recent activity, as displayed in the seismic reflection profiles. Whereas the first rejuvenates an older passive margin, the second plays along a main frontal thrust, a more external lateral ramp of the accretionary complex. In this case, an extensional reactivation is testified by the growth structure visible in the synkinematic strata. The direction of extension is thus mainly E-W, similar to that shown by other faults along the eastern side of Hyblean plateau. This recent activity could be related to tectonic reorganization of the south-central Mediterranean according to Goes et al. (2004). These faults then could be the transfer zone between the outer front of the Calabrian accretionary prism and the new compression front located at the front of the Sicily in the southern Tyrrhenian Sea (Billi et al., 2006). In our model, the extensional reactivation of an older lateral ramp can be related to a collapse of the entire accretionary wedge due to a slowdown in convergence velocity or represents an example of how at present the deformation is accommodated in the inner sector of the wedge rather than at the front. A strike-slip motion has been proposed for this fault or alternatively can be interpreted as a STEP-fault accommodating the retreating trench (Govers and Wortel, 2005). A possible stike-slip mechanism is instead suggested for a fault zone located slightly toward the west. This fault zone, running NS parallel to the Malta Escarpment, is characterized by salt diapiric ascents, which deform the seafloor, and by abrupt reduction on the ME unit.

7.2.2 Eastern boundary of the Calabrian accretionary prism

The eastern boundary of the prism is characterized, toward the north, by the termination of the Southern Apennines. The thrust belt, its foredeep (Taranto Valley) and foreland (Apulian Ridge) are well visible in seismic profiles. Moving southward, the Apulian Ridge has not been affected by downfaulting and flexure due to advancing and load of the Apennines. The Apulian platform is instead truncated by an erosional Messinian escarpment. The two foreland basins, the Ionian basin for the Calabrian arc and the Apulian platform for the southern Apennines, are not connected in the Ionian offshore. This implies a different history, at least in the recent time, for these two margins. The linking segment of the Ionian offshore, in fact, is not flexed. It is then possible to imagine that these two margins developed independently in the recent part due to a slab tear. This is also consistent with a 150 km slab windows imaged by tomographic analyses below the southern Apennines (Chiarabba et al., 2008). This windows should have been induced by ultrafast retreat of the Ionian slab compatible with high velocity spreading (19 cm/yr) of the oceanic Marsili basin (Nicolosi et al., 2006). This ultrafast retreating could be related to the formation of the huge post-Messinian outer accretionary wedge in the Ionian offshore whose propagation has been facilitated by the presence of a weak décollement layer. In any case, the linkage between Apennines-Calabrian arcs remains unclear and needs further studies.
Also the contact zone between Mediterranean Ridge and Calabrian Arc is still unclear. The eastern sector of the Ionian sea is the sector less covered by seismic reflection profile. According to the structural synthetic map, the narrowing of both the outer wedge and the foreland basin is evident in the area, where the two accretionary wedge collides. Moving towards the Kephalonia island, the Mediterranean Ridge is intercept by the dextral Kephalonia transform fault (Kahle et al., 1993) and is displaced toward the east, whereas the Calabrian arc is still active. According to Chamot-Rooke et al. (2005) the Mediterranean Ridge proper is overlain by gravity folds and thrusts.

7.2.3 The outer front of the accretionary prism

The quality and the resolution (vs. penetration) of the multichannel seismic profiles utilized in the study cannot help to define the recent activity of the subduction process. It is however clear that not evident frontal thrust has been recognized in the Ionian offshore. In the Ionian abyssal plain, the Plio-Quaternary sediments show only small wavelenght folds, which, have been in the past ascribed to karst processes or salt movements (Morlotti et al., 1984). Compressive post-Messinian (or post-M reflector) deformations are instead distributed on the whole accretionary prism as testified by several thrusts and backthrusts that involve the M reflector. In the past, the Calabrian accretionary prism was by Finetti (1982) and Rossi and Borsetti (1981) interpreted,

because of its resemblance to the adjacent Mediterranean Ridge (Ryan and Heezen, 1965), as a compressional structure. Other authors relate the Calabrian Arc to the emplacement of olistostrome. The frontal thrust of the Calabrian accretionary prism has been identified in the past in different sector of the wedge. For Finetti (1982) the forearc scraping zone of the accretionary complex ends where we locate the main frontal thrust. For Rossi e Sartori (1981) the Calabrian ridge s.l. consists of recent sediments mobilized by gravity sliding. This should be related to the existence of one or more potential décollement layers within the sedimentary cover of the Ionian plate above which compressional tectonics and associate gravity processes may develop. Recently (Chamot-Rooke et al., 2005) identified in the Ionian abyssal plain the outer deformation front characterized by a shallow décollement layer in the evaporites formation. But the boundary between the deformed outer prism and the undeformed basin is not clear. This outer prism has been interpreted by several authors as a sliding deformation front without accretion.

7.3 Discussion about the outer accretionary prism

We consider the outer prism as the frontal toe of the Calabrian accretionary prism. It is comprised between the main frontal ramp and the onset of the foreland basin, where the PQ unit is undeformed. Further northeast it collides against the advancing Mediterranean Ridge. In the western Ionian offshore the outer wedge extends along a relatively narrow, north-south band located just to the east of the faults forming the Malta Escarpment and it is confined by the escarpment and the re-activated lateral ramp. The extension of this wedge has not been discussed in previous works. Some authors have identified the outer wedge only along the section running roughly NW-SE.

The outer prism is a wedge like body involving in deformation only the upper part of the sedimentary sequences of the Ionian plate. The seafloor and B reflectors are the upper and lower boundary respectively of the outer prism. It includes the Plio-Quaternary succession (PQ) and the Messinian unit (ME).

The refraction survey (ESP 4-5), acquired in the Ionian offshore along the Calabrian Arc by de Voogd et al. (1992), shows, below a thin layer of unconsolidated recent sediments of Plio-Quaternary age, constrained also by the DSDP 374, a Messinian sequence consisting of two layers with a clear velocity inversion inside. This inversion is connected with the passage between the high velocity upper evaporite sequence and a lower layer of terrigenous deposits. The refraction data display a progressive thickening of the two Messinian units upslope toward the north (Fig.17).

In the seismic reflection profiles the PQ unit is a well-layered sequence of about 0.2–0.4 s (TWT) thickness. The Messinian sequence is instead bounded by the A and B reflectors. The velocity inversion, found inside, relates to an infra-Messinian layer which is not well detectable along all the profiles. Probably this represents the base

of the evapotiric sequence. The seismic facies of this unit is largely transparent without outstanding reflectors inside. Below the Messinian wedge a Tortonian sequence lies above the undisturbed foreland section, made of calcareous pelagic sequences of probably Eocene-Mesozoic age (Casero et al., 1984; Cernobori et al., 1996; Finetti, 1982).

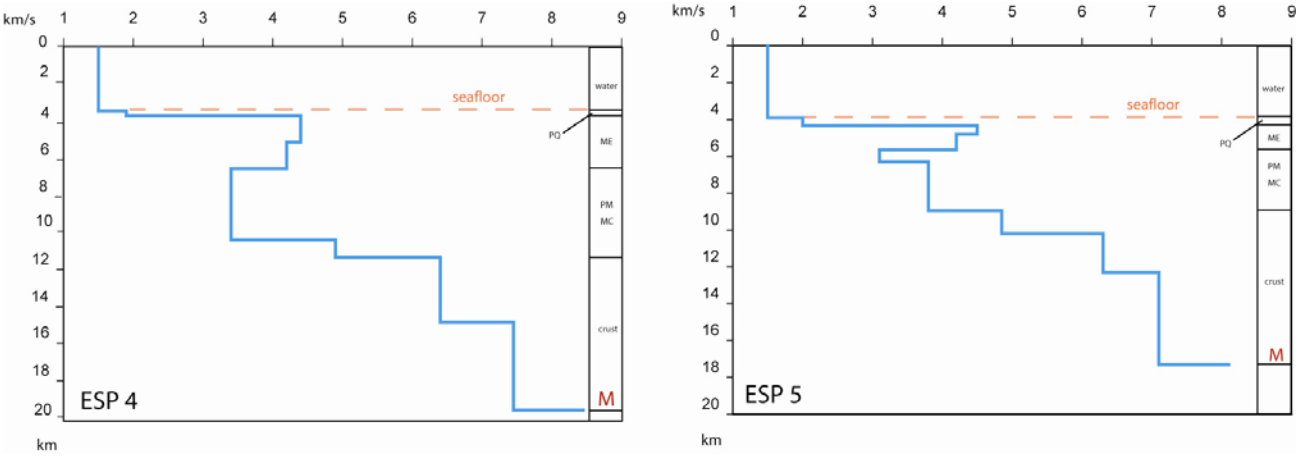

Figure 17 – Velocity model of de Voogd et al. (1992) obtained for ESP 4 /5 located in the Ionian offshore. For the location see Fig. 5

The thickness of the outer prism, considering the unit between A and B reflectors, varies from 1.6 s (two-way traveltime) near the frontal ramp to 0.2 s in the abyssal plain. In the same track, the PQ unit does not seem to significantly change its thickness. Toward the west, an abrupt change in thickness of the wedge is connected with a faulted zone running roughly NS, further east to the Malta Escarpment. Salt diapirs ascent seems connected to the movement along this faulted zone.

The nature and the age of the basal reflection of the outer prism is debated. The B reflector, a very low frequency and high amplitude continuous horizon, dipping toward north, has been defined as the first flat reflector below the sequence with diapiric structure according to Finetti (1982), and should represent the base of the Messinian evaporitic sequence.

In the Ionian abyssal plain, where a pre-Messinian intraplate phase of deformation is present, the B reflector seems instead to constitute the upper boundary of a post-rift sequence (Sioni, 1996). This second interpretation led to consider the B reflector as an intra-Tortonian surface similar to the same surface in the Apenninic chain.

The presence of this outer wedge and its nature, sedimentary or tectonic, opens several questions about: (1) the recent activity of the subduction process, as discussed by several authors (D'Agostino e Selvaggi, 2004; Mattei et al., 2007) using different data (paleomagnetic, seismicity and GPS), and (2) the geodynamic setting of the Ionian sea.

Therefore this outer wedge represents a key area to understand the evolution and the history of accretionary mechanisms. Two different hypotheses are proposed below.

Model 1 : sedimentary wedge

Following Holton (1999), the outer wedge can also be interpreted as an allochthonous sedimentary wedge connected with the destruction of the Calabrian accretionary wedge. The lack of internal reflectors suggests that this structure is an olistostrome, similar to allochthonous Miocene sections of the adjacent Caltanissetta basin of southern Sicily. According to this second intriguing mode, the wedge accommodates a Messinian preevaporitic flexural domain. The bottom and the top of the wedge are, in fact, marked by the B and A horizons, Tortonian and evaporitic Messinian respectively. The Messinian preevaporitic age of the wedge is inferred by Casero et al. (1984) who made a litostratigraphic calibration using the borehole in the Malta Ragusa continental platform. Foredeep basins of the same age (Terravecchia, Laga or uppermost Marnoso-Arenacea) are recognized along the Appenninic Maghrebian fold-and-thrust belt (Casero, 2004) and in Tunisia offshore (Sicily channel) (Casero & Roure, 1994). According to this model, and by analogy with the Sicily channel (Casero & Roure, 1994), there no post-evaporitic flexure should occur in the Ionian offshore. Indeed, there are not other younger flexural basins developing in front of Messinian foredeep.

Model 2 : tectonic salt wedge

This model suggests that the outer wedge is the expression of the Plio-Quaternary subduction. The outer wedge should be mostly made up of Messinian sediments, clastic and evaporitic. According to the seismic interpretation, the deep-water Messinian evaporitic section in the Mediterranean Sea, corresponds to an acoustically transparent interval, without clear reflection inside due to intense ductile deformation, between a strong, irregular high-amplitude top reflector (M) and a high-amplitude flat and continuous basal reflector (B) that can be mapped over wide areas (Finetti, 1976). The thickening of the wedge toward the main frontal thrust is the result of tectonic thickening related to ductile deformation of salt rocks. The seismic facies (Montadert et al., 1978) and the velocity model of de Voogd et al. (1992) support this idea, suggesting for the outer wedge a mean velocity of 4.3 km/s compatible with a wedge made up of salt rocks. According to this hypothesis, the chaotic seismic facies of the body is due to the extreme deformation. The Plio-Quaternary wedge has grown on top of a flat décollement localized within the Messinian lower evaporites.

The geodynamic implications of these two different models are significant and will be discussed in the following paragraph.

8. **Time-space evolution of the Calabrian accretionary prism**

The growing history of the Calabrian accretionary wedge has been reconstructed through geological interpretation of the seismic reflection profiles located in the Ionian offshore. The used seismic reflection profiles have time-recording of 8-10 s TWT on average.

Fig. 18 shows from the forearc to the foreland basin a progressive thickening of the prism made up of stacking of the sediments scraped off by the downgoing subducting plate and accreted into the wedge front. Apart from refraction velocity, seismic character and few superficial wells that constrain the incoming subduction unit, we do not have direct information on the material constituting the wedge. Few cores, taken in the Northern Ionian Sea, found chaotic deposits corresponding to a rather continuous sedimentary sequence ranging from Upper Cretaceous to Messinian (Morlotti et al., 1982). This supports the idea of the inner accretionary prism is made up mainly by pre-Messinian sediments.

According to Cernobori et al. (1986), the basal décollement, which divides the undeformed subducting sequence from the accreted one cuts into the Tertiary and Mesozic sequence. In the inner sector of the wedge, it lies at about 14 s TWT, whereas at the main frontal thrust, the décollement is flat, and is localized at the base of the evaporites unit (B reflector) below the outer wedge (Finetti, 1982). This ramp divides the pre-Messinian accretionary wedge, visible in the inner sector of the wedge up to the Calabria crystalline unit from the outer wedge which corresponds instead to a wedge made up exclusively of deformed post-Messinian deposits.

The outer Calabrian accretionary wedge has a basal decollement characterized by $\beta = 0.96°$, and a topographic slope characterized by $\alpha = 0.36°$. These values have been calculated making a conversion in depth of the seismic profiles using as reference the velocity for the different units the refraction velocities of de Voogd et al. (1992). In particular 1500 m/s water, 1800 m/s Plio- Quaternary unit (PQ) and 4300 m/s as average value for Messinian unit (ME). This critical taper clearly falls into the field of salt orogenic wegde.

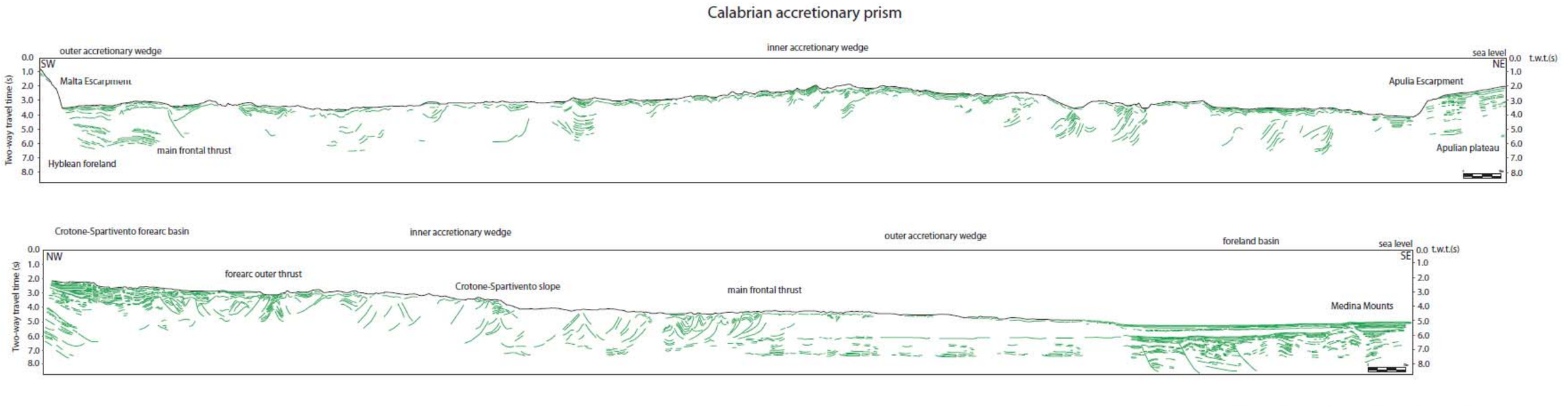

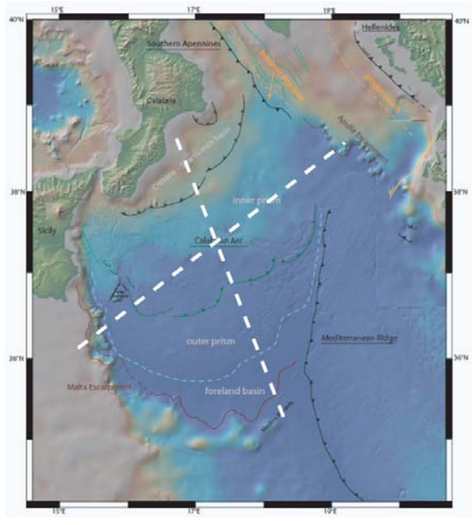

Figure 18 – Line drawing crossing the Calabrian accretionary prism running (a) SW-NE and (b) NW-SE showing the general setting of the wedge. Vertical scale in seconds TWT. Inset shows location of the profile.

The hypothesis of a décollement localised at the outer wedge, at the base of Messinian sequence (B reflector), is in agreement with the following observations:

- the very low taper of the outer wedge requires a very weak detachment layer, and it is thus likely that the Messinian evaporites represent the weakest horizon of the Neogene sedimentary succession of the Ionian foreland basin.
- The base of the evaporites (B reflector) is often divergent from their top (A or M reflector), which is folded, whereas the former is flat.
- A specific deformational style characterizes the outer wedge which does not show imbricated thrust sheets but rather a reflection free, progressively thickening, wedge only draped by thin, well stratified and slightly folded sediments.
- The peculiar hummoky topography of the outer wedge.
- The similarity with the structures and the time-space evolution of the near Mediterranean Ridge.

This schematic outline is compatible with the idea that the deposition of the Messinian evaporite bearing formation along the top of the accretionary wedge as well as the frontal deformation zone (the foreland basin, Ionian abyssal plain) played an important role and could have affected the style of wedge deformation, similarly to the Mediterranean Ridge (Kastens et al., 1992; Chaumillon et al., 1996; Kukowsky et al., 2002; Costa et al., 2004).

Moreover, unlike the Mediterranean Ridge, the Calabrian Arc shows clear deformation in the inner wedge. The age of such deformation is certainly post-Messinian (post M reflector). This deformation implies a back-stepping in the propagation of the deformation or suggests synchronous movements in different sectors of the wedge. Probably, the post- Messinian deformation in the inner accretionary prism have exploited older thrust planes formed during the pre-Messinian phase of growing and thickening of the wedge. This condition follows the rules of the critical taper for the accretionary wedge., Out-of - sequence thrusting in the inner portion of the wedge could have re-activated pre-existing structures once the wedge propagated outwards along a Messinian evaporites.

The origin of one of the main structure of the inner accretionary wedge, i.e., the Crotone- Spartivento slope, which is localized where the wedge changes its slope, can be explained with two different hypotheses: (1) it could represent the present accretionary front where the deformation is accomodated or (2) it marks the difference between two sectors of the wedge characterized by different internal strength, producing a progressive transfer from a ductile deformation zone to a more brittle type: Messinian salt unit on one hand and Tertiary to Mesozoic cover of the Ionian plate on the other hand. Being the accretionary process very sensible to variations of boundary conditions, this change could be related to a stopping or slowing down of

the convergence process, to a change in the erosion/sedimentation rate, or to a change in basal shear stress (see the critical wedge theory, Platt, 1986; Chapple, 1978; Davis et al., 1983; Dahlen et al., 1984).

The lack of stratigraphic data on the Pliocene–Quaternary sequences filling the syntectonic basins does not allow us to reconstruct the actual sequence of fold-and-thrust propagation in the Calabrian Arc frontal area. In any case, the rapid forward progression of deformation structures in salt-bearing wedges would have made it difficult to unravel the propagation sequence even if the stratigraphy of these basins had been known (Costa and Vendeville 2002).

The end of the outer prism, or the contact with the undeformed Plio-Quaternary sequences of the foreland basin is not marked by a clear deformation front. The wedge front is hidden below upper Pliocene turbidites (Sioni, 1996). For this reason, the activity of the subduction process in the Calabrian arc is still a matter of debate. A similar situation is observed along the outer deformation front of the Mediterranean ridge.

8.1 Wedge detaching on salt

Some analogue experiments (Costa e Vendeville, 2002) demonstrate that the sequence of thrust propagation in fold-and-thrust belts detaching above a very weak viscous décollement is drastically different from that in belts detaching on stronger décollement.

The fold-and-thrust belts detaching on non-evaporitic horizons, have been extensively studied. It is demonstrated that they grow and advance by maintaining a self-similar geometry. As the wedge lengthens by forward propagation of its front, it also thickens to maintain its critical taper, whose value is controlled by the angle of the internal fiction and the cohesion of the cover rocks and the coefficient of friction along the detachment horizons (Dahlen et al., 1984). The general trend is that fold and thrust belts advance toward the foreland by nucleation of younger structures at or in front of the toe of the wedge, whereas older structure within the wedge continue to grow or rotate passively in order to accommodate the thickening required to maintain a constant wedge taper.

Commonly, the geometrical characteristics of fold-belts detaching on salt are the more symmetrical (forward and backward) structural vergence of folds or thrusts, whereas the detached cover is deformed by folding or faulting in function of its lithologies.

All foldbelts detaching on salt exhibit a very low taper of 1° or less (Davis and Engelder, 1987). Moreover, the low taper of fold-belts above salt allows them to advance and propagate much faster than those belts detaching on stronger decollements. Several studies have documented break-back thrusts that form behind older thrusts or have indicated that many structures within a foldbelt can grow simultaneously.

The basal shear stress (τ) resisting the advance of a fold-belt above a frictional material depends on the thickness (h) and density (ρ) of the sedimentary cover, the amount of frictional resistance along the detachment plane (***ƒ***), and the coefficient of fluid pressure (λ) along that detachment:

$$\rho g h f (1-\lambda) = \tau$$

By contrast, the estimated strength of a low-viscosity decollement is at least one order of magnitude lower. The resistance to translation of the overlying brittle cover does not take place by slip along one or several fault planes but is accommodated by simple shear over the entire thickness of the viscous decollement layer (Kehle, 1970; Weijermars et al., 1993). The viscous shear stress resisting deformation is mostly independent of the thickness of the brittle cover, but depends on the thickness of the viscous layer (h) and shear-strain rate (v) (Weijermars et al., 1993).

$$T = (v/h)\eta \qquad \eta = \text{viscosity}$$

The value for basal shear stress will further decrease if the salt layer is thicker or if salt viscosity is reduced by temperature increase, by strain softening due to crystal-size reduction, or by an increase in fluid content. The principal result of such low basal shear resistance is that the associated critical wedge taper should be extremely low (Davis e Engelder, 1987). Therefore, even for minor amounts of shortening and displacements of the backstop, a fold-belt detaching on salt would rapidly advance and lengthen, as its tip would rapidly propagate forward. As a consequence, the fold-belt will experience only minor thickening and deformation. Theoretically, such minor deformation may occur by formation of numerous, closely spaced folds or thrusts that subsequently do not grow, or by formation of few, widely-spaced structures that undergo significant growth. Experiments suggest that the latter pattern prevails during the early deformation history of fold-and-thrust belts. Because the front of the fold-belt advances rapidly, it can theoretically reach the foreland pinch out of the salt decollement early, when the amount of regional shortening is still small and the belt comprises only a few, widely-spaced folds and thrusts. Once the foldbelt front has reached the salt pinch-out, it can no longer obey the condition of geometric self-similar growth, according to which the wedge's length and height increase proportionally so that the wedge taper remains constant. Instead, additional shortening could no longer be accommodated by forward advance of deformation front because there was no potential detachment plane beyond the pinch-out of the viscous decollement. Further advance of the wedge's tip beyond the decollement pinch-out would have required a much steeper wedge taper. Consequently, shortening was accommodated by formation of new thrusts and folds deforming the wedge itself, which thickened but no longer advanced.

8.2 Final model

In the Central Mediterranean, orogenic wedging was associated, from 30 Ma onward, with trench retreat and back-arc extension. The late Neogene evolutionary stage of the belt, related to the extensional processes, obliterated the structure associated with the early thickening event, partly outcropping in Calabria basement. The most evident expression of the extensional process is the formation of large-scale detachments that place the HP unit below non-metamorphosed or slightly metamorphosed units (Rossetti et al., 2004). This extensional regime is contemporaneous with the accretion of the outer fold and thrust belt. The external envelop of the orogenic wedge is constituted by a stack of Meso- Cenozoic sedimentary units derived from the African-Adria margin.

The formation of the arcuate shape of the Calabrian arc was attained mostly between the late Miocene and the Pleistocene, during the opening of the Tyrrhenian sea. Between 15-10 Ma the velocity of retreat drastically decreased (Faccenna et al., 2001 a). Nicolosi et al. (2006) concludes that the evolution of Tyrrhenian arc-backarc system occurred through a succession of ultra-rapid (2.1-1.6 My at 19 cm/yr) and slow spreading events (post 0.78 My, magmatic inflation of Marsili Seamount) separated by periods of relative quiescence (about 1 My).

Despite the slab is still defined by the narrow Wadati-Benioff zone below Calabria (Selvaggi e Chiarabba, 1995) the trench should have nearly ceased its retrograde motion as suggested by geodetic (Hollestein et al., 2003; D'Agostino and Selvaggi, 2004) and paleomagnetic (Mattei et al., 2007) data. This evidence suggests that subduction in the central Mediterranean is decaying.

The recent history (last 10 Ma) of the Calabrian subduction system and, in particular, of the Calabrian offshore accretionary wedge, has been poorly studied. Lots of knowledge of the Calabrian subduction zone arise mainly from deep geology and only little from shallow data. Although the paucity of stratigraphic data represents the real problem for better constraining this key sector of the Mediterranean geology, our study improves the knowledge about the structure and the structural domain of the Calabrian accretionary prism, trying to propose a valid model of time space evolution of the accretionary complex, based on objective observation. To reconstruct the growing history of this subduction complex, we are therefore forced to combine data from very different disciplines.

According to Faccenna et al. (2004), the total amount of subduction for the Tyrrhenian system should be derived by summing up the amount of convergence (Dewey et al., 1989) with the amount of back-arc extension (Patacca et al., 1990). The value obtained is, since 10 Ma onward, about 60 km of convergence and 380 km of retreat for a total amount of subduction of 440 km. This is the shortening that should have been

accommodated in the Calabrian accretionary wedge and subduction zone (Fig. 19). The Calabrian foreland fold-and-thrust belt, which formed during Neogene time, consists of a system of NNE-SSW and NE-SW directed thrusts with a SE directed sense of transport. Starting from these constraints, we point out the geodynamic implications of the two different models regarding the outer wedge and then we propose our model.

Sedimentary wedge**:** The presence of a Messinian foredeep in the centre of the Ionian basin should imply that the frontal thrust before 5 Ma was already in its present day position. Two possible scenarios can be put forward. In the first reconstruction, the accretionary complex should be about three hundred kilometres longer than the present day one, accounting for the drifting of the Calabrian Arc. A second hypothesis is that a transcurrent fault system, as the Tindari-Letojanni Fault and the Malta Escarpment, to the west (Casero & Roure, 1994), and Crati-Sangineto Line, to the east, should have translated southeastward the Messinian accretionary prism for about three hundreds kilometres. In the Ionian offshore, similar crustal structure could be recognized along the eastern border of Sicily. The extensional reactivation of the lateral ramp of the wedge opposite to the Malta escarpment represents, in fact, an existing crustal scale plate boundary with strike-slip kinematics. This lineament shows a displacement of the basement of c. 0.4 – 0.5 s TWT. The age of this lateral escape of the Calabrian Arc, with respect to Sicily (African margin), may have occurred during post-Messinian time. The main problem arising from this interpretation is the lack of post-Messinian deformation in the belt. Such deformation, in fact, should have occurred to account for the opening of the Tyrrhenian basin. Our data, in fact, show that compressive structures in the inner wedge cannot accommodate such a large contractional displacement (i.e., the one connected with the opening of the Tyrrhenian basin).

Tectonic wedge**:** This model is similar to the Mediterranean Ridge and well explains the low taper of the outer wedge. In this case, the retreat of the subducting slab and the convergence should have been accommodated by deformation in the inner wedge along several thrust planes after the Messinian salinity crisis in the outer wedge. A portion of deformation may have also been accommodated in the inner wedge by reactivating pre-existing thrust planes. This out of sequence thrusting could be related to the readjustment of the critical taper of the wedge.

The sedimentary nature of the outer wedge represents certainly an attractive and innovative idea, but needs further research for the complexity brought in the geodynamic framework of Mediterranean area. A more conservative hypothesis for the evolution of the accretionary wedge may be the following.

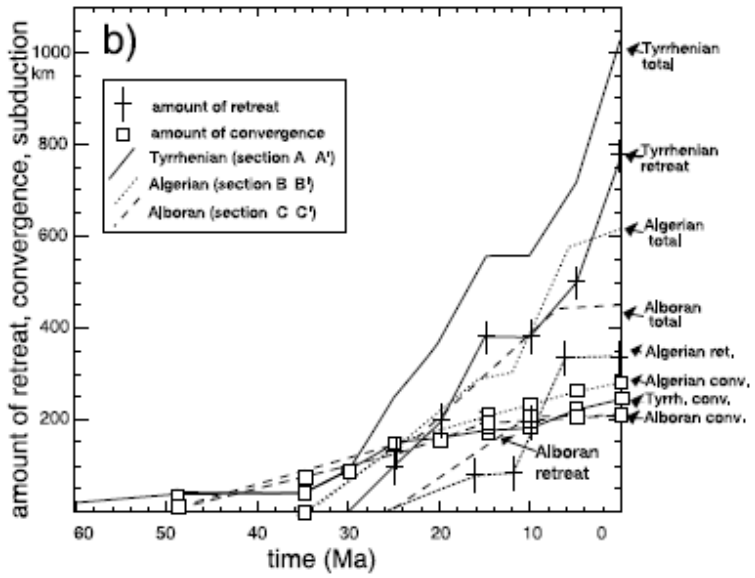

Figure 19 - Amount of relative plate convergence and back-extension calculated along the Tyrrhenian, cross-sections. The total amount of subduction is derived by summing up the amount of convergence with the amount of back-arc extension.

Summing up, the accretionary history of the Calabrian arc is characterized by several steady points: (1) the accretion of the wedge does not follow the normal rule of forward propagation, but, in Pliocene time, most of the older structures in the internal wedge have been compressionally reactivated, (2) in the meantime, near the Calabrian coasts, a forearc basin developed above the inner prism. This subsident area is closely related to the evolution of the wedge, (3) during post-Messinian time, the decollement layer moved up and become localized in the evaporitic layer, making up the outer prism.

Taking into account these preliminary remarks, we summarize the evolution of the wedge in four main stages, i.e., between 15 and 10 Ma, after the Messinian salinity crisis, after the opening of the Vavilov basin, and during recent and present times (Fig. 20).

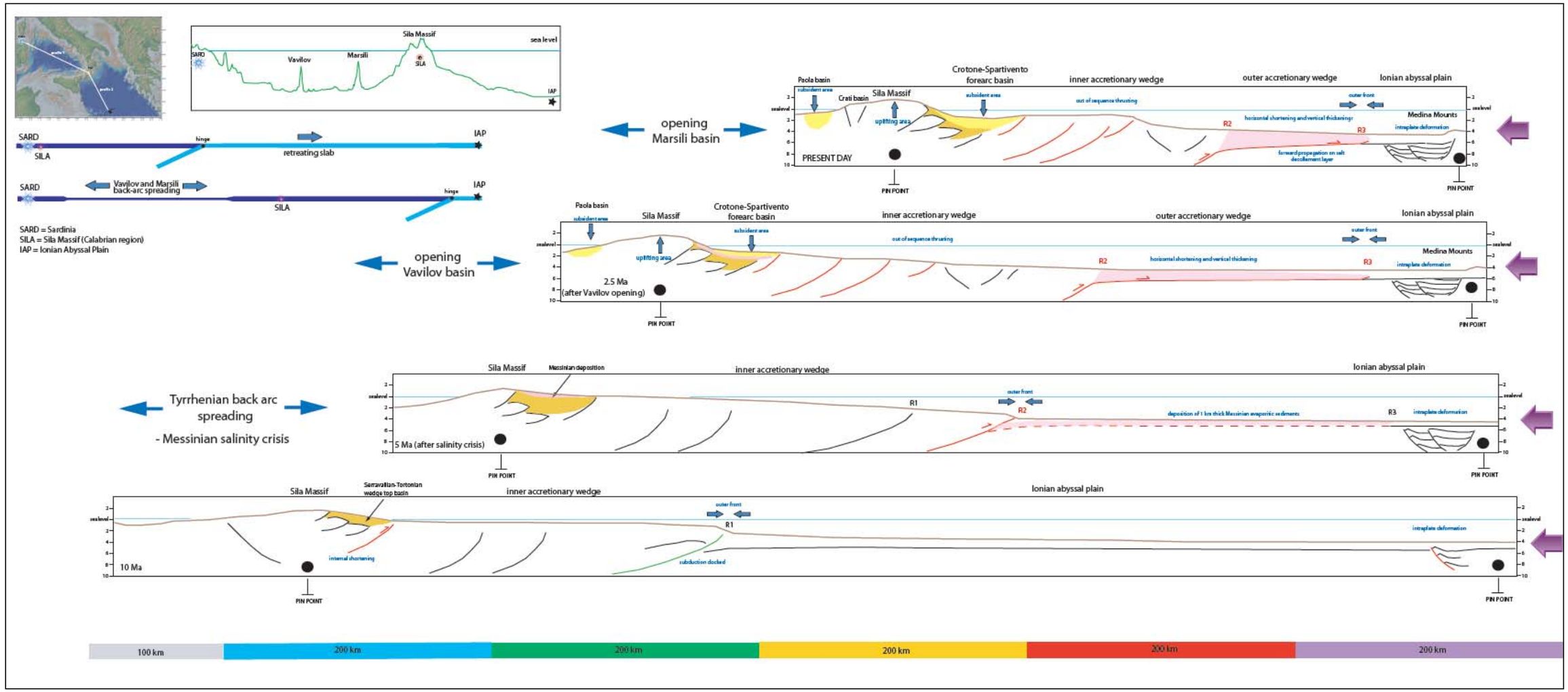

Figure 20 - Schematic time - space evolution of the Calabrian accretionary prism during the last 15 Ma. The subduction history is represented in four steps from 15 to 10 Ma, from 10 to 5 Ma (after the Messinian salinity crisis and the deposition of salt layer in the Ionian abyssal plain), from 5 to 2.5 Ma (after the opening of the Vavilov basin), and from 2.5 Ma to present day (after the opening of the Marsili basin). The evolutionary model take into account the total amount of subduction data used in previous work (Faccenna et al., 2004). In red are indicated the active structures. The green outer front at 10 Ma indicates the locked subduction. In pink are represented the Messinian sediments that constitute mainly the outer wedge. In yellow the subsident areas (Paola, and Crotone-Spartivento forearc basins).

- Phase 15-10 Ma

This time interval is characterized by a decrease of subduction with little convergence and zero retreat (Fig. 20). The opening of backarc basin is jumping from the Liguro-Provencal basin to the Tyrrhenian one. The growth of the wedge is mostly interrupted as testified by intraplate compressive deformation recognized in the Ionian abyssal plain. The shortening accommodated in these structures is about 10 km (Chamot-Rooke et al., 2005) and is comparable with the amount of shortening for this period (Fig. 20). We hypothesize that the subduction process stopped (R1 is locked), the deformation being then localized in the downgoing plate. Also, we suggest that this episode was related to the entrance in the subduction zone of continental blocks. Several out of sequence thrusts can be observed in the internal sector of the wedge as testified by the presence on top of the inner portion of the wedge of the Crotone and Rossano wedge top basin (Barone et al., 2008).

- Phase 10-5 Ma

According to Faccenna et al. (2004), during this time, the amount of convergence should be about 40 km and the amount of retreat about 100 km. The total subduction has been accommodated in the inner wedge and the accretionary complex has grown forward accreting sedimentary sequences at its toe (R1 → R2). The deformation is probably accommodated along several thrust faults. Unfortunately, from the seismic lines, we cannot distinguish the synkinematic basins induced by this deformation phase except for the Calabrian offshore shallow water area, where the structure of Luna field formed in late Tortonian times (Roveri et al., 1992).

- Phase 5 Ma – present

After the Messinian salinity crisis and the deposition in the Ionian abyssal plain of no more than 1 km of Messinian sediments, the foreland propagation of the accretionary complex develop using the base of the Messinian deposits as the main decollement. At this time, we observe a fast forward propagation of the outer deformation front favoured by the presence of weak decollement layers. After the outer propagation and incorporation of Messinian sediments, the outer wedge starts to be deformed by internal shortening and vertical thickening. The deformation (note that convergence should be about 20 km and retreat about 280 km connected with the opening of Vavilov and Marsili basins) occurred in the outer wedge for a maximum of 200 km. The remaining 100 km were possibly accommodated in the inner wedge by reworking previous structures. We suggest that the 100 km of shortening accommodated in the inner wedge represents the total spreading of the Marsili basin occurred between 2.1 – 1.6 Ma at an ultrafast velocity (Nicolosi et al., 2006). Due to the high strain rate, it is likely that deformation was localized in the inner wedge. On the other hand, slow convergence rates produce above a weak decollement the progressive forelandward propagation of the deformation front. This suggests that, at fast convergence rates, the basal decollement (i.e. a low viscosity/strength zone) does not

propagate outwards during wedge growth (Rossetti et al., 2000). Fast convergence produce also steep surface taper and localised deformed area. This suggests also that the growth of the outer wedge may have occurred during periods of slow subduction rates.

In the same time the reactivation of the internal thrust can also be related to a readjustment of the taper of the wedge due to the lowering of topographic slope and increase of total length of the wedge owing to fast foreward propagation on the Messinian decollement (Fig. 21). This forward propagation and lengthening of the wedge created the spaces and the subsequent subsidence of the inner sector of the wedge that became localized in the Plio-Quaternary Crotone-Spartivento forearc basin. The timing of the subsidence in the basin is marked by the deposition of undeformed Plio-Quaternary sequence on top of Messinian unconformity. In the same time also on the other side of the Sila Massif we observe the onset of subsidence (Paola basin).

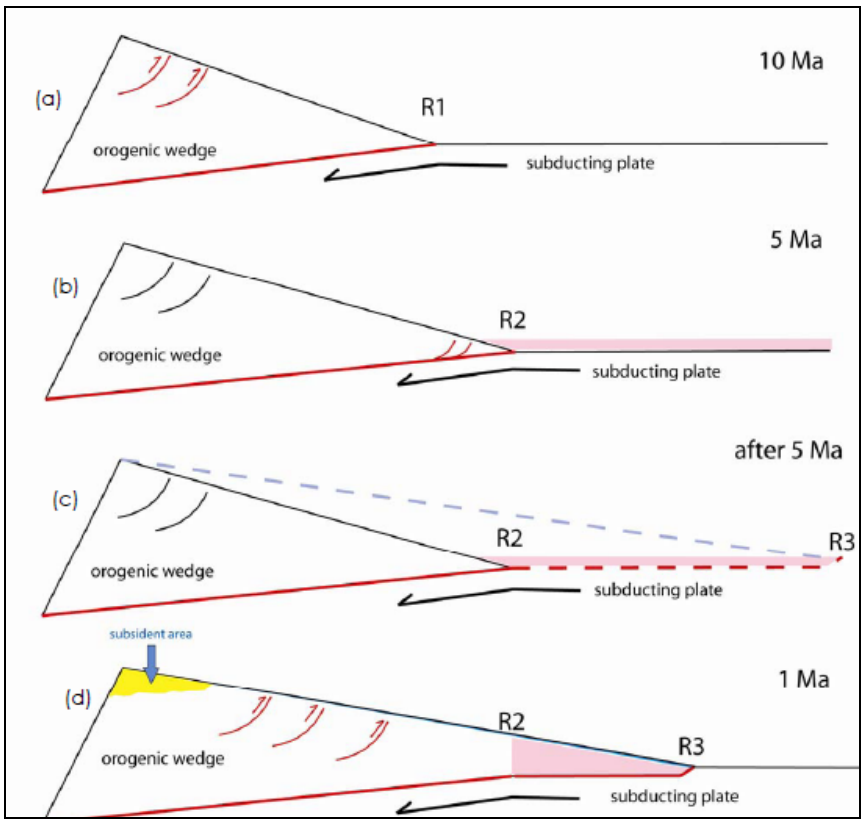

Figure 21 – Conceptual evolutionary model of the Calabrian accretionary prism from 10 Ma to 1 Ma ago. In pink the deposition of Messinian sediments (b), subsequently incorporated and ductile deformed in the outer wedge (c) and (d). Forearc subsident area in yellow (d). The figure is not in scale.

9. Conclusions

Main conclusions and products from the analysis of a large set of seismic reflection profiles in the Ionian offshore are as follows:

- A complete structural map of the Ionian offshore based on a dense grid of seismic profiles, which allowed an accurate location and drawing of all mapped structures over the entire basin.
- For the first time, geometry and kinematics of the Calabrian accretionary prism are defined. In particular, four major structural domains are recognized and depicted by considering their stratigraphy, style and time of deformations, and internal seismic characters. The recognized domains are the following ones: the Crotone- Spartivento foreland basin, the inner accretionary prism, the outer accretionary prism, and the foreland basin.
- Definition of time-space evolution of the Calabrian accretionary prism during the last 15 Ma. The growth of the prism included both forward propagation stages characterized by frontal accretion, and out-of-sequence internal thrusting. In addition to the rheology of the prism, the prism growth was mostly controlled by two main external factors: (1) the presence of a thick evaporitic deposit, which allowed the fast propagation of the prism by using the evaporitic deposit as the main decollement. The involvement of the evaporitic deposit in the accretionary prism reduced, in turn, its critical taper, thus resuming deformation at the rear of the wedge; (2) the dynamic of the subduction system including, in particular, the temporal evolution and velocity of the southeastward retreat of the slab and the associated opening of the two back arc basins.

Main limits of this work are as follows:

- Except for several wells in the shallow water area near the coasts, few dredges and gravity/piston cores, and the DSDP 374 drill in the Ionian abyssal plain, the substantial lack of stratigraphic constraints, in particular, in the inner sector of the prism, did not allow a detailed tectonostratigraphic reconstruction of the prism.
- The lack of high-resolution seismic profiles did not allow us to understand the present-day activity of the subduction process.

Main open questions are as follows:

- It is unknown whether the subduction is presently active and, if so, where the compressional displacements are being accommodated. Moreover, a clear structure acting as frontal thrust has not been recognized yet. To clarify these issues, a set of high-resolution seismic profiles is necessary.

• The Southern Apennines and the Calabrian arc fold-and-thrust belts are presently not linked. The southern prolongation of the Apulian Ridge, westward bounded by the Apulian escarpment, is not involved in the compressional deformation and constitutes the boundary between the two fold-and-thrust belts. It follows that further studies are necessary to better define this complex tectonic area at the junction between the Southern Apennines and the Calabrian arc fold-and-thrust belts.

• The nature of the outer wedge, i.e., sedimentary or tectonic, is questionable and should be further investigated. Only direct analysis (drilling) shall clarify this issue.

REFERENCES

Adam J., Reuther C.-D., Grasso M. & Torelli, L., 2000. Active fault kinematics and crustal stresses along the Ionian margin of southeastern Sicily. Tectonophysics, 326, 3-4, 273-288.

Amodio Morelli L., Bonardi G., Colonna V., Dietrich D., Giunta G., Ippolito F., Liguori V., Lorenzoni S., Paglionico A., Perrone V., Piccarreta G., Russo M., Scandone P., Zanettin-Lorenzoni, Zuppetta E.A., 1976. L'Arco Calabro- Peloritano nell'orogene Appenninico-Maghrebide. Memorie della Società Geologica Italiana, 17, 1-60.

Argnani A. and Bonazzi C., 2005. Malta escarpment fault zone offshore eastern Sicily: Pliocene- Quaternary tectonic evolution based on new multichannel seismic data. Tectonics, 24, TC4009, doi:10.1029/2004TC001656.

Argnani A., 2002, Tectonics of eastern Sicily offshore: Preliminary results from the MESC 2001 marine seismic cruise, Boll. Geofis. Teor. Appl., 43(3– 4), 177–193.

Argus, D. F., R. G. Gordon, C. DeMets, and S. Stein, 1989. Closure of the Africa-Eurasia-North American plate motion circuit and tectonics of the Gloria fault, J. Geophys. Res., 94, 5585–5602.

Aris Rota F, Fichera R., 1985. Magnetic interpretation connected to ‘‘Geo-Magnetic Provinces’’: The Italian case History. In: 47_ Meeting EAEG, 4–7 June, Budapest-Hungary.

Barbieri F., Morlotti E., Poerio L. & Torelli L., 1982. Dati geologici preliminari sul Bacino di Crotone- Spartivento (Mar Ionio). Ateneo Parmense, Acta Naturalia, 18, 141-155.

Barone A., Fabbri A., Rossi S. and Sartori R., 1982. Geological Structure and Evolution of the Marine Areas Adiacent to the Calabrian Arc. Earth. Ev. Sc., 3, 207-221.

Bianca M., Monaco C., Tortorici L. & Cernobori L., 1999. Quaternary normal faulting in southeastern Sicily (Italy): a seismic source for the 1693 large earthquake. Geophys. J. Int., 139, 370-394.

Biju-Duval B., Dercourt J. and Le Pichon X., 1977. From the Tethys Ocean to the Mediterranean Seas: a plate tectonic model of the evolution of the western Alpine system, in Biju-Duval, B. and Montadert, L. (eds.): Structural History of the Mediterranean Basins (Sympos).

Biju-Duval B., Morel Y., Baudrimont A., Bizon G., Bizon J.J., Borsetti A.M., Burollet P.F., Clairefond P., Clauzon G., Colantoni P., Mascle G., Montadert L.. Perrier R., Orsolini P., Ravenne C., Taviani M. and Winnock E., 1982. Donnés nouvelles sur les marges du bassin Ionien profond (Mediterranee Orientale). Resultats des campagnes Escarmed, Revue Inst. France Petrole 37, 713–731.

Billi A., Barberi G., Faccenna C., Neri G., Pepe F., Sulli A., 2006. Tectonics and seismicity of the Tindari Fault System, southern Italy: Crustal deformations at the transitino between ongoing contractional and extensional domains located above the edge of a subducting slab. Tectonics, 25, doi:10.1029/2004TC001763.

Bizon G., Bizon J.J., Biju-Duval B., Borsetti A., Burollet P.F., Colantoni P., Mascle G., Morel Y., Tixier M., 1983. Données nouvelles sur le Néogène et le Quaternaire des escarpements ioniens (Méditerranée Orientale), Revue de l'Institut Francais du Pétrole, 38, 5, 575-603.

Boccaletti M., Nicolich R., Tortorici L., 1984. The Calabrian Arc and the Ionian Sea in the dynamic evolution of the central Mediterranean. Marine Geology, 55, 219-245.

Boccaletti M., Ciaranfi N., Cosentino D., Deiana G., Gelati R., Lentini F., Massari F., Moratti G., Pescatore T., Ricci Lucchi F. and Tortorici L., 1990. Palinspastic restoration and paleogeographic reconstruction of the peri-Tyrrhenian area during the Neogene. Palaeogeography, Palaeoclimatology, Palaeoecology, 77, 41-50.

Bosellini, A. 2002. Dinosaurs ''re-write'' the geodynamics of the eastern Mediterranean and the paleogeography of the Apulia Platform. Earth-Sci. Rev. 59, 211–234.

Casero, P., Cita, M.B., Croce, M., and De Micheli, A., 1984. Tentativo di interpretazione evolutiva della scarpata di Malta basata su dati geologici e geofisici, Mem. Soc. Geol. It. 27, 233–253.

Casero, P., Roure, F., 1994. Neogene deformations at the Sicilian– North African plate boundary. In: Roure, F. (Ed.), Peri-Tethyan Platforms. Ed. Technip, Paris, pp. 27– 50.

Catalano R., Doglioni C. and Merlini S., 2001. On the Mesozoic Ionian Basin, Geophys. J. Int., 144, 49–64.

Catalano R., Franchino A., Merlini S., and Sulli A., 2000. A crustal section from the Eastern Algerina basin to the Ionian ocean (Central Mediterranean), Mem. Soc. Geol. It., 55, 71 – 85.

Cavazza W., De Celles P.G., 1998. Upper Messinian siliciclastic rocks in southeastern Calabria (southern Italy): palaeotectonic and eustatic implications for the evolution of the central Mediterranean region. Tectonophysics, 298, 223-241.

Cernobori L., Hirn A., McBride J.H., Nicolich R., Petronio L., Romanelli M., the Streamers-Profiles Working Group, 1996. Crustal image of the Ionian basin and its Calabrian margin. Tectonophysics, 264, 175-189.

Chamot-Rooke et al., 2005. DOTMED, A synthesis of deep marine data in the Eastern Mediterranean. Mémoires de la Société géologique de France, n.s., n° 177.

Chapple W.M., 1978. Mechanics of thin-skinned fold-and-thrust belts. Geol. Soc. Am. Bull., 89, 1181-1198.

Chaumillon E., Mascle J., Hoffmann H.J., 1996. Deformation of the western Mediterranean Ridge : Importance of Messinian evaporitic formations. Tectonophysics, 263, 163-190.

Chiarabba C., De Gori P., Speranza F., 2008. The southern Tyrrhenian subduction zone: Deep geometry, magmatism and Plio-Pleistocene evolution. Earth and Planetary Science Letters, 268, 408-423.

Costa E., Camerlenghi A., Polonia A., Cooper C., Fabretti P., Mosconi A., Murelli P., Romanelli M., Sormani L., Wardell N., 2004. Modeling deformation and salt tectonics in the eastern Mediterranean Ridge accretionary wedge. GSA Bulletin, 116, n° 7/8, 880-894.

Costa E., Vendeville B.C., 2002. Experimental insights on the geometry and kinematics of fold-and-thrust belts above weak, viscous evapori tic décollement. Journal of structural geology, 24, 1729-1739.

D'Agostino, N., and G. Selvaggi (2004), Crustal motion along the Eurasia-Nubia plate boundary in the Calabrian Arc and Sicily and active extension in the Messina Straits from GPS measurements, J. Geophys. Res., 109, B11402, doi:10.1029/ 2004JB002998.

Davis D.M., Suppe J., Dhalen A., 1983. Mechanics of fold-and-thrust belts and accretionary wedges. Journal of Geophysical Research, 88, 1153-1172.

Davis D.M., Engelder T., 1987. Thin-skinned deformation over salt. In: Lerche I., O'Brien J.J. (Eds.). Dynamical Geology of Salt and Related Structure. Academic Press, London, 301-337.

Dhalen F.A., Suppe J., Davis D., 1984. Mechanics of fold-and-thrust belts and accretionary wedges: cohesive Coulomb theory. Journal of Geophysical Research, 89, 10087-10101.

De Mets, C., R. G. Gordon, D. F. Argus, and S. Stein (1994), Effect of recent revisions to the geomagnetic reversals time scale on estimates of current plate motions, Geophys. Res. Lett., 21, 2191– 2194.

De Voogd B., Truffert C., Chamot-Rooke N., Huchon P., Lallemant S., and Le Pichon X., 1992. Twoship deep seismic soundings in the basins of the Eastern Mediterranean Sea (Pasiphae cruise), Geophys. J. Int., 109, 536–552.

Della Vedova B. & Pellis G., 1992. New heat flow density measurements in the Ionian sea. Atti VIII Convegno GNGTS, Roma, 1133-1145.

Dewey J.F., Helman M.L., Torco E., Hutton D.H.W., Knott S., 1989. Kinematics of the Western Mediterranean, in Alpine Tectonics, edited by M.P. Coward and D. Dietrich, Geol. Soc. Spec. Publ., 45, 265-283.

Doglioni C., Merlini S., Cantarella G., 1999. Foredeep geometries at the front of the Apennines in the Ionian Sea (central Mediterranean), Earth and Planetary Science Letters, 168, 243-254.

Emeis K.C., Robertson A.H.F., Richter C., et alii, 1996. Site 963. In: Proceedings of the Ocean Drilling Program. Initial reports, 160, 55-84.

Emery K.O., Heezen B.C. and Allan T.D., 1966. Bathymetry of the eastern Mediterranean Sea. Deep Sea Res, 13, 173-192.

Fabbri A., Rossi S., Sartori R., Barone A., 1982. Evoluzione neogenica dei margini marini dell'Arco Calabro-Peloritano: Implicazioni geodinamiche, Mem. Soc. Geol. It., 24, 357-366.

Faccenna C., Funiciello F., Giardini D. and P. Lucente, 2001. Episodic back-arc extension during restricted mantle convection in the Central Mediterranean, Earth and Planetary Science Letters, 187, 105-116.

Faccenna, C., F. Funiciello, D. Giardini, and F. P. Lucente (2001b), Episodic back-arc extension during restricted mantle convection in the central Mediterranean, Earth Planet. Sci. Lett., 87, 105– 116.

Faccenna C., Piromallo C., Crespo-Blanc A., Jolivet L., Rossetti F., 2004. Lateral slab deformation and the origin of the western Mediterranean arcs. Tectonics, 23, TC1012, doi:10.1029/2002TC001488.

Ferrucci F., Gaudiosi, G., Hirn, A., Nicolich R., 1991. Ionian basin and calabrian arc: some new element from DSS data. Tectonophysics, 195, 411-419.

Finetti, I., 1985. Structure and evolution of the central Mediterranean (Pelagian and Ionian Seas). In: Stanley, D.J., Wezel, F.C. (Eds.), Geological Evolution of the Mediterranean Basin. Springer, New York, pp. 215 230.

Finetti, I., Del Ben, A., 2000. Crustal stratigraphy and tectono-dynamics of the Pelagian Sea region from new ''CROP'' seismic data. Geology of Northwest Libya, Second Symp., Abstracts, Tripoli, 42.

Finetti I. and Morelli C., 1973. Geophysical exploration of the Mediterranean Sea. Boll. Geof. Teor. Appl., 15, 263–340.

Finetti I., 1982. Structure, stratigraphy and evolution of Central Mediterranean. Boll. Geof. Teor. Appl., 247–426.

Finetti I., Lentini F., Carbone S., Catalano S., Del Ben A., 1996. Il sistema Appenninico Meridionale – Arco Calabro– Sicilia nel Mediterraneo Centrale: studio geofisico–geologico. Boll. Soc. Geol. Ital. 115, 529–559.

Finetti, 1976. Mediterranean Ridge: a young submerged chain associated with the Hellenic Arc. Bull. Geol. Teor. Appl., 28, 69, 31-62.

Goes, S., D. Giardini, S. Jenny, C. Hollenstein, H. G. Kahle, and A. Geiger (2004), A recent tectonic reorganization in the south-central Mediterranean, Earth Planet. Sci. Lett., 226, 335 – 345.

Govers, R., Wortel, M.J.R., 2005. Lithosphere tearing at STEP faults: response to edges of subduction zones. Earth Planet. Sci. Lett. 236, 505–523.

Gueguen E., Doglioni C. and Fernàndez M., 1998. On the post-25 Ma geodynamic evolution of the Western Mediterranean. Tectonophysics, 298, 259-269.

Hersey J.B., 1965. Sedimentary basins of the Mediterranean Sea. Submarine Geology and Geophysics, Proceed. XVII Symp. Colston Res. Soc., Butter worths, London, 75-91.

Hieke W., Cita M.B., Forcella F., Muller C., 2006. Geology of the Victor Hensen Seahill (Ionian Sea, Eastern Meditteranean): insight from the study of cored sediment sequences. Bollettino della Società Geologica Italiana, 125(2), 245-257.

Hieke, W., Hirschleber, H., Dehghani, G. A., 2003. The Ionian Abyssal Plain (central Mediterranean Sea): Morphology, subbottom structures and geodynamic history - an inventory. Marine Geophysical Researches, 24, 279-310.

Hieke W. & Wanninger A., 1985. The Victor Hensen seahill (central Ionian sea): morphology and structural aspects. Marine Geology, 64, 343-350.

Hieke W., 2000. Transparent layers in seismic reflection records from the central Ionian Sea (Mediterranean) – evidence for repeated catastrophic turbidite sedimentation during the Quaternary. Sedimentary Geology, 135, 89-98.

Hinz, K., 1974, Results of seismic refraction and seismic reflection measurements in the Ionian Sea, Geol. Jb. E 2, 33–65.

Hirn A., Nicolich R., Gallart J., Laigle M., Cernobori L., and ETNASEIS Scientific Group, 1997. Roots of Etna volcano in faults of great earthquakes, Earth Planet. Sci. Lett. 148, 171-191.

Hollenstein Ch., Kahle H.G., Geiger A., Jenny S., Goes S., Giardini D., 2003. New GPS constraints on the Africa-Eurasia plate boundary zone in southern Italy. Geophysical Research Letters, 30, 18, doi:10.1029/2003GL017554.

Holton J., 1999. Apennines productive sequences identified off southern Italy. Oil & Gas Journal, 97, 51.

Hsü K.J., Montadert, L., Bernoulli, D., Bizon, G., Cita, M.B., Erickson, A., Fabricius, F., Garrison, R.E., Kidd, R.B., Melieres, F., Muller, C. and Wright, R.C., 1978, Site 374: Messina Abyssal Plain, in Hsu¨ , K.J., Montadert, L. et al., Init. Rep. DSDP XLII, (part 1) 175–217.

Ismail-Zadeh, A.T., Nicolich, R., Cernobori, L., 1998. Modelling of geodynamic evolution of the Ionian Sea basin. Comput. Seismol. Geodyn. 30, 32– 50.

Jolivet, L., Faccenna, C., Goffé, B., Mattei, M., Rossetti, F., Brunet, C., Storti, F., Funiciello, R., Cadet, J.P., Parra, T., 1998. Mid-crustal shear zones in post-orogenic extension: the northern Tyrrhenian Sea case. J. Geophys. Res. 103 (B6), 12123–12160.

Kahle H.G., Muller M.V., Muller S., Veis G., 1993. The Kephalonia transform fault and the rotation of the Apulian platform: evidence from satellite geodesy. Geophysical Research Letters, 20, 651-654.

Kastens K.A., Nancy A.B. and Cita M.B., 1992. Progressive deformation of an evaporates-bearing accretionary complex: Sea-Marc I, SeaBeam and Piston core observations from the Mediterranean Ridge. Mar. Geophys. Res., 14, 249-298.

Kehle R.O., 1970. Analysis of gravity sliding and orogenic translation. Geological Society of American Bulletin, 81, 1641-1663.

Kukowski N., Lallemand S.E., Malavieille J., Gutscher M.A., Reston T.J., 2002. Mechanical decoupling and basal duplex formation observed in sandbox experiments with application to the Western Mediterranean Ridge accretionary complex. Marine Geology, 186, 29-42.

Le Pichon, X., Lyberis, N., Angelier, J., Renard, V., 1982. Strain distribution over the East Mediterranean Ridge: a synthesis incorporating new sea-beam data. Tectonophysics 86, 243-274.

Lucente, F. P., C. Chiarabba, G. B. Cimini, and D. Giardini, Tomographic constraints on the geodynamic evolution of the Italian region, J. Geophys. Res., 104, 20,307– 20,327, 1999.

Makris J., Nicolich R. and Weigel W., 1986. A seismic study in the western Ionian Sea, Annales Geophysicae 4B, 665–678.

Mattei M., Cifelli F., D'Agostino N., 2007. The evolution of the Calabrian Arc: Evidence from paleomagnetic and GPS observations. Earth and Planetary Sciences, 263, 259-274.

Malinverno A. & Ryan W.B.F., 1986. Extension in the Tyrrhenian Sea and shortening in the Apennines as result of arc migration driven by sinking of the lithosphere. Tectonics, 5, 227-245.

Mele, G., A. Rovelli, D. Seber, T. M. Hearn, and M. Barazangi,1998. Compressional velocity structure and anisotropy in the uppermost mantle beneath Italy and surrounding regions, J. Geophys. Res., 103, 12,529 – 12,543.

Monaco C., Tapponier P., Tortorici L. and Gillot P.Y., 1997. Late Quaternary slip rates on the Acireale–Piedimonte normal faults and tectonic origin of Mt Etna (Sicily). Earth and Planetary Science Letters, 147, 125–139.

Montandert et al., 1978. Messinian event. Seismic evidence. Initial report of the Deep Sea Drilling Project, 42, 1037-1048.

Montuori, C., Cimini, G.B., Favali, P., 2007. Teleseismic tomography of the southern Tyrrhenian subduction zone: new results from seafloor and land recordings. J. Geophys. Res. 112. doi:10.1029/2005JB004114.

Morelli C., Pisani M., Gantar C., 1975. Bathymetric, gravity and magnetism in the Strait of Sicily and in the Ionian Sea. Boll. Geof. Teor. Appl., 17, 39-58.

Morlotti, E., Sartori, R., Torelli, L., Barberi, F. and Raffi, I., 1982. Chaotic deposits from the External Calabrian Arc (Ionian Sea, Eastern Mediterranean), Mem. Soc. Geol. It. 24 (1982), 261–275.

Mostardini, F., Merlini, S., 1986. Appennino centro-meridionale: sezioni geologiche e proposta di modello strutturale. Mem. Soc. Geol. Ital. 35, 177– 202.

Müller J., Hieke W. and Fabricius F., 1978. Turbidites at site 374: their composition, provenance and paleobathymetric significance. In: Hsü K.J., Montadert L., et alii, Init. Repts DSDP, 42, 397-400.

Nicolich R., Laigle M., Hirn A., Cernobori L., and Gallart J., 2000. Crustal structure of the Ionian margin of Sicily: Etna volcano in the frame of regional evolution. Tectonophysics, 329, 121– 139.

Nicolosi I., Speranza F., Chiappini M., 2006. Ultrafast oceanic spreading of the marsili basin, southern Tyrrhenian Sea: Evidence from magnetic anomaly analysis. Geology, 34, 9, 717-720.

Patacca E., Scandone P., 1989. Post-Tortonian mountain building in the Apennines. The role of the passive sinking of a relic lithospheric slab. In: Boriani, A., Bonafede, M., Piccardo, G.B., Vai, G.B. (Eds.), In: The Lithosphere in Italy, Accad. Naz. Lincei., vol. 80, pp. 157–176.

Patacca, E., R. Sartori, and P. Scandone (1990), Tyrrhenian basin and Apenninic arcs. Kinematic relations since late Tortonian times, Mem. Soc. Geol. Ital., 45, 425–451.

Piromallo C. & Morelli A., 2003. P wave tomography of the mantle under the Alpine Mediterranean area. J. Geophys. Res., 108, 2065, doi:10.1029/2002JB001757.

Platt J.P., 1986. Dynamics of orogenic wedges and the uplift of high-pressure metamorphic rocks. Geological Society of American Bulletin, 97, 1037-1053.

Polonia A., Camerlenghi A., Davey F. and Storti F., 2002. Accretion, structural style and syncontractional sedimentation in the Eastern Mediterranean Sea. Marine Geology, 186, 127-144.

Rehault J.P., Mascle J., Boillot G., 1986. Evolution géodynamique de la Méditerranée depuis l'Oligocène, Mem. Soc. Geol. It., 27, 85-96.

Reston T. J., Fruehn J., Huene R., 2002. The structure and evolution of the western Mediterranean Ridge . Marine Geology 186, 1-2, 83-110.

Ricci Lucchi F., 1986. The Oligocene to Recent foreland basins of the northern Apennines, Spec. Publ. Int. Assoc. Sedimentol., 8, 105-140.

Rossetti F., Goffé B., Monié P., Faccenna C., Vignaroli G., 2004. Alpine orogenic PTt deformation history of the Catena Costiera area and surrounding regions (Calabrian Arc, southern Italy): the nappe edifice of Northern Calabria revised with insights on the Tyrrhenian–Apennine system formation. Tectonics, 23, 1-26.

Rossi, S., Borsetti, A.M., 1974. Dati preliminari di stratigrafia e di sismica del Mare Ionio settentrionale. Mem. Soc. Geol. Ital. 13, 251– 259.

Rossi S., Auroux C., Mascle, J., 1983. The gulf of Taranto (southern Italy): seismic stratigraphy and shallow structure. Mar. Geol., 51, 327-346.

Rossi S., and Sartori R., 1981. A seismic reflection study of the external Calabrian Arc in the northern Ionian Sea (eastern Mediterranean). Mar. Geophys. Res., 4, 403 – 426.

Roveri M., Bernasconi A., Rossi M.E., Visentin C., 1992. Sedimentary evolution of the Luna Field Area, Calabria, Southern Italy. Generation, Accumulation, and Production of Europe's Hydrocarbons (Edited by Spencer A.M.), Europ. Assoc. Petrol. Geosci., Spec. Publ., 2, 217-224.

Ryan W.B.F., Cita M.B., 1978. The nature and distribution of Messinian erosional surfaces – indicators of several kilometer deep Mediterranean in the Miocene. Mar. Geol., 27, 193-230.

Ryan, W. B. F. and B. C. Heezen 1965, Ionian Sea submarine canyons and the 1908 Messina turbidity current, *Geol. Soc. Am. Bull.*, *76*, 915-932.

Ryan W.B.F., 1969. The stratigraphy of the Eastern Mediterranean, PhD tesi, Columbia University, New York.

Ryan W.B.F., Hsü K.J., et alii, 1973. Initial Reports of the Deep Sea Drilling Project, Government Printing Office, Washington, 13, 517-1447.

Sartori R., Colalongo M.L., Gabbianelli G., Bonazzi C., Carbone S., Curzi P., Evangelisti D., Grasso M., Lentini F., Rossi S., Selli L., 1991. Note stratigrafiche e tettoniche sul "Rise di Messina" (Ionio nord occidentale)", Giornale di geologia, 53(2), 49-64.

Scandone, P., Patacca, E., Radoicic, R., Ryan, W.B.F., Cita, M.B., Rawson, M., Chezar, H., Miller, E., McKenzie, J. and Rossi, S., 1981, Mesozoic and Cenozoic rocks from Malta Escarpment (Central Mediterranean), Amer. Assoc. Petrol. Geol. Bull. 65, 1299–1319.

Selvaggi G., Chiarabba C., 1995. Seismicity and P-wave velocità image of the Southern Tyrrhenian subduction zone. Geophys. J. Int. 121, 818-826.

Sioni, 1996. Mer Ionienne et Apulie depuis l'overture de l'Ocean Alpin. PhD tesi.

Tortorici L., Monaco C., Tansi C. & Cocina O., 1995. Recent and active tectonics in the Calabrian arc (Southern Italy). Tectonophysics, 243, 37-55.

Truffert C., Chamot-Rooke N., Lallemant S., de Voogd B., Huchon P., Le Pichon X., 1993. The crust of the Western Mediterranean Ridge from deep seismic data and gravity modelling. Geophysical Journal International 114, 360–372.

Turner J.P., Williams G.A., 2004. Sedimentary basin inversion and intra-plate shortening. Earth-Science Reviews, 65, 277-304.

Weijermars R., Jackson M.P.A., Vendeville B.C., 1993. Rheological and tectonic modelling of salt provinces. Tectonophysics, 217, 143-174.

Wortel M. J. R. and Spakman W., 2000. Subduction and Slab Detachment in the Mediterranean- Carpathian Region. Science, 290, 1910-1917.

Ziegler P.A., van Wees J.D., Cloetingh S., 1998. Mechanical controls on collision-related compressional intraplate deformation. Tectonophysics, 300, 103-129.

Ziegler P.A., 1987. Late Cretaceous and Cenozoic intra-plate compressional deformations in the Alpine foreland – a geodynamic model. Tectonophysics, 137, 389-420.

Abstract

The eastern side of the Sila Massif, in the northern Calabria-Peloritani Arc (Italy), provides the opportunity to examine the age and the deformational style, both onshore and offshore, of a pre-Messinian growing phase of the Calabrian accretionary wedge. Stack of thrust sheets involving both basement units (Sila and Longobucco Unit) and syn-orogenic Aquitanian sediments (Paludi Formation) have been observed, in the internal sector of the wedge, from geological survey and well log data. Post-orogenic sediments (Rossano and Crotone Basin) have been partially involved in deformation, only in more recent time, and the structures are visible in the Ionian offshore. Apatite fission track analyses performed on the basement rocks (Sila unit) indicate that basement exhumed above the partial annealing zone in a time spans from 18 to 13 Ma.

1. Introduction

The Calabria-Peloritani Arc (CPA) represents a narrow orogenic segment, characterized by the occurrence of Alpine HP-rocks sandwiched between pre-Alpine or non-metamorphic units, then covered by post-orogenic transgressive sedimentary deposits. It defines a key sector of the western Mediterranean dynamics characterized by the subduction of the Liguro-Piedmont and Ionian basins in a setting of general African and European plate convergence (e.g. Amodio-Morelli et al., 1976; Van Dijk et al., 2000; Bonardi et al., 2001 and references therein). The present-day position of the CPA is attributed to the general retreat of the subducting slab, followed by foreword migration of the sedimentary domain of the Apennine-Maghrebian thrust-belt system, since the Late Eocene, accomplished with opening of two back-arc basins (Liguro-Provencal and the Tyrrhenian) and partial oceanization of the Tyrrhenian one (e.g. Dewey et al., 1989; Faccenna et al., 2001; Rosenbaum & Lister, 2004) (Fig. 1a). Both metamorphic and non metamorphic rocks crop out in the CPA, grouped into three main complexes. From top to bottom, these are (e.g. Dubois, 1970; Ogniben, 1976; Amodio Morelli et al., 1976; Acquafredda et al., 1994): (i) the Calabride Complex (pre-Alpine metamorphic and igneous rocks with their Meso-Cenozoic covers); (ii) the Liguride Complex (Jurassic to Early Cretaceous ophiolitic sequences), and (iii) the Apennine Chain (Meso-Cenozoic dominantly carbonatic sequences). All these units show different distribution and thickness throughout the CPA (e.g. Bigi et al., 1990; Bonardi et al., 2001; Messina et al., 2004). The crystalline units, although diffuse in all the CPA, and oceanic rocks belonging to the Liguro-Piedmont domain cropping out in circumscribed tectonic units, are juxtaposed on top of the sedimentary units belonging to the Apenninic-Maghrebian Chain by regional-scale tectonic structures, responsible for this complex stacking (e.g. Cello et al., 1996; Rossetti et al., 2004).

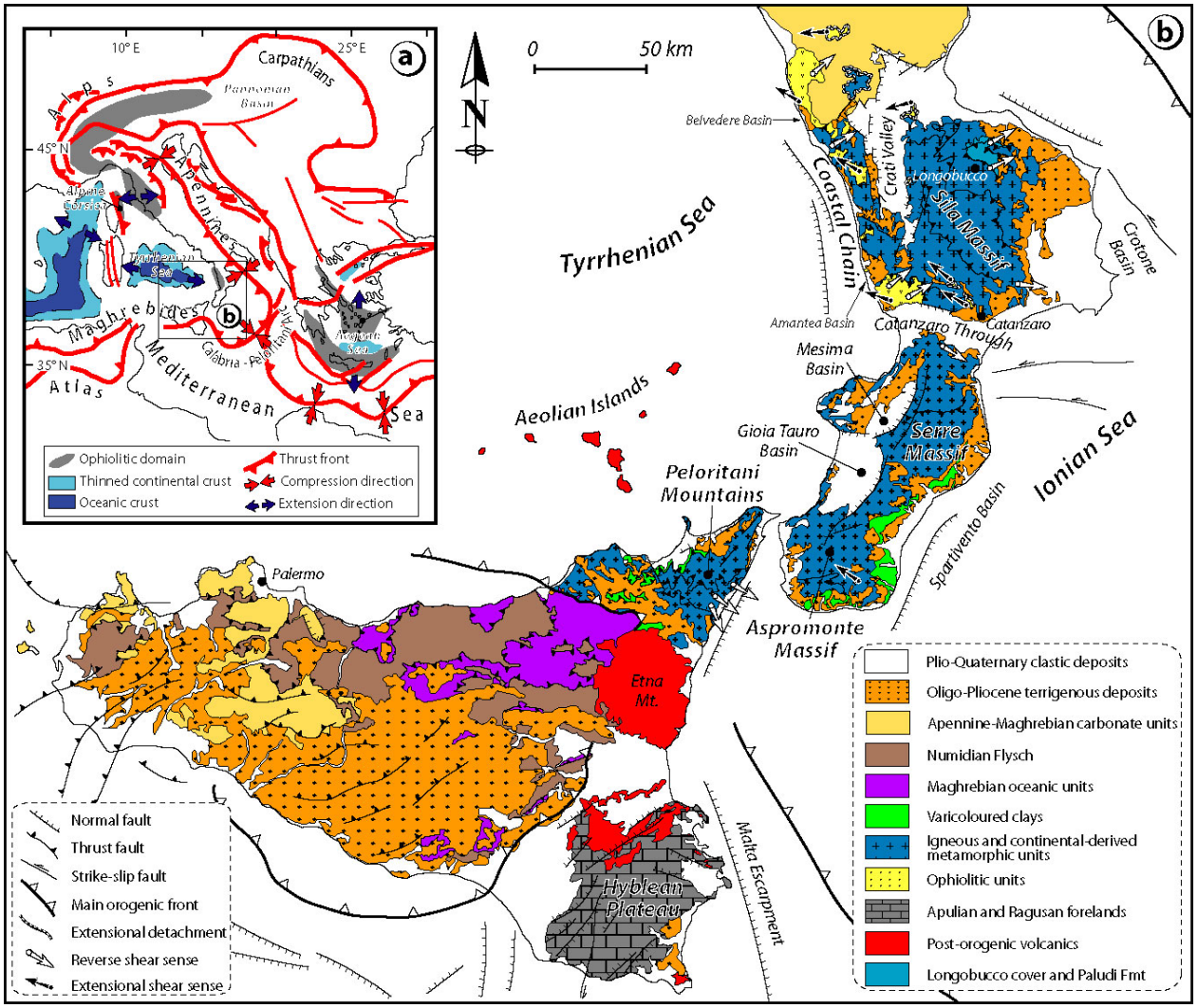

Figure 1 - a) Schematic tectonic map of the central Mediterranean region illustrating the trend of the main Alpine thrust fronts and the location of back-arc extensional domains (modified after Jolivet et al., 1998). b) Geological map of the Calabria-Peloritani Arc showing the main ductile and brittle tectonic features described in both metamorphic and non-metamorphic domain (modified after Bigi et al., 1990 and Cifelli et al., 2004). Reverse shear senses are from: Rossetti et al., 2001, 2004 (Coastal Chain and central Sila Massif); Langone et al., 2006 (Serre Massif); Heymes et al., 2008 (Apromonte Massif); Cirrincione & Pezzino, 1994, Giunta & Somma, 1996 and Vignaroli et al., 2008 (Peloritani Mountains); this study (eastern Sila Massif). Extensional shear senses are from: Rossetti et al., 2201, 2004 (Coastal Chain and central Sila Massif); Heymes et al., 2008 (Apromonte Massif).

Our contribution is based on a structural geological study integrated with apatite fission track (AFT) analysis performed in the eastern sector of the Sila Massif (Calabria region; Fig. 1), where pre-Alpine basement derived units are stacked to form the upper portion of the Calabrian accretionary wedge. Our data are finalised to reconstruct the geometry and the timing of the thrusting process in the upper levels and internal portion of the Calabrian orogenic wedge, visible only on land and in shallow water sector. Offshore and onshore data have been merged. The onshore setting was interpreted by correlating the surface and sub-surface geological

information. Then, with the review and integration of published geochronology and tectonic scenarios for the other tectonic units, we propose a snapshot sequence for the dynamics of the Calabria-Peloritani wedge since the onset of orogenic growth to the final post-orogenic episodes.

2. Geological overview of the Calabria-Peloritani Arc

Three main tectonic models have been proposed for the kinematics in the CPA:

- the superimposition of two compressive tectonic processes, ascribed to an Eo-Alpine (westverging) and a subsequent Apennine (east-verging) orogenic event (e.g. Haccard et al., 1972; Amodio Morelli et al., 1976; Bonardi et al., 1994; 2001; Cello et al., 1996; Iannace et al., 2005; 2007);
- the superimposition of a regional extensional (WNW-verging) tectonic event on an early compressive (east-verging) stage during the Apennine orogenesis, responsible of the present-day structural architecture of the tectonic units and the exhumation and exposure of the HP-rocks in Coastal Chain and Sila Massif (Rossetti et al., 2001; 2004), in the Aspromonte Massif (Platt & Compagnoni, 1990) and in the Calabria-Lucania boundary (Wallis et al., 1993);
- the occurrence of a thick-skinned transpressive tectonic evolving towards shallowl thrust and back-thrust systems (Van Dijk et al., 2000).

Alpine metamorphism occur in both continental- and oceanic-derived rocks in the CPA. HP/LT Alpine metamorphism, associated to deep underthrusting, was recorded by the oceanic rocks (De Roever et al., 1974; Spadea et al., 1976; Beccaluva et al., 1982; Cello et al., 1996; Rossetti et al., 2001; 2004; Iannace et al., 2007), equilibrated into the blueschist facies field. MP/LT metamorphism has been described for the European units of the Sila Massif (the Castagna Unit; Rossetti et al., 2001), of the Serre Massif (Langone et al., 2006) and in the Adria-derived units of the eastern Peloritani Mountains (e.g. Cirrincione & Pezzino, 1994; Vignaroli et al., 2008). Finally, retrogressive syn-greenschist metamorphism has been described for the exhumation trajectory followed by the HP-metaophiolitic sequences of the Coastal Chain and Sila Massif, related either to extensional (Rossetti et al., 2001; 2004) or compressive structural features (Iannace et al., 2007). Diffuse late-to-post-orogenic reverse shear zones mostly affect the upper portions of the CPA tectonic edifice in the Calabrian region (e.g. Dietrich, 1988; Rossetti et al., 2001; 2004; Iannace et al., 2005; 2007) and in the Peloritani Mountains (Giunta & Somma,1996; Vignaroli et al., 2008). Finally, post-orogenic normal fault systems controlled the evolution of sedimentary deposits mostly located on the Tyrrhenian side of the CPA (e.g. Argentieri et al., 1998; Mattei et al., 2002; Cifelli et al., 2004).

2.1 Geochronological and Stratigraphic constraints

Figure 2 shows a synthesis of published geochronological and stratigraphic data obtained for the different regions of the CPA. The huge of published geochronological data has been related to the main tectonic events recognized for the CPA geodynamic evolution (the metamorphic peak, the metamorphic retrogression and the final late exhumation). The isotopic geochronological method applied on individual mineral specimen as well as the geological setting (i.e. extensional or compressive) controlling the dynamic of sedimentation are specified in legends of the same figure.

The Alpine orogenic metamorphism in the CPA is described by using different methods on different rock types (Borsi and Dubois, 1968; Schenk, 1980; Beccaluva et al., 1981; Bonardi et al., 1987; Atzori et al., 1994; Rossetti et al., 2001; De Gregorio et al., 2003), systematically showing Tertiary (Eocene to Oligo-Miocene) ages. Syn-blueschist facies conditions (8-14 kbar) in both oceanic- and continental-derived rocks of the Costal Chain and the Sila Massif occurred in the Late Eocene-Oligocene (e.g. Rossetti et al., 2001; 2004). Recently, Iannace et al. (2007) described metamorphic sequences of the Coastal Chain sector containing Mg-carpholite and preserving stratigraphic contacts. Based on ^{40}Ar-^{39}Ar dating on phengite, the authors rejuvenated the age of the metamorphic peak at the Aquitanian-Burdigalian boundary. A further younger age for the Alpine metamorphism has been proposed by Macciotta et al. (1986) for the Adria derived units in the Costal Chain (the San Donato Unit) equilibrated under low-grade greenschist condition. These divergences impose a discussion on the relative tectonic models. The only available Alpine age, at 42-43 Ma, for the Serre Massif is based on Rb/Sr method on phengite from Europe-derived units (Schenk, 1980). Greenschist transitional to amphibolitic facies Alpine metamorphism occurred in European continental units of the Aspromonte Massif during the Oligocene-Miocene boundary (Bonardi et al., 1992; 2000). Alpine metamorphic peak in the Peloritani Mountains equilibrated under greenschist facies conditions in Adria-derived units (e.g. Atzori et al., 1994; Vignaroli et al., 2008) during the continental collision. The age of this event is not so well constrained, despite a Middle Eocene-Late Oligocene time span has been proposed (e.g. Atzori et al., 1994; De Gregorio et al., 2003). Summarizing this complex geochronological framework, the Alpine orogenic metamorphism seems to be almost synchronous in both the axial (the Costal Chain and the Sila Massif) and the frontal (the Peloritani Mountains) portions of the Calabria- Peloritani wedge. In terms of wedge dynamic, this metamorphism can be related to the deep underplating of oceanic and subordinate continental units at its bottom (the present-exposed HP-units in the Coastal Chain and the Sila Massif) and by accretion at its front (the Adria-derived greenschist units in the Peloritani Mountains) during self-similar (steady-state) growth of the wedge.

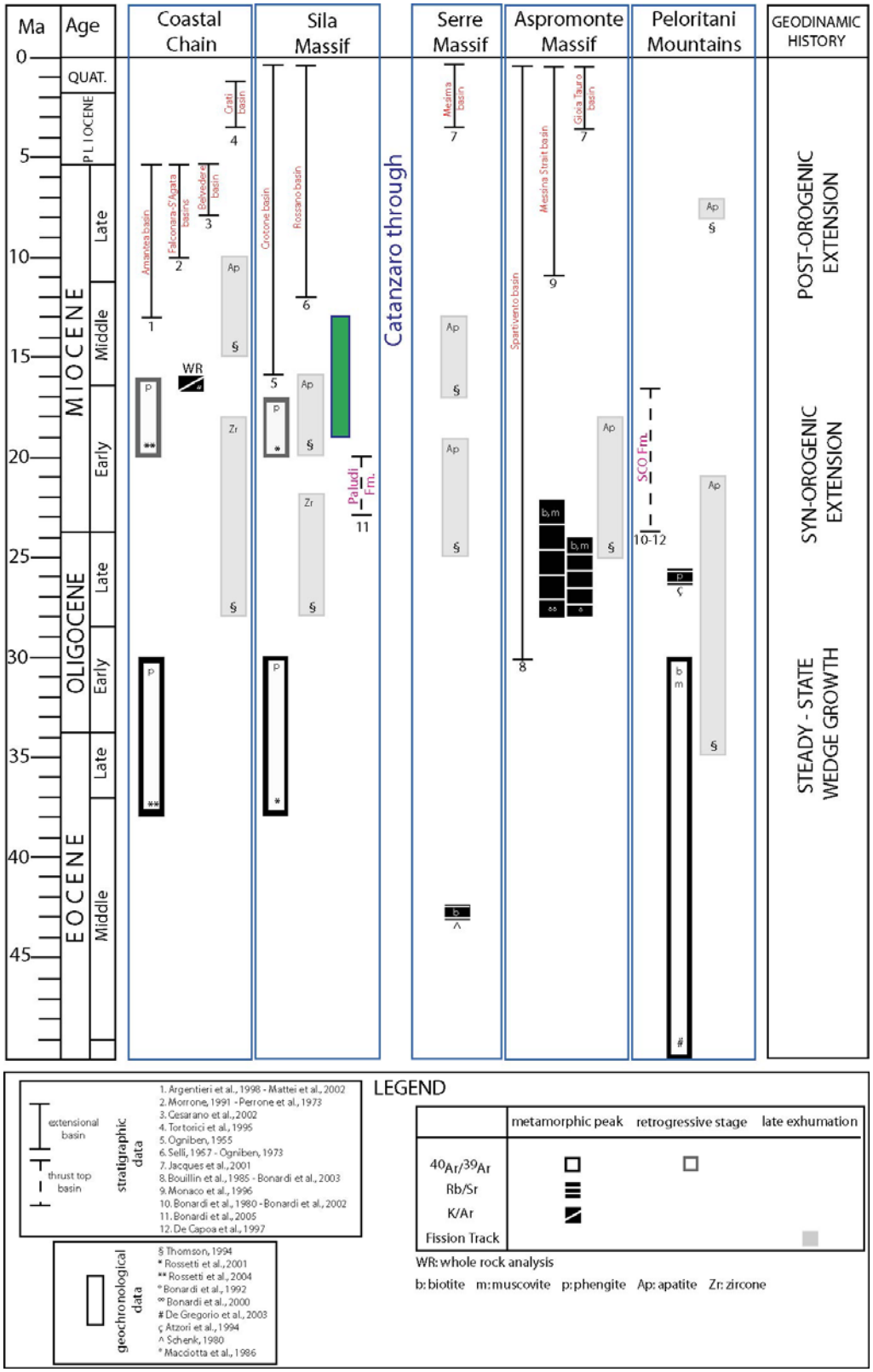

Figure 2 - Review of the geochronological/stratigraphical data in the Calabria-Peloritani Arc

Ages of the retrogressive metamorphism have been obtained for both the continental- and oceanic-derived rocks of the Coastal Chain and the Sila Massif. The 20-16 Ma interval obtained by Rossetti et al. (2001; 2004) has been related to the crustal thinning operated by extensional detachment in between the over-thickened wedge. No further second-phase ductile extensional features have been recognized in other sectors of the CPA.
Thermo-chronological data relative to the latest exhumation stage come from the extensive study by Thomson (1994) on continental-derived (European and Adriatic) units widely dispersed in all the CPA. Making a synthesis of that study (Fig. 2), apatite and zircon from 65 rock samples were analyzed. On the Ionian side, Thomson obtained apatite FT ages ranging between 42.5 ± 20.1 and 12.7 ± 1.4 Ma. Thomson interpreted this older apatite FT ages, that are from the Ionian side, they are characterized by shorter mean lengths and higher standard deviations, indicating a slower cooling through the partial annealing zone (PAZ) and probably Thomson also predicted the cooling of the Tyrrhenian side but, as he didn't obtain apatite FT ages older than 40 Ma, he concluded that any rock that resided at temperatures below ca. 120° C before ca. 35 Ma was subsequently removed by erosion from the crustal section. On the basis of the whole data-set, Thomson concluded that the basement rocks of the Calabrian arc experienced a phase of rapid cooling related to exhumation between ca. 35 and ca. 15 Ma and attributed the exhumation to extension caused by the instability of the accretionary prism due to continuous underplating. By comparing the age of AFT with respect to their location in the CPA, we note that there is a general rejuvenation passing from the Peloritani Mountains to the Coastal Chain (Fig. 2). In particular, European continental units in the Peloritani Mountains cooled through the PAZ in the whole Oligocene, while the similar units in the Coastal Chain exhumed up to Late Miocene.
Stratigraphic constraints come from ages of the syn-to post-orogenic sedimentary basins cropping out on both the Ionian and Tyrrhenian sides of the CPA. Oldest sedimentary sequences are represented by the lowermost levels of the Spartivento basin located in offshore position with respect to the Aspromonte Massif (Fig. 1). Then, the Paludi Formation and the Stilo-Capo d'Orlando Formation were dated at the Aquitanian-Burdigalian interval on the basis of their nannofloras content (Bonardi et al., 1980; 2002; 2005). In particular, the age of Paludi Fmt was previously referred to the Early–Middle Eocene (e.g. Dubois, 1976); subsequently, Bonardi et al. (2005), after a stratigraphic revision, proposed an Aquitanian age of the formation, obtained by nannofloras analyses. These sedimentary deposits come from the erosional unroofing of the European units during their nappe stacking. Structural observation allowed to consider that their sedimentation was, at least in part, coeval with respect to the nappe stacking (e.g. Vignaroli et al., 2008). All other sedimentary deposits are younger than the Middle Miocene and were deposited in wedge-top basins in the Ionian side of the chain and in post-orogenic extensional basins in the Tyrrhenian side.

2.2 Geological setting of the eastern Sila Massif

The eastern Sila Massif (Sila unit) is composed by pre-Mesozoic crystalline units intruded by late Hercynian granitoids (*Sila batholith*) with relative Mesozoic sedimentary cover (Longobucco Unit) and flyschoid sequences (the Paludi Formation; Bonardi et al., 2005). The Hercynian units consist of rocks affected by various metamorphic grade (e.g. Borsi & Dubois, 1968; Lorenzoni et al., 1978; Messina et al., 1994; Graessner & Schenk, 2001). The Mesozoic succession consists of continental red beds (red conglomerates, quartzose sandstone and red mudstone) overlain by shelf limestones and calcarenites, slope shale and deep-water turbidites (e.g. Lanzafame & Tortorici, 1980; Zuffa et al., 1980). The clastic deposits of the Paludi Formation (Dubois, 1976) rest unconformably above the Sila units. The Paludi Formation consists of a conglomeratic basal part followed by pink-red marls and by arenaceous marls and sandstones. Its depositional age, previously referred to the Early-Middle Eocene by Dubois (1976), has been subsequently rejuvenated to the Aquitanian by Bonardi et al. (2005) on the basis of nannofloras content. The entire tectonic edifice is sealed by the Middle to Late Miocene sedimentary deposits of the Rossano Basin (Ogniben 1962; Roda, 1964; Barone et al., 2008). The onset of sedimentation includes transgressive basal alluvial and fan-delta conglomerate overlain by Serravallian (?)-Tortonian fossiliferous sandstones. The succession passes upward to deeper water marls and clays that are overlain by an interval of olistostrome bodies of varicoloured clays, equivalent to the typical succession of the Sicilide Complex of southern Apennines (e.g. Critelli, 1999). In the Rossano Basin, the Tortonian-Messinian boundary results in deposition of evaporitic limestone overlain by a transgressive sequence along an erosional angular unconformity. In the upper levels of the Messinian deposits, olistostromes of undifferentiated sandstones may occur (the Cariati nappe). Finally, the Pliocene and Pleistocene sedimentation in the Rossano Basin is characterized by mudstone and locally sandstone.

The Hercynian nappe structure has been described for these units (e.g. Gurrieri et al., 1978; Lorenzoni & Zanettin Lorenzoni, 1983), as well as Pressure-Temperature conditions during Hercynian metamorphism have been quantitatively estimated (e.g. Graessner & Schenk, 2001). No penetrative Alpine ductile deformation has been recognised in the eastern Sila Massif. Alternatively, the classic cross-sections identify W and SW dipping thrust systems which are responsible for the general NE-verging stacking of the Hercynian units on top of flyschoid sequences (e.g. Lanzafame & Tortorici, 1980; Ghisetti & Vezzani, 1981; Van Dijk et al., 2000; Bonardi et al., 2001; Caggianelli & Prosser, 2001; Liotta et al., 2004). Also the Paludi Formation has been involved in the orogenic phase related to the accretion of the Calabrian wedge with Apulia-verging orogenic transport (Bonardi et al., 2005).

3. Structural Geology of the eastern Sila Massif

3.1 Onshore structural analysis

Our structural and kinematics investigations have focused on the main tectonic boundaries between the different exposed unit which constitute the nappe pile of the Longobucco area. Large-scale mapping of the main structures was extrapolated by considering published geological cartography (e.g. Bigi et al., 1990). The results of such information are synthesized in the geological map of Fig. 3, where we described the collected structural data in terms of trend and kinematics of the main thrust surfaces and thrust-related structures. The structural-geometrical relationships between different units are schematised in the cross-sections of Fig. 4a.

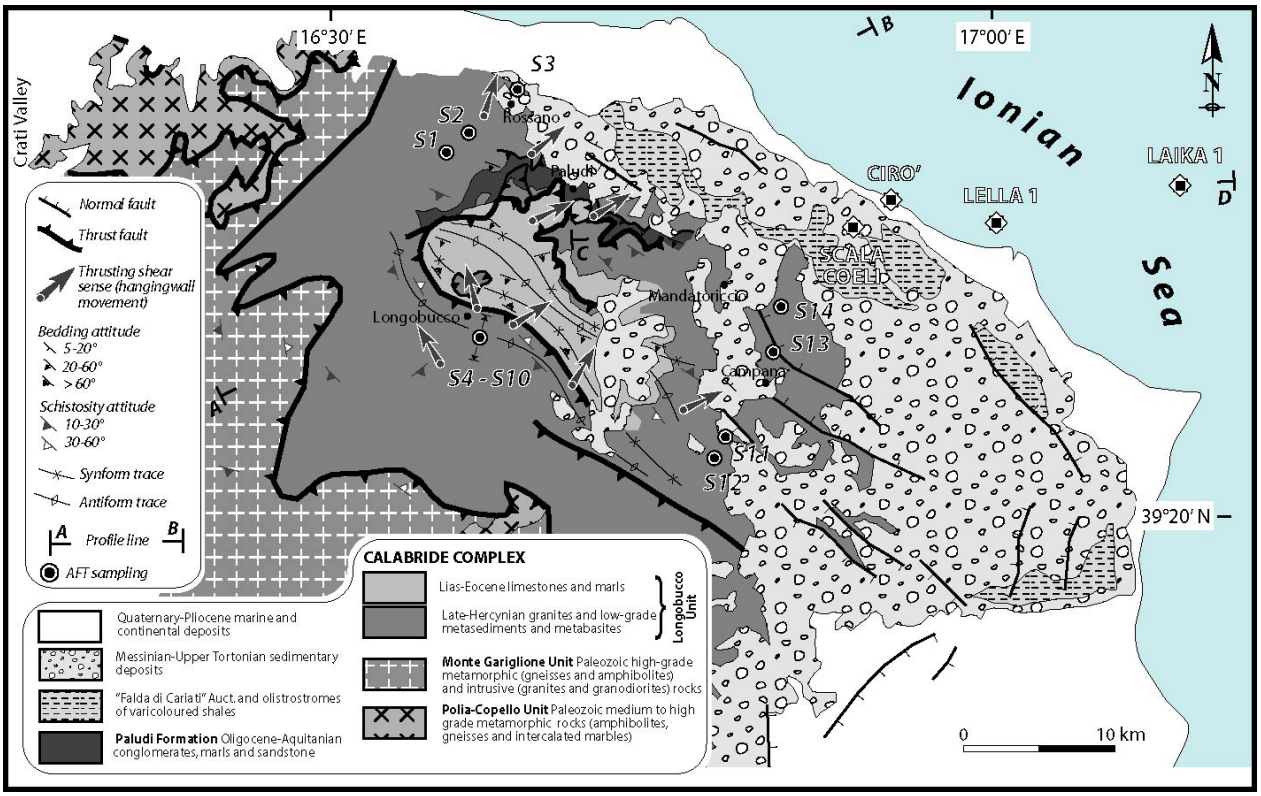

Figure 3 - Structural-geological map of the Longobucco area.

The first order structures in the Longobucco area are NW-SE-striking thrust systems juxtaposing thrust sheets in an Ionian-verging nappe pile (Fig. 3). Major thrust systems control (i) the superimposition of the Hercynian high-grade metamorphic and intrusive rocks of the Monte Gariglione Unit on top of the Longobucco Unit, (ii) the double stacking of the basement- and sedimentary cover rocks, and (iii) the superimposition of the

Longobucco Unit on top of the Paludi Formation (Figs. 3, 5a). All the stacked tectonic pile is sealed by Middle Miocene unconformable sedimentary deposits (Fig. 3).

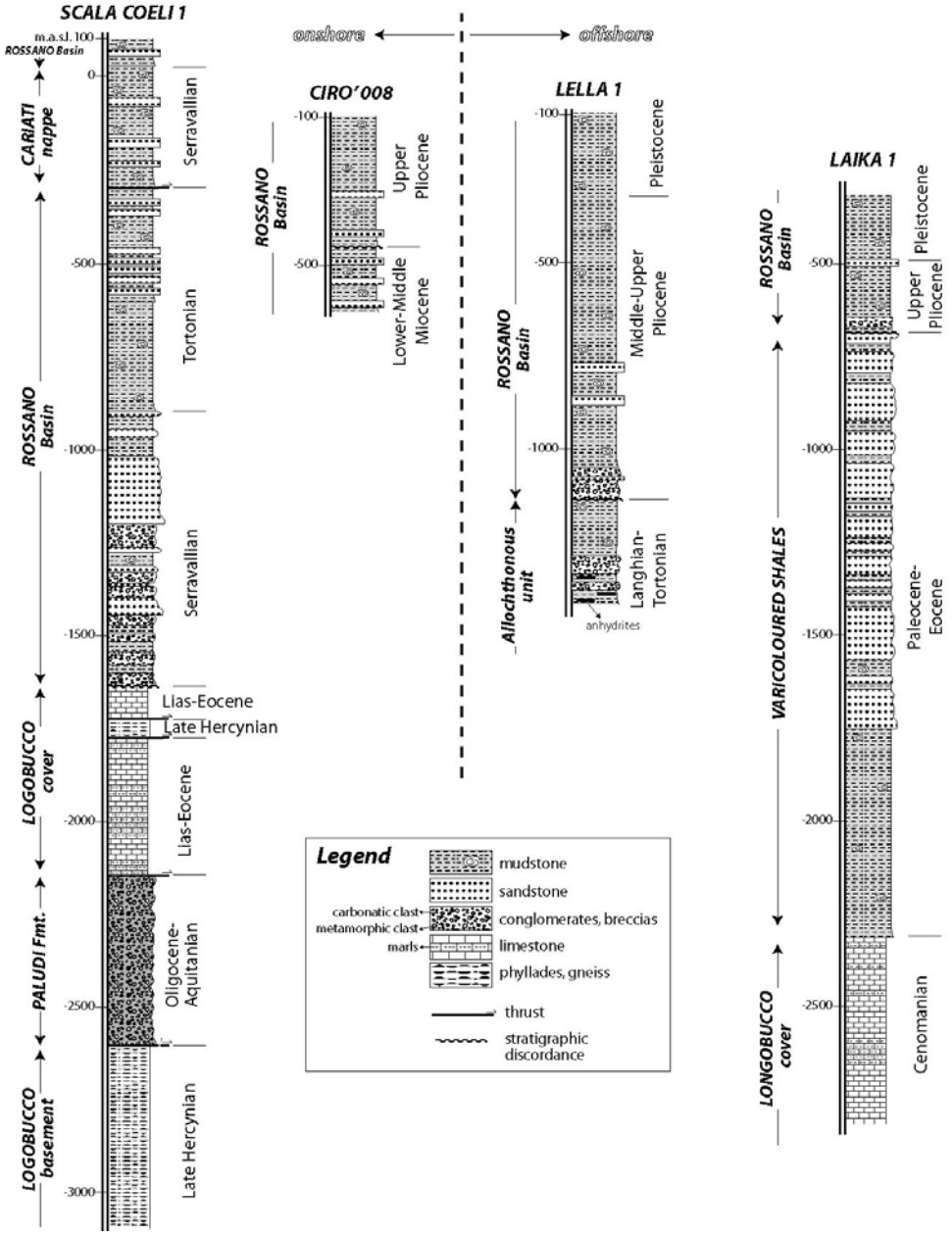

Figure 4 - Schematic stratigraphic logs of the wells in the eastern Sila Massif (see Fig. 3 for locations).

The uppermost tectonic slice (the intrusive rocks of the Monte Gariglione Unit) lies on top of the Longobucco Unit along a thrust contact gently dipping to the WSW (Fig. 5a) and showing an articulated, laterally discontinuous trace in map. This contact is locally reactivated by late transcurrent faults. To the east, the granite of the Longobucco Unit displays an antiform structure, with westward gently dipping western flank and

high-dipping eastern one, proximal to the vertical approaching to the contact with the underlying Jurassic-Eocene sequence (Figs. 5a and 6a).

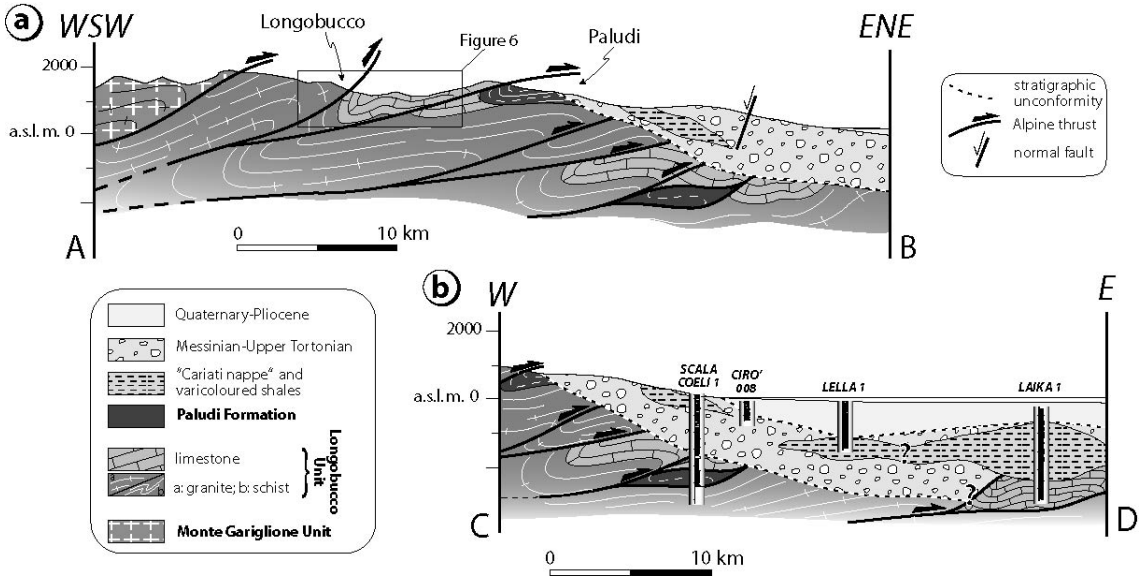

Figure 5 - Geological cross-sections illustrating the structural relationships between units exposed on-shore (a) and off-shore (b).

No pervasive deformative fabric (such as mylonitization or intensive cleavage) is present in the granite. Discrete brittle-dominated shear systems have been recognised. Kinematics of deformative structures affecting granite is not clear because of the superimposition of late transcurrent movement on an early reverse one. Meso-scale top-to-the-NW thrust surfaces (Fig. 6b and stereographic projection n° 1 in Fig. 6a) have been seldom observed. In the Longobucco village, a tectonic contact, marked by *ca.* 3 metres-thick of breccias and cataclasite, defines the juxtaposition of the granite on top of the Jurassic- Eocene sequences (Fig. 6b). In the gouge domain, NW-SE striking *C'*-shear planes show both top-to-the NE and top-to-the-NW sense of shear and are characterised by a high transcurrent component. The Jurassic sequence at the foot-wall is defined by red conglomerates and quartzarenites constituting the lowermost levels of the sedimentary series (Lanzafame & Tortorici, 1980). These anagenites form a strongly cuspateto- lobate sinform showing a vertical-to-overturned western flank (Fig. 6a). Thrust-related folds in the anagenites and limestone show roughly N-S sub-horizontal hinge and gently westward dipping axial plane (stereographic projection n° 2 in Fig. 6a). High-angle (up to 65°) reverse-faults cut the folds in the limestone, showing both top-to-the NE and top-to-the-NW sense of shear (stereographic projection n° 2 in Fig. 6a). From a structural point of view, the Longobucco Unit is deformed in a fold-thrust-belt geometry (Fig. 6a) in which a sequence of large NW-trending synforms-antiforms can be recognised (Figs. 3 and 6a). The Jurassic-Eocene sequence defines a mega-lens embedded in the basement

rocks, laterally confined between two main thrust splays (Fig. 3). In the northeastern part of the section (the Castellaccio locality; Fig. 6a), imbrication of schists and limestone sheets occurs along WSW dipping thrust planes.

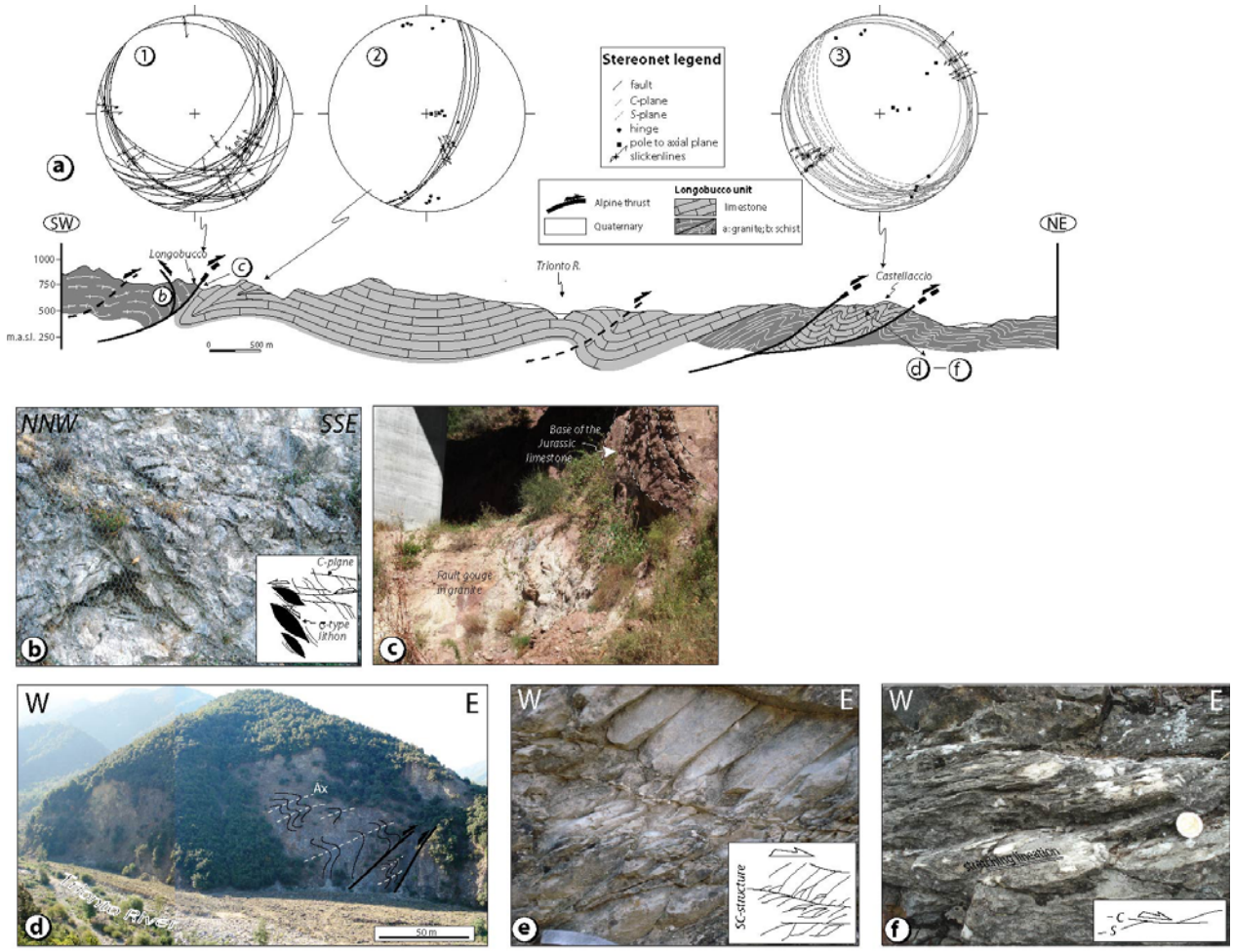

Figure 6 - (a) Detailed cross-section illustrating the tectonic relationships between the basement and the cover in the Longobucco Unit; (b) top-to-the-NNW shear sense in the Longobucco granites related to back-thrusting; (c) detail of the fault gouge produced at the tectonic contact between the carbonatic sequence and the granite at the Longobucco village; (d) syn-thrusting plicative structures in the Longobucco carbonatic cover; (e-f) top-to-the-E shear senses in the Longobucco cover.

The largest part of the deformation is accommodated by plicative and brittle shear zones occurring into the sedimentary rocks. Open-type folds of metric amplitude are widespread along the section, evolving to cuspate-type and overturned when approaching to the thrust planes (Fig. 6d). Folds show hinge trending NW-SE and axial planes dipping to the SW (stereographic projection n°3 in Fig. 6a). Folding is accomplished by the development of a pervasive plano-linear fabric sub-parallel to the main thrust. Flexural slip between carbonate layers is very common. Intense calcite re-crystallization and striation occurred on both stratigraphic and

cleavage surfaces. Aligned calcite assemblages define the stretching lineation, generally trending N60. Kinematic indicators are widespread. *SC*-structures and *C'*-shear planes consistently indicate thrusting towards the ENE (hanging-wall movement) (stereographic projection n°3 in Fig. 6a; Fig. 6e,f). The thrust contact between the Longobucco Unit and the Paludi Formation shows trace generally trends NW-SE. At its north-western end, it evolves in a lateral ramp dissecting the underlying splays (Fig. 3). The Paludi Formation consists of conglomeratic basal part, overlain by pink–red marls and by arenaceous marls and sandstones (e.g. Dubois, 1976). According to Van Dijk et al. (2000), the contact between these two units near the Paludi village is defined by a NE-verging thrust (Fig. 7a,b).

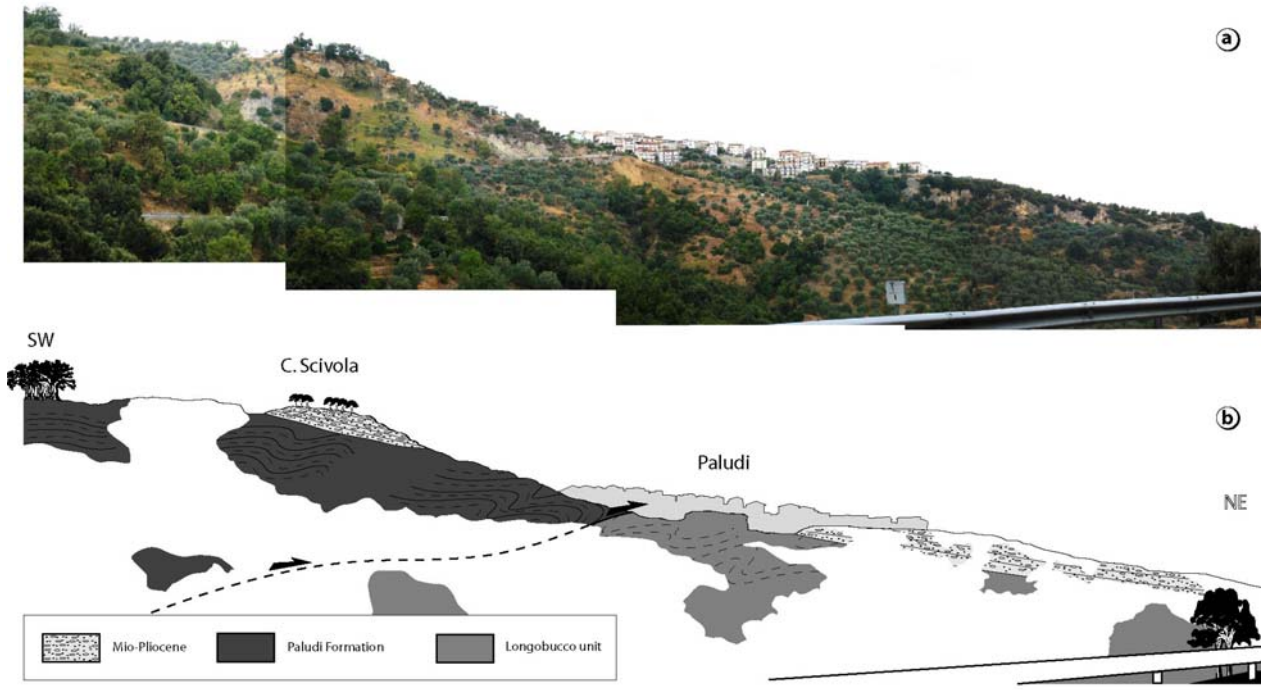

Figure 7 - Structural data: panoramic view of the tectonic contact near the Paludi village

Internal deformation of the Paludi Formation is represented by both plicative and shear structures.
Recumbent folds show NW-SE-trending hinge and are often dissected by *C'*-like shear planes (Fig. 8a). In pelitic layers, non-coaxial deformation style is evidenced by *SC*-structures. Carbonate-dominant layers are often re-shaped in sigma-type lithons by shear structures (Fig. 8b). Shearing planes display striations trending from N45° to N60°. The analysis of kinematic indicators on meso-scale sections parallel to the striations and perpendicular to the sedimentary layers allow recognising a top-to-the NE sense of shear (Fig. 8b-d). The thrust contact

between the Paludi Formation and the Longobucco Unit is sealed by the transgressive deposits of the Middle Miocene, uncomformably dipping to the E/NE (Fig. 7).

These deposits consist carbonates and red pelagic limestones at the bottom, being overlain by red marls and sandstones containing olistoliths of evaporites (see also Van Dijk et al., 2000). Undeformed stratigraphic contacts with the underlying tectonic units are well exposed.

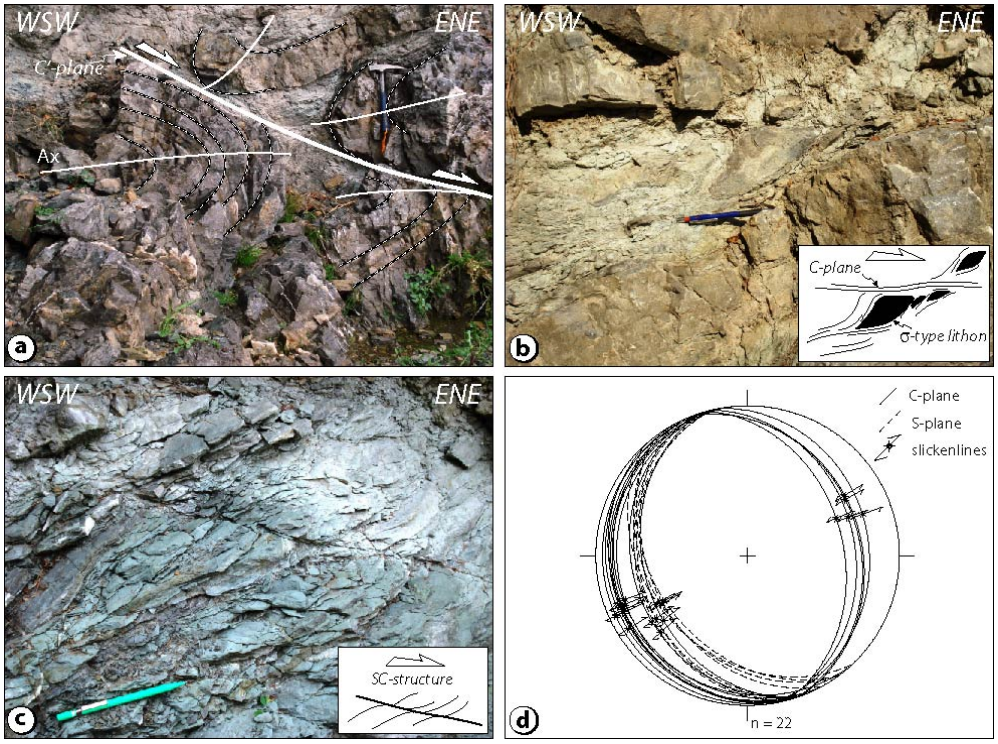

Figure 8 - Structural data: details of the shear senses of the Paludi Formation

Locally, synsedimentary fault systems occur. Sediments cropping out in the Rossano village show a dominant normal fault system and subordinate dextral-component transcurrent one (Fig. 9). SW gently-dipping sedimentary layers are cut by fluid-filled low-angle normal faults, in which sub-sequent high-angle normal and transcurrent faults root (Fig. 9a, b). Structural analyses on the kinematics of the faults provide a rough N-S maximum extension direction (Fig. 9c).

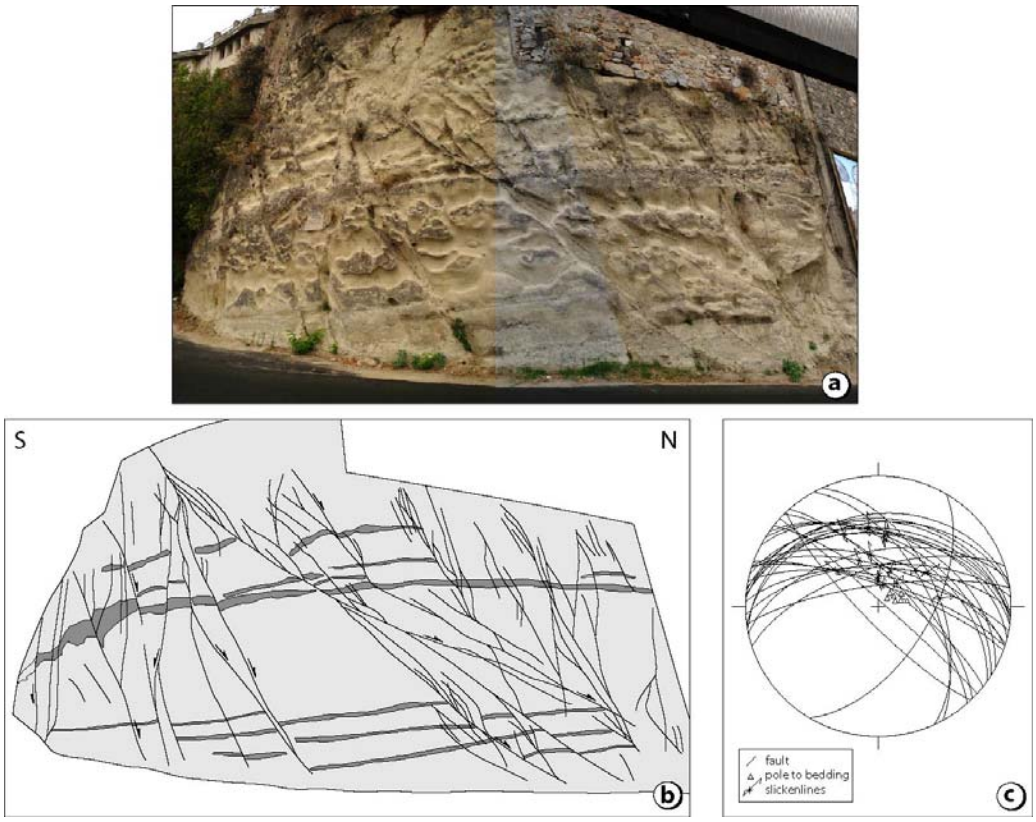

Figure 9 - Rossano village: syn-sedimentary normal and subordinate transcurrent fault system in Pliocene (?) sediments.

3.2 From onshore to offshore

Information carried out from the geological survey in the eastern Sila Massif has been extended to the offshore by using stratigraphic well data published by oil industries during the last 40 years. Four wells (Fig. 1b) have been taken into consideration, aligned along an E-W strike (Fig. 3), nearly perpendicular to the major outcropping structures. The wells were drilled in the Rossano Basin and are: Scala Coeli1 and Cirò008 onshore, Laika1 and Lella1 offshore. Figure 4 reports the schematic stratigraphic log for each well, specifying the attribution of lithologies to the unit and the nature of the contact between different lithologies (stratigraphic or tectonic).

Scala Coeli 1: this stratigraphic log allows constraining onshore lithologies and geometries at depth deduced by the geological survey. First 50 m are represented by the Upper Messinian sediments of the Rossano Basin (the Palopoli Molasse). Then, a stratigraphic unconformity separates these sediments from the underlaying alternation of ~350 m composed by mudstone and sandstone referable to the allochthonous Cariati nappe, Serravallian in age. The base of the Cariati nappe is tectonic. This thrust unit overlying ~1300 m thick of the Serravallian-Tortonian sediments of the Rossano Basin. These are dominantly composed by mudstone and

siltstone with metre-thick levels of sandstone in the upper portion. At the bottom, the arenaceous component prevails then passing to breccias and conglomerates containing calcareous and subordinately metamorphic (basement) clasts. The sediments of the Rossano Basin lye above a carbonate sequence, representing the cover Longobucco Unit along an erosional angular unconformity. Tectonic discontinuities affect the upper part of the carbonate sequence, involving ~50 m of basement rocks. At the bottom, a major tectonic element marks the contact with the underlying Paludi Fmt. The latter is composed of conglomerates and breccias, made up of calcareous and metamorphic clasts. Metamorphic clasts are dominant in the lower part of the formation, close to the tectonic contact with the underlying Longobucco Unit basement, which is made up of phyllades and intercalated gneiss down to the bottom of the well.

Cirò 008: the well was the upper portion of the stratigraphic sequence of the Rossano Basin, which is made up of ~50 m thick of Upper Pliocene-Pleistocene mudstone unconformably lying on alternation of Tortonian mudstone and sandstone.

Lella 1: its stratigraphic column is composed by about 1000 m thick of Pliocene-Pleistocene sediments resting unconformably on top of a Langhian-to-Tortonian allochthonous unit. The Plio-Pleistocene sequence is part of the Rossano Basin and is made up of dominant mudstone passing to a basal breccia with carbonate and metamorphic clasts. An erosional unconformity marks the boundary with the underlying allochthonous unit. The latter is composed by an alternation of mudstone and sandstone containing traces of anhydrite at the base.

Laika 1: first 500 m recover the Upper Pliocene-Pleistocene succession of the Rossano Basin, made up of dominant mudstone and a basal breccia. The sediments unconformably cover a large thickness (~1600 m) of Paleocene-Eocene olistostrome sequence made up of the Varicoloured Shales (e.g. Critelli, 1999). The latter is composed by sandstone at the top, gradually passing to mudstone towards the bottom. Then, a stratigraphic discordance marks the boundary between the Varicoloured Shales and the underlying limestone sequence, Cenomanian in age, probably referable to the Longobucco cover.

Correlation of geological data extrapolated from the stratigraphic wells allows the reconstruction of the main offshore stratigraphic-structural relationships among units of the eastern Sila Massif (Fig. 5b). The sedimentary deposits of the Rossano Basin constitute a roughly monoclinal succession dipping toward the offshore. Two main stratigraphic unconformities can be recognised: the upper one marks the Pliocene-Miocene boundary; the lower one represents the erosive contact of the Rossano Basin on top of the basement units.

Onshore, the Scala Coeli1 well allows reconstructing the deep structural geometries of the tectonic units underlying the Rossano Basin. In particular, we can documented a double stacking of the Sila and Longobucco Units, with involvement of the Paludi Formation (Fig. 5b), very similar to the structural architecture recognised during the geological survey (Figs. 3 and 5a). Above, the thrust horizons do not affect the regular Serravallian-

Tortonian sedimentary deposition of the Rossano Basin, but the thrust sheets are sealed by the erosive angular unconformity. Offshore, the correlation of the Miocene-Pliocene unconformity between the Cirò008 and Lella1 wells suggests a deepening of the Rossano Basin (Fig. 5b). Nevertheless, the juxtaposition of Varicoloured Shales on top of the Cenomanian limestones (the Laika1 well) implies that the series are, at least in part, involved in deformation. Although an accurate thrust sheet geometry cannot be reconstructed, it is plausible to consider that the base of the basin is truncated by a thrust horizon bounding the limestone (Fig. 5b).

4. Apatite Fission Track Thermochronology

Fission tracks represent linear damage zones produced by the radioactive decay of 238U. The density of fission tracks depends on the time over which tracks have accumulated. Over geological time, fission tracks are fully retained in apatite at temperature below 60°C while they are only partially retained between 60° and 120°C (Partial Annealing Zone, PAZ) with a mean closure temperature at 110°±10°C (Green and Duddy, 1989). Measurement of fission-track lengths gives information on the thermal history of the rocks in the PAZ temperature range. A quantitative evaluation of thermal history can be obtained through the application of statistical modelling procedures that find T-t path compatible with the fission-track data (Gallagher, 1995; Ketcham et al., 2000; 2005).

This methodology is considered an ideal technique for testing the age and the rates of rock denudation in the upper structural levels of an orogenic wedge (e.g. O'Sullivan and Wallace, 2002; Fügenschuh and Schmid, 2003).

4.1 Method

A new set of 14 apatite samples were analyzed. They come from granitoid lithotype of the Longobucco Unit collected along three vertical sections and in a strongly constrained structural position, i.e. all the samples belong to the hanging-wall of the Longobucco thrust (Fig. 10). Apatite grains were separated from about 5 kg bulk samples using standard heavy liquids and magnetic separation techniques. Mounts were ground, polished and etched with 5N HNO3 at 20° C for 20 seconds to reveal the spontaneous tracks. Samples were then irradiated with thermal neutrons in the Lazy Susan facility of the Triga Mark II reactor of the University of Pavia (Italy). To measure the neutron fluency, standard glass CN5 was used as dosimeters. After irradiation, the low-U muscovite detectors were etched in 40% HF at 20° C for 45 minutes to reveal the induced fission tracks. Apatite fission-track ages were measured and calculated using the externaldetector and the zeta-calibration methods (Hurford and Green, 1983) with a zeta value (referred to Fish Canyon Tuff and Durango apatite

standards, Hurford, 1990) of ζ= 360±11. The details of the data are reported in Table 1 and Fig. 10. Thermal history reconstructions were performed using the HeFTy program by R. Ketcham (2005) and results from representative samples (i.e. with a consistent number of length determinations) are reported in Fig. 11.

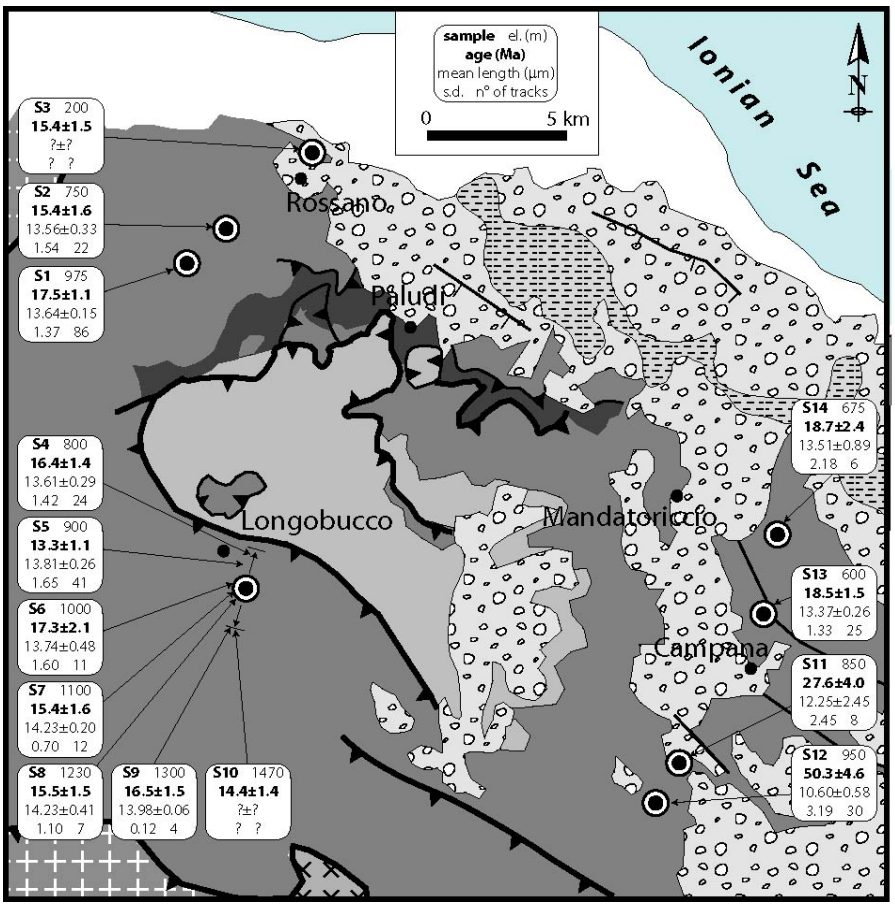

Figure 10 - Zooming of Figure 4 showing locations of apatite fission track samples collected for this study. For each sample, the elevation, fission track age, mean tack length, standard deviation and number of confined tracks measured are shown. Errors are in ±1σ.

The program defines envelopes in a time-temperature space that contains all paths that statistically yield the good fit (the T-t path is supported by the data) and the acceptable fit (the T-t path is not excluded by the data).

4.2 Results and interpretation

Section 1: Three samples (S1, S2, S3) were collected between 975 and 200 m of elevation. Apatite FT ages vary between 17.5 and 15.4 Ma with long mean track length (13.4 -13.6 µm) and low standard deviations (1.5 µm - 1.4 µm) (table 1).

Section 2: Seven samples were collected along a topographic profile with elevation spanning between 1470 and 800 m. Apatite FT ages, bracketed between 16.4 and 13.3 Ma, do not show an evident correlation to the elevation (Fig. 11). Mean track length varies between 13.6 and 14.2 µm with standard deviations between 1.6 and 1.1 µm.

Section 3: Four samples were collected with elevations ranging between 950 and 600 m. Apatite FT ages are in a wider range between 50.3 and 18.5 Ma. Mean track length are between 10.6 and 13.5 µm with standard deviation varying between 3.20 µm to 1.10 µm (Table 1).

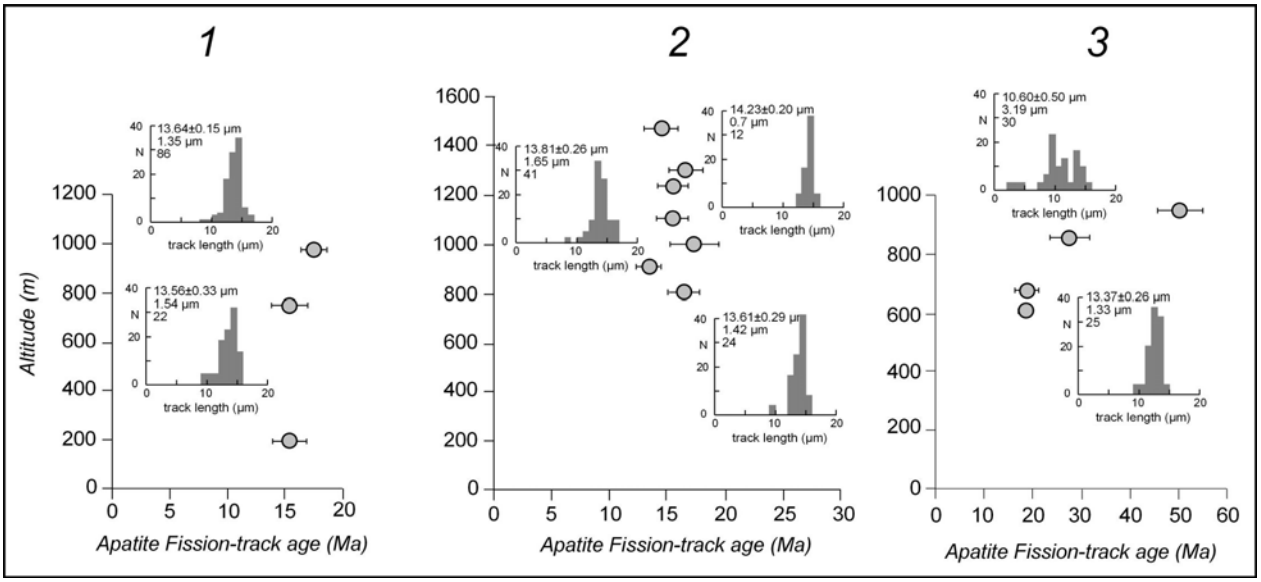

Figure 11 - FTA: Altitude/age graphics. Track-length distributions are normalised to 100 tracks.

All the samples, with the exception of samples S11 and S12, show unimodal length distributions with relatively long mean lengths and small standard deviations that are indicative of moderate to rapid cooling across the PAZ. Therefore, all samples from section 1 and 2 indicate a cooling event from temperatures above about 110°C at about 17 -15 Ma (see Fig. 12, a, b, c). Conversely, in section 3, only the fission-track ages of the two lowest samples are cooling ages (for sample S13 see Fig.12, f). In fact, the two uppermost samples (S11, 12) show older ages with sample S12 showing an age as old as 50.3±4.6 accompanied with reduced track mean length (10.6±0.58 µm) and large standard deviation (3.19 µm). This indicates that before the final cooling event

these two samples were already at temperatures inside the PAZ (for sample S12 see also the modelling in Fig.12, e). They can be interpreted as belonging to an exhumed paleo-PAZ. It is possible to infer the presence of a break in slope in the age-elevation profile probably placed at ca. 17-18 Ma and 600 m of altitude (Fig. 12, 3). Samples above the break show confined track length distribution with significantly shortened mean length and broad standard deviation, the distribution being composed by tracks formed in the pre-exhumation PAZ and by a later set of post-exhumation tracks. Confined track length distributions below the break reflect rapid cooling (long mean track lengths and small standard deviations; Fitzgerald et al., 1995). A break-in-slope represents the base of the paleo-PAZ and the corresponding age indicates the onset of an exhumation phase.

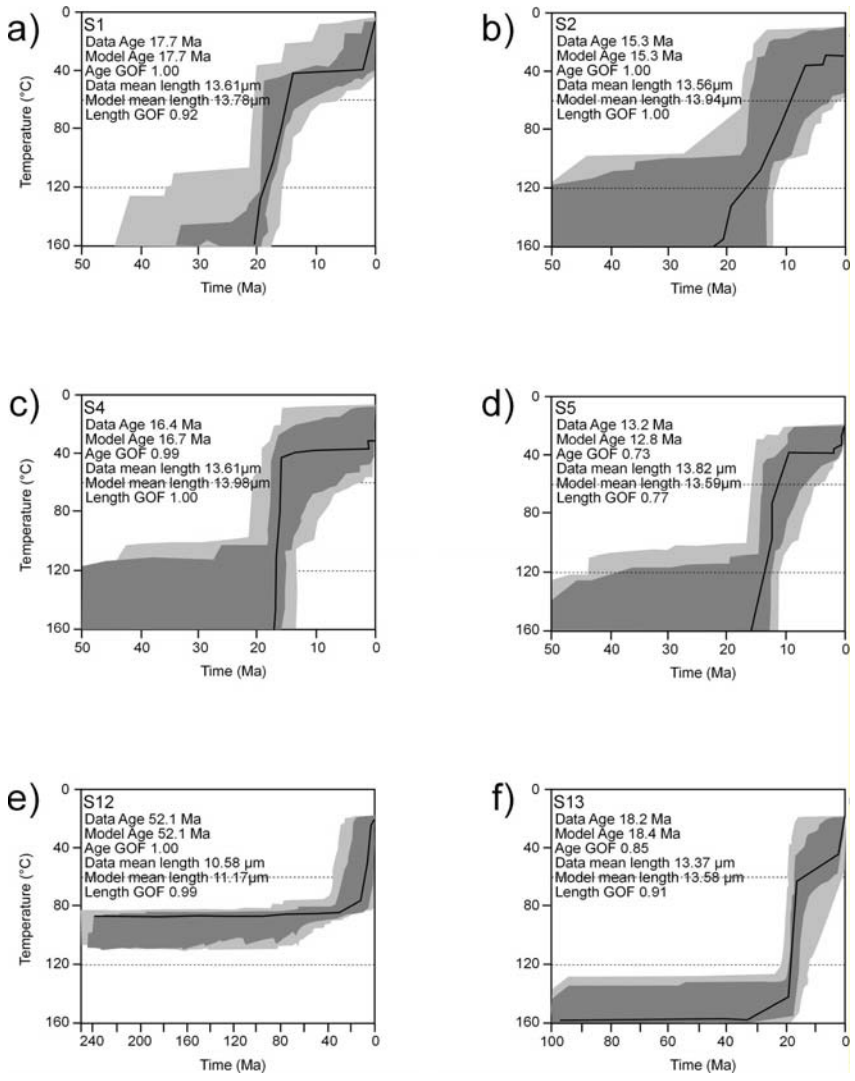

Figure 12 - Thermal modelling of representative samples based on the annealing model (Ketcham et al., 1999). Grey field represents the good-fit result predicted by the model, while the solid line is the best-fit result.

Samples belonging to the paleo- PAZ are preserved only in section 3 while in the other two sections they were removed by erosion from above the collected samples. Samples analyzed from section 1 and 2 belong to the so called “exhumation profile”. Information about the sample exhumation/erosion rate can be inferred from the slope of a best fitting line through the data belonging to the exhumation profile (data below the break in slope). But, in the case of section 2 (Fig. 11) in which we have 7 samples to define the slope of the best-fitting line, we statistically obtain a negative values. However the correlation coefficient R is very low (R2=0.0133) indicating in practice no correlation of the data.

	Sample	El. (m)	$\rho_a x10^5$ (cm^{-2}) n_d	$\rho_s x10^5$ (cm^{-2}) n_s	$\rho_i x10^5$ (cm^{-2}) n_i	n_g	$P(\chi^2)$ (%)	Central Age±1σ (Ma)	Lm (μm)	s.d. (μm)	n
SECTION 1	**S1**	975	6.58 5153	8.24 411	55.02 2743	25	77	**17.5±1.1**	13.64±0.15	1.37	86
	S2	750	6.58 5153	2.74 200	22.70 1654	25	7.54	**15.4±1.6**	13.56±0.33	1.54	22
	S3	200	6.58 5153	3.51 192	27.45 1502	32	6.9	**15.4±1.5**	13.37±0.25	1.05	17
SECTION 2	**S4**	800	6.58 5153	3.01 190	21.69 1370	30	64.6	**16.4±1.4**	13.61±0.29	1.42	24
	S5	900	6.58 5153	3.17 215	28.44 1931	30	33.9	**13.3±1.1**	13.81±0.26	1.65	41
	S6	1000	6.58 5153	1.24 89	8.46 607	30	99.9	**17.3±2.1**	13.74±0.48	1.60	11
	S7	1100	6.58 5153	3.18 169	24.59 1307	20	7.1	**15.4±1.6**	14.23±0.20	0.7	12
	S8	1230	6.58 5153	2.61 144	19.84 1095	30	55.4	**15.5±1.5**	14.23±0.41	1.10	7
	S9	1300	6.58 5153	2.46 173	15.69 1237	38	79.8	**16.5±1.5**	13.98±0.06	0.12	4
	S10	1470	6.58 5153	4.04 141	33.05 1154	25	71.9	**14.4±1.4**	14.34±1.04	1.47	2
SECTION 3	**S11**	850	6.58 5153	2.26 170	8.89 668	30	<1	**27.6±4.0**	12.25±0.87	2.45	8
	S12	950	6.58 5153	3.34 308	7.80 3.44	30	7.01	**50.3±4.6**	10.60±0.58	3.19	30
	S13	600	6.58 5153	3.56 214	23.16 1393	20	7.46	**18.5±1.5**	13.37±0.26	1.33	25
	S14	675	6.58 5153	2.06 126	13.72 811	20	<1	**18.7±2.4**	13.51±0.89	2.18	6

Table 1 – AFT data

Notes: ρ_d, ρ_i: standard and induced track densities measured on mica external detectors; ρ_s: spontaneous track densities on internal mineral surfaces; n_d, n_i and n_s: number of tracks on external detectors and on mineral surfaces. n_g: number of counted mineral grains; $P(\chi^2)$: χ^2 probability (Galbraith, 1981). Lm: mean length of confined tracks length distribution ± standard error, s.d.: standard deviation, n: number of measured lengths.

Probably, the recent normal faults that cut across the whole nappe stacking may have affected also section 2, displacing the samples and breaking their correlation with the altitude. From section 1, composed by only three samples, we obtain a mean exhumation rate of 0.2 mm/yr.

5. Discussion

The Sila Massif represents a key-sector to investigate the structural characteristics of the most internal (i.e. east-southeast foreland-ward) tectonic units of the Calabrian accretionary wedge. Published regional-scale cross-section (e.g. Caggianelli & Prosser, 2001) outline that structuration in this area occurred by thrust systems involving both lower crust rocks and sedimentary units. In this work, we detailed the structural architecture and the kinematic features relative to this thrusting event. Structural data show that the major thrusting direction is mostly towards the ENE. Imbrication of thrust sheets determines a complex structured edifice composed of allochthonous sheets bounded by major south-westward dipping thrust surfaces.

As aheads proposed in previously published regional-scale cross-sections (e.g. Lanzafame & Tortorici, 1980; Caggianelli & Prosser, 2001; Liotta et al., 2004), our observations on the geometrical-structural architecture (i.e. attitude of the foliation) of rocks at the hanging-wall (granite antiform) and at the foot-wall rocks (overturned sinform in the anagenites and limestone) account for a ENE-verging thrust geometry (Fig. 3). Nevertheless, meso-scale structural dataset indicate that the early thrust tectonic was subsequently reworked by NW-SE striking transpressive (or back-thrust) tectonics, responsible of the final juxtaposition between the granite and the Jurassic sequence.

In the Longobucco area, structural work outlines that the structural architecture is controlled by thrust-sheet systems inducing the stacking of granitic bodies on top of the Paludi Formation (Eocene flysch unit). All the nappe stacking edifice was sealed by Tortonian to Messinian sedimentary deposits (Rossano basin, Barone et al., 2008). Subordinate late transcurrent faults rework the nappe stacking. Absolute timing of deformation is constrained by recent stratigraphic work (Bonardi et al., 2005) that describes an Aquitanian nannoflora in the Paludi Formation. Our thermochronological dataset confirms that exhumation of granitic bodies of the Sila Unit passed throughout the PAZ in a time spanning from 18 to 13 Ma. A break-in-slope in the age versus altitude diagram (Fig. 11) shows the base of the paleo-PAZ and the corresponding age indicates the onset of this exhumation phase. Rock exhumation occurs either tectonically in the footwall of low-angle extensional faults, or through erosion (Ring et al., 1999). In compressive settings, tectonics may exert an indirect control on exhumation because of erosion promoted by upward motion of fault-bound blocks. We interpret the cooling event starting at 17-18 Ma, as revealed through the apatite FT data, as caused by erosion enhanced by the upward movement of the rocks due to the activity of the Longobucco thrust.

The nature of the Longobucco thrusting episode can be revealed throughout the integration with the published dataset for the Calabria complex (Fig. 3). This dataset implies that structuration of the Calabrian basement units is generally younger toward the foreland, then reflecting a forward-propagating sequence. Our fission track analyses suggest that the activity of the Longobucco thrusting (i) truncates a formerly emplaced tectonic edifice (mostly defined by the deep-seated metamorphic units), (ii) is coeval with episode of post-orogenic extension affecting the innermost domains (Coastal Chain and Sila Piccola), (iii) occurred in a structural position behind the outer deformation front. These data suggest that the Longobucco thrusting is out-of-sequence with respect to the eastward-southeastward thrust toward the foreland.

The NE-thrusting episode revealed in the Longobucco area represents part of a broader accretionary process related to the growth of the Calabrian wedge. A similar structure is evident below the Crotone-Spartivento forearc basin, in front of the Crotone peninsula (Fig. 13). There we can observe the crystalline unit of the Sila Massif, thrust on top of Eocene-Oligocene flysch unit or pre-Tertiary carbonates (not well defined).

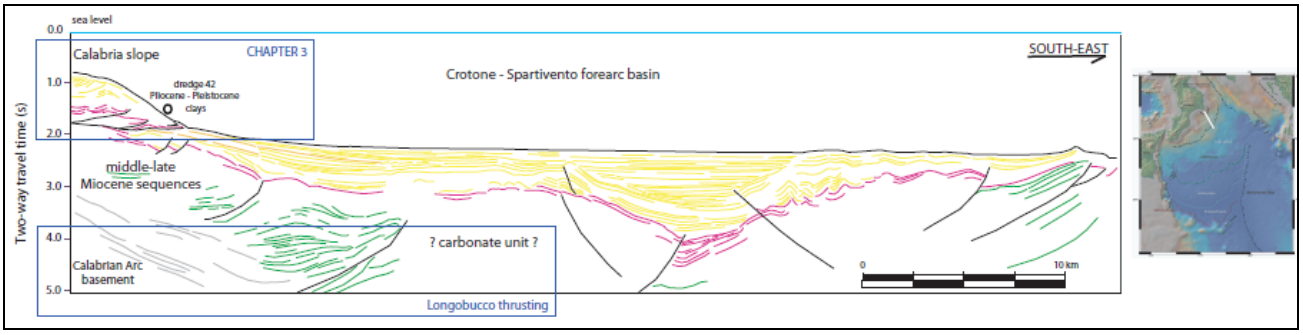

Figure 13 – Line drawing, NW-SE oriented, crossing the Crotone-Spartivento basin. Similar of Longobucco thrusting in lower blue box.

6. Dynamic of the Calabrian accretionary complex

The integration of the presented dataset and the published one helps to propose a tectonic model for the evolution of the Calabrian accretionary complex from its onset until to 16 Ma, which can be summarized in four key steps: the orogenic accretion (frontal accretion and underplating); the syn-orogenic exhumation of HP rocks; the out-of-sequence thrusting; the late-to-post-orogenic extension of the wedge.

The orogenic accretion (45?-30 Ma): underplating of the oceanic and some continental-derived rocks (mostly from Adria domain and subordinate European ones, such as the Castagna Unit in the Coastal Chain) accreted at the base of the orogenic wedge. The wedge thickened, and HP metamorphism developed in both oceanic and continental rocks in the axial region of the wedge (the present-day Coastal Chain and Sila Piccola: Gimigliano area). Frontal accretion was only at the expenses of more surficial terrains and not induce metamorphism. In

terms of dynamic of the wedge, one can be assumed that its growth was achieved under steady-state condition, such as vertical thickness (*h* parameter) and propagation of the thrust front (*l* parameter) increased constantly and independently.

The syn-orogenic exhumation period (30-25 Ma): with the onset of continental collision, continental material was introduced in the subduction and MP-metamorphism developed in the continental units of the Peloritani Mountains (the Mandanici and the San Marco d'Alunzio units). During this step, the strong coupling between upper and lower continental plates induced the migration of the frontal thrust. Thus, continuous tectonic plate convergence was absorbed by internal deformation of the wedge and its subsequent thickening (the *h* parameter increases). In terms of wedge dynamics, the wedge reached the overcritical configuration and a drastic change in dynamic from continuous underplating to syn-orogenic extensional setting occurred in the axial portion of the wedge (e.g. Platt, 1986). Crustal thinning developed by elision of material within the wedge and exhumation of deep-seated rocks along major normal detachment structures was favoured.

The out-of-sequence thrusting period (20-16 Ma): at the end of the syn-orogenic exhumation, probably the wedge fell in the undercritical condition and a new assessment of its structure was necessary. At this time, probably, diffuse (out-of-sequence) thrusting occurred in the CPA, in order to regain the steady-state configuration of the wedge. In this framework, we relate the formation of the Longobucco thrusting and the emplacement of European granitic bodies on top of Paludi Formation in the Sila Massif. Furthermore, this precise event can be recognised as responsible for the Aspromonte Unit emplacement on top of the Peloritani units in the eastern Sicily. These two situations are also chronologically constrained by the involvement of late-orogenic sediments: the Paludi Formation in the Sila Massif and the Stilo-Capo d'Orlando in the Peloritani Mountains). Evidences of post-detachment thrusting in Sila Massif were also described by Rossetti et al. (2001). The out of sequence thrusting recognized in the Longobucco area can be related to a diffuse phase of shortening observed in the internal sector of the Calabrian accretionary prism, which probably occurred when both retrograde migration of the slab and back-arc extensional processes stopped (Faccenna et al., 2004). This phase can be related to continental collision along different segments of the subduction front or to interaction and deformation of the slab at its arrival at the 660 km discontinuity (Faccenna et al., 2001).

The late-to-post-orogenic assessment of the wedge (16 Ma onward): although (out-of-sequence) thrusting occurred to restore the critical configuration of the wedge, post-orogenic extensional setting dominating the inner portions of the wedge (e.g. the Coastal Chain), and brittle normal structures controlled the deposition of sedimentary sequences in the Tyrrhenian facing basins (e.g. Amantea, Belvedere basins). In the Sila Massif, occurrence of transpressive structures (e.g. Van Dijk et al., 2000) might be occurred being partially superimposed on the previous structured belt. These structures might rework the kinematic and the geometry of the Longobucco thrust producing top-to-the-NW transpressive shear planes.

On the other hand, in the frontal portions of the CPA the wedge remained dominated by accretion and foreward propagation as testified by the wedge top basin outcropping both onland and offshore (Crotone and Rossano basin) afterwards deformed.

7. Conclusions

This work provides timing and structural constraints on the accretionary phase of the Calabrian wedge in pre-Messinian time. The Sila massif represents key area to understand the geometry of the nappe stacking in the internal portion of the Calabrian accretionary wedge. Structures, similar in age and by the units involved, are clear by observed in seismic reflection profiles in shallow water area near the Ionian Calabrian coast, below the present Crotone-Spartivento forearc basin. The AFT analysis constitute a valid tool for constraining the time-space evolution of the Calabrian accretionary wedge. Geological relationship between Sila crystalline unit, carbonate platform unit and synorogenic flysch are in agreement with the geometry hypothesized from the geological interpretation of the seismic reflection profiles for the inner portion of the accretionary wedge. This work adds information on the reconstruction of time-space evolution of the wedge between 40-30 Ma to 15 Ma.

REFERENCES

Acquafredda P., Lorenzoni S., Zanettin Lorenzoni E., 1994. Paleozoic sequences and evolution of the Calabrian-Peloritan Arc (Southern Italy). Terra Nova, 6, 582-594.

Alvarez W., Cocozza T., Wezel F. C., 1974. Fragmentation of the Alpine orogenic belt by microplate dispersal. Nature, 248, 309-314.

Amodio Morelli L., Bonardi G., Colonna V., Dietrich D., Giunta G., Ippolito F., Liguori V., Lorenzoni S., Paglionico A., Perrone V., Piccarreta G., Russo M., Scandone P., Zanettin-Lorenzoni, Zuppetta E.A., 1976. L'Arco Calabro- Peloritano nell'orogene Appenninico-Maghrebide. Memorie della Società Geologica Italiana, 17, 1-60.

Argentieri A., Mattei M., Rossetti F., Argnani A., Salvini F., Funiciello R., 1998. Tectonic evolution of the Amantea Basin (Calabria, southern Italy): Comparing in-land and off-shore data. Annales Tectonicae, XII, 79–96.

Atzori P., Cirrincione R., Del Moro A., Pezzino A., 1994. Structural, metamorphic and geochronologic features of the Alpine event in the south-eastern sector of the Peloritani mountains (Sicily). Periodico di Mineralogia, 63, 113- 125.

Barone M., Dominici R., Muto F., Critelli S., 2008. Detrital modes in a late Miocene wedge-top basin, Northeastern Calabria, Italy: compositional record of wedge-top partitioning . Journal of Sedimentary Research, 78, DOI: 10.2110/jsr.2008.071.

Beccaluva L., Chiesa S., Delaloye M., 1981. K/Ar age determinations on some Tethyan ophiolites, Rend. Soc. Ital. Mineral. Petrol., 37, 869-880.

Beccaluva L., Macciotta L., Spadea P., 1982. Petrology and geodynamic significance of the Calabria-Lucania ophiolites, Rend. Soc. Ital. Mineral. Petrol., 38, 937-982.

Bigi G., et al., 1990. Structural model of Italy, sheets 4–6, in Progetto Finalizzato Geodinamica, SELCA, Florence.

Bonardi G., Compagnoni R., Del Moro A., Messina A., Perrone V., 1987. Riequilibrazioni tettonometamorfiche alpine nell'Unita` dell'Aspromonte (Calabria meridionale), Rend. Soc Ital. Mineral. Petrol., 42, 301.

Bonardi G., De Capoa P., Di Staso A., Perrone V., Sonnino M., Tramontana M., 2005. The age of the Paludi Formation: a major constraint to the beginning of the Apulia-verging orogenic transport in the northern sector of the Calabria–Peloritani Arc. Terra Nova, 17, 331–337.

Bonardi G., De Capoa P., Fioretti B., Perrone V., 1994. Some remarks on the Calabria-Peloritani Arc and its relationships with the southern Apennines. Bollettino di Geofisica Teorica e Applicata 36, 483-492.

Bonardi G., Cavazza W., Perrone V., Rossi S., 2001. Calabria-Peloritani Terrane and northern Ionian Sea, in Anatomy of an Orogen: The Apennines and the Adjacent Mediterranean Basins, edited by G. B. Vai and J. P. Martini, pp. 287-306, Kluwer Acad., Norwell, Mass.

Borsi S. and Dubois R., 1968. Données géochronologiques sur l'histoire hercynienne et Alpine de la Calabre Centrale, C. R. Acad. Sci., Ser. D, 266, 72-75.

Brunet C., Monié P., Jolivet L., Cadet J.P., 2000. Migration of compression and extension in the Tyrrhenian Sea, insights from 40Ar/39Ar ages on micas along a transect from Corsica to Tuscany. Tectonophysics, 321, 127-155.

Caggianelli A. & Prosser G., 2001. An exposed cross-section of late Hercynian upper and intermediate continental crust in the Sila nappe (Calabria, southern Italy). Periodico di Mineralogia, 70, 277-301.

Carmignani L., Kligfield R., 1990. Crustal extension in the Northern Apennines: the transition from compression to extension in the Alpi Apuane core complex. Tectonics, 9, 1275-1303.

Cello G., Mazzoli S., 1996. Kinematics of primary contacts between low- and relatively high-pressure rocks in orogens, J. Struct. Geol., 18, 519-522.

Cifelli F., Mattei M., Hirt A.M., Gunther A., 2004. The origin of tectonic fabrics in "undeformed'' clays: The early stages of deformation in extensional sedimentary basins: Geophysical Research Letters, v. 31, L09064, doi: 10.1029/2004GL019609.

Cirrincione R. & Pezzino A., 1994. Nuovi dati strutturali sulle successioni mesozoiche metamorfiche dei M. Peloritani orientali. Bollettino della Società Geologica Italiana 113, 195-203.

Critelli S., 1999. The interplay of lithospheric flexure and thrust accommodation in forming stratigraphic sequences in the Southern Apennines foreland basin system, Italy: Accademia Naturale dei Lincei, Rendiconti Lincei Scienze Fisiche e Naturali, serie IX, v. 10, p. 257–326.

De Gregorio S., Rotolo S.G., Villa I.M., 2003. Geochronology of the medium to high-grade metamorphic units of the Peloritani Mts., Italy. International Journal of Earth Sciences 92, 852-872.

Dercourt, J., Zonenshain, L.P., Ricou, L.E., Kazmin, V.G., Le Pichon, X., Knipper, A.L., Grandjacquet, C., Sbortshikov, I.M., Geyssant, J., Lepvrier, C., Pechersky, D.H., Boulin, J., Sibuet, J.C., Savostin, L.A., Sorokhtin, O., Westphal, M., Bazhenov, M.L., Lauer, J.P., Biju-Duval, B., 1986. Geological evolution of the Tethys belt from the Atlantic to the Pamirs since the Lias. *Tectonophysics*, **123**, 241-315.

De Roever E.W.F., Piccarreta G., Beunk F.F., 1974. Blue amphiboles from northwestern and central Calabria (Italy), Period. Mineral., 43, 1-37.

Dewey J.F., Helman M.L., Turco E., Hutton D.H.W., Knott S.D., 1989. Kinematics of the western Mediterranean. In Alpine Tectonic, edited by M. P. Coward and D. Dietrich. Geological Society London Special Publication, 45, 265- 283.

Dubois R., 1970. Phases de serrage, nappes de socle et métamorphisme alpin à la junction Calabre Apennin: Sur la suture calabro-apenninique, Rev. Geol. Dyn. Geogr. Phys., 12, 221-254.

Dubois R., 1976. La suture calabro-apenninique Crétacé-Eocène et l'ouverture tyrrhènienne Néogène: étude pétrographique et structurale de la Calabre centrale, 567 pp. Thèse, Université P. et M. Curie, Paris.

Faccenna C., Becker T.W., Lucente F.P., Rossetti F., 2001. History of subduction and back-arc extension in the central Mediterranean. Geophysical Journal International, 145, 809-820.

Faccenna C., Mattei M., Funiciello R., Jolivet L., 1997. Styles of back-arc extension in the Central Mediterranean. Terra Nova, 9, 126-130.

Faccenna C., Piromallo C., Crespo-Blanc A., Jolivet L., Rossetti F., 2004. Lateral slab deformation and the origin of the western Mediterranean arcs. Tectonics, 23, TC1012, doi:10.1029/2002TC001488.

Fügenschuh B. and Schmid S.M., 2003. Late stages of deformation and exhumation of an orogen constrained by fission-track data: a case study in the Western Alps. Geological Society of American Bulletin, 115, 1425-1440.

Gallagher K., 1995. Evolving temperature histories from apatite fission-track. Earth and Planetary Science Letters, 136, 421-435.

Graessner T., Schenk V., Bröcker M., Mezger K., 2000. Geochronological constraints on the timing of granitoid magmatism, metamorphism and post-metamorphic cooling in the Hercynian crustal cross-section of Calabria. Journal of Metamorphic Geology, 18, 409-421.

Green P. F., Duddy I. R., Gleadow A. J. W., Tingate P.R., and Laslett G. M.,1986. Thermal annealing of fission tracks in apatite 1. A qualitative description. Chem. Geol., 59, 237-253.

Green P.F. and Duddy I.R., 1989. Some comments on paleotemperature estimation from apatite fission tracks analysis. J. Petr. Geol., 12, 111-114.

Heymes T., Bouillin J.P., Pêcher A., Monié P., Compagnoni R., 2008. Middle Oligocene extension in the Mediterranean Calabro-Peloritan belt (southern Italy): Insights from the Aspromonte nappes pile. Tectonics, 27, TC2006, doi:10.1029/2007TC002157.

Gurrieri S., Lorenzoni S., Zanettin-Lorenzoni E., 1978. L'aureola metamorfica di contatto dei "graniti" dell'Unità di Longobucco (Sila). Bollettino della Società Geologica Italiana, 97, 717-726.

Haccard, D.C., Lorenz C., Grandjacquet C., 1972. Essai sur l'évolution tectogénétique de la liasion Alpes-Apennines (de la Ligurie à la Calabre), Mem. Soc. Geol. Ital., 11, 309-341.

Hurford A.J., and Green P.F., 1983. The zeta age calibration of fission-track dating. Isotope Geoscience. 1, 285-317.

Hurford A.J., 1990. Standardization of fission track dating calibration: recommendation by the Fission Track Working Group of the I.U.G.S. Subcommission on Geochronology: Chemical Geology, 80, 171-178.

Iannace A., Bonardi G., D'Errico M., Mazzoli S., Perrone V., Vitale S., 2005. Structural settino and tectonic evolution of the Apennine Units of northern Calabria. Compte Rendu Geoscience, 337, 1541-1550.

Iannace A., Vitale S., D'Errico M., Mazzoli S., Di Staso A., Macaione E., Messina A., Reddy S.M., Somma R., Zamparelli V., Zattin M., Bonardi G., 2007. The carbonate tectonic units of northern Calabria (Italy): a record of Apulian palaeomargin evolution and Miocene convergence, continental crust subduction, and exhumation of HP–LT rocks. Journal of the Geological Society, London, 164, 1165-1186.

Jolivet L., Faccenna C., Goffé B., Mattei M., Rossetti F., Brunet C., Storti F., Funiciello R., Cadet J.P., d'Agostino N., Parra T., 1998. Midcrustal shear zones in post-orogenic extension: Example from the northern Tyrrhenian Sea (Italy). Journal of Geophysical Research, 103, 12123-12160.

Ketcham R.A., 2005. Forward and Inverse Modeling of Low-Temperature Thermochronometry Data. Reviews in Mineralogy & Geochemistry, 58, 275-314.

Langone A., Gueguen E., Prosser G., Caggianelli A., Rottura A., 2006. The Curinga-Girifalco fault zone (northern Serre, Calabria) and its significance within the Alpine tectonic evolution of the western Mediterranean. Journal of Geodynamics, 42, 140-158.

Lanzafame G. and Tortorici L., 1980. Le successioni Giurassico-Eoceniche dell'area compresa tra Bocchigliero, Longobucco e Propalati (Calabria). Riv. Ital. Paleont., 86, 31-54.

Lentini F., Catalano S., Carbone S., 2000. Carta geologica della Provincia di Messina (scala 1:50000). Società Elaborazioni Cartografiche (S.EL.CA. eds), Florence.

Lotta D., Festa V., Caggianelli A., Prosser G., Pascazio A., 2004. Mid-crustal shear zone evolution in a syn-tectonic late Hercynian granitoid (Sila Massif, Calabria, southern Italy). International Journal of Earth Sciences, 93, 400-413.

Lorenzoni S., Messina A., Russo S., Stagno F., Zanettin Lorenzoni E., 1978. Le magmatiti dell'Unità di Longobucco (Sila - Calabria). Bollettino della Società Geologica Italiana, 97, 727-738.

Lorenzoni S. & Zanettin Lorenzoni E., 1983. Note illustrative alla Carta Geologica della Sila alla scala 1:200.000. Memorie della Società Geologica Italiana, 36, 317-342.

Malinverno A. & Ryan W., 1986. Extension in the Tyrrhenian Sea and shortening in the Apennines as result of arc migration driven by sinking of the lithosphere. Tectonics, 5, 227–245.

Massoli D., Koyi H.A., Barchi M.R., 2006. Structural evolution of a fold and thrust belt generated by multiple décollements: analogue models and natural exmaples from the Northern Apennines (Italy. Journal of Structural Geology, 28, 185-199.

Mattei M., Cipollari P., Cosentino D., Argentieri A., Rossetti F., Speranza F., 2002. The Miocene tectonic evolution of the southern Tyrrhenian Sea: Stratigraphy, structural and paleomagnetic data from the on-shore Amantea Basin (Calabrian arc, Italy). Basin Research, 14, 147-168.

Messina A., Russo S., Borghi A., Colonna V., Compagnoni R., Caggianelli A., Fornelli A., and Piccarreta G., 1994. Il Massiccio della Sila. Settore settentrionale dell'arco Calabro–Peloritano: Societa` Geologica Italiana Bollettino, 113, 539-586.

Messina A., Somma R., Macaione E., Carbone G. & Careri G., 2004. Peloritani continental crust composition (southern Italy): geological and petrochemical evidence. Bollettino della Società Geologica Italiana, 123, 405-441.

Ogniben L., 1962, Le Argille Scagliose e i sedimenti messiniani a sinistra del Trionto (Rossano, Cosenza). Geologica Romana, 1, 255–282.

Ogniben L., 1973. Schema geologico della Calabria in base ai dati odierni. Geologica Romana, 12, 243-585.

Patacca E., Sartori R. Scandone P., 1990. Tyrrhenian basin and Apenninic arcs: kinematic relation since late Tortonian times. Memorie della Società Geologica Italiana, 45, 425-451.

Platt, J.P. and Compagnoni, R. 1990. Alpine ductile deformation and metamorphism in a Calabria basement nappe (Aspromonte, South Italy). *Eclogae Geologicae Helvetiae* **83**, 41-58.

Roda C., 1964. Distribuzione e facies dei sedimenti neogenici nel Bacino Crotonese. Geologica Romana, 3, 319-366.

Rosenbaum G. & Lister G.S., 2004. Neogene and Quaternary rollback evolution of the Tyrrhenian Sea, the Apennines, and the Sicilian Maghrebides. Tectonics, 23, TC1013, doi: 10.1029/2003TC001518.

Rossetti F., Faccenna C., Goffé B., Monié P., Argentieri A., Funiciello R. and Mattei M., 2001. Alpine structural and metamorphic signature of the Sila Piccola Massif nappe stack (Calabria, Italy): Insights for the tectonic evolution of the Calabrian Arc. Tectonics 20, 112-133.

Rossetti F., Goffé B., Monié P., Faccenna C., Vignaroli G., 2004. Alpine orogenic PTt deformation history of the Catena Costiera area and surrounding regions (Calabrian Arc, southern Italy): the nappe edifice of Northern Calabria revised with insights on the Tyrrhenian–Apennine system formation. Tectonics, 23, 1-26.

Royden L., Patacca E., Scandone P., 1987. Segmentation and configuration of subducted lithosphere in Italy: an important control on thrust belt and foredeep-basins evolution. Geology, 15, 714-717.

Schenk V., 1980. U-Pb and Radiometric Dates and their Correlation with Metamorphic Events in the Granulite-Facies Basement of the Serre, southern Calabria (Italy). Contributions to Mineralogy and Petrology, 73, 23–38.

Spadea P., Tortrici L., Lanzafame G., 1976. Serie ofiolitifere fra Tarsia e Spezzano Albanese (Calabria): Stratigrafia, petrografia, rapporti strutturali. Mem. Soc. Geol. Ital., 17, 135-174.

Tansi C., Muto, F., Critelli, S., Iovine, G., 2007. Neogene-Quaternary strike-slip tectonics in the central Calabrian Arc (southern Italy). Journal of Geodynamics, 43, 393-414.

Van Dijk J.P., Bello M., Brancaleoni G.P., Cantarella G., Costa V., Frixa A., Golfetto F., Merlini S., Riva M., Torricelli S., Toscano C., Zerilli A., 2000. A regional structural model for the northern sector of the Calabrian Arc (southern Italy). Tectonophysics, 324, 267-320.

Vignaroli G., Rossetti F., Theye T., Faccenna C., 2008. Styles and regimes of orogenic thickening in the Peloritani Mountains (Sicily, Italy): new constraints on the tectono-metamorphic evolution of the Apennine belt. Geological Magazine, 145, 552-569.

Wallis S.R., Platt J.P. and Knott S.D., 1993. Recognition of syn-convergence extension in accretionary wedges with examples from the Calabrian Arc and the eastern Alps, Am. J. Sci., 293, 463-495.

Zuffa G.G., Gaudio W., Rovito S., 1980. Detrital mode evolution of the rifted continental-margin Longobucco Sequence (Jurassic), Calabrian Arc. Journal of Sedimentary Petrology, 50, 51-61.

INTRODUCTION

In the last years, several studies and research were focused on geohazards in marine coastal areas (platform and slope) and offshore environment. The Ionian sea is characterized by active subduction processes and relative growth and accretion of a huge sedimentary wedge. It records also physical phenomenon related to evolution of geologically active and young area (volcano, earthquake, landslide, tsunami). More recent origin of Italian continental margin implies the existence of dangerous for coastal urban area for mobility and instability of sediments related to morphosedimentary trend, as for example Ionian side of Calabro-Peloritani Arc, regional uplifting area and centre of compressive events, and Malta Escarpment, steep continental slope tectonically reactivated.

The analysis of seismic reflection profiles in the Ionian offshore allow to describe the recent evolution of an active continental margin in two target area, which are characterized by gravity instability triggered by very different causes.

- Messina tsunami. In the central sector of the Malta escarpment the 1908 Messina and Reggio Calabria earthquake have triggered a medium size landslide, resulting in tsunami that struck the Italian coast. The critical point is the instability of sedimentary cover along this steep continental slope.
- Crotone landslide. The gravity instabilities that involves the recent unit of the Crotone basin is related to the presence at depth of thick unit of Messinian evaporitic sediments which movements induced by basal slope can produce active deformation on the upper level (Brun & Fort, 2004).

Abstract

A century after the catastrophic event, the sources of the 1908 Messina, Southern Italy, earthquake and tsunami, which caused at least 60,000 deaths, remain uncertain. Through a simple backward ray-tracing method, we convert the tsunami travel-time data reported in a 100-years-old paper into distances and find that the sources of the earthquake and tsunami are different. Overturning a long-held assumption, reconsideration of the available tsunami, bathymetric, seismic, and seismological data indicates that the tsunami was generated by an underwater landslide.

1. Introduction

As coastal settlements expand, locating and monitoring areas threatened by tsunami are concerns for local and international authorities responsible for mitigation of this hazard. On 28 December 1908, at 5.21 a.m., local time, a catastrophic earthquake (MCS maximum intensity = XI, estimated magnitude = 7.1) struck the region of the Messina Straits, Ionian Sea, Southern Italy. Within minutes after the passage of the seismic waves, a tsunami with maximum observed runup of about 10 m hit the coasts of Calabria and Sicily (Figure 1) [*Platania*, 1909; *Baratta*, 1910; *Boschi et al*., 1989, 2000]. The earthquake and tsunami caused major destruction and at least 60,000 deaths. One hundred years later, the source of the tsunami is still uncertain. Our hypothesis is that the 1908 Messina tsunami was not caused by vertical displacement of the seafloor during coseismic rupture as previously thought (www.noaa.gov) but by an underwater landslide. To test this hypothesis, we analyzed all available tsunami, bathymetric, seismic, and seismological data to revue previous interpretations and present our new conclusions.

2. Brief Seismotectonic Setting

Eastern Sicily and southern Calabria (Figure 1) have a historical record of destructive earthquakes [*Boschi et al*., 2000]. These regions lie along the Africa-Eurasia convergent plate boundary in the central Mediterranean area, where the Apenninic-Maghrebian orogenic wedge has grown since at least the Oligocene. Geodetic and seismological data show that both the Messina Straits and Ionian Sea are actively undergoing extension [*Goes et al*., 2004], possibly in connection with the south-eastward rollback of the Ionian slab that is subducting beneath Calabria and Sicily. Accordingly, an earthquake has been interpreted as the source of the 1908 Messina tsunami, with the rupture located along a N-to-NE-striking normal fault located in the northern sector of the Messina Straits [*Boschi et al*., 1989; *Tinti and Armigliato*, 2003]. A N-striking, E-dipping fault has been recently proposed through a refined inversion of seismological and geodetic data (Figure 1a) [*Amoruso et al*.,

2006]. Among all the various faults proposed as the source of the 1908 Messina earthquake [*Tinti and Armigliato*, 2003], the fault proposed by *Amoruso et al*. [2006] has the southernmost central portion, which is the most tsunamigenic portion of a fault because it is where the maximum slip occurs.

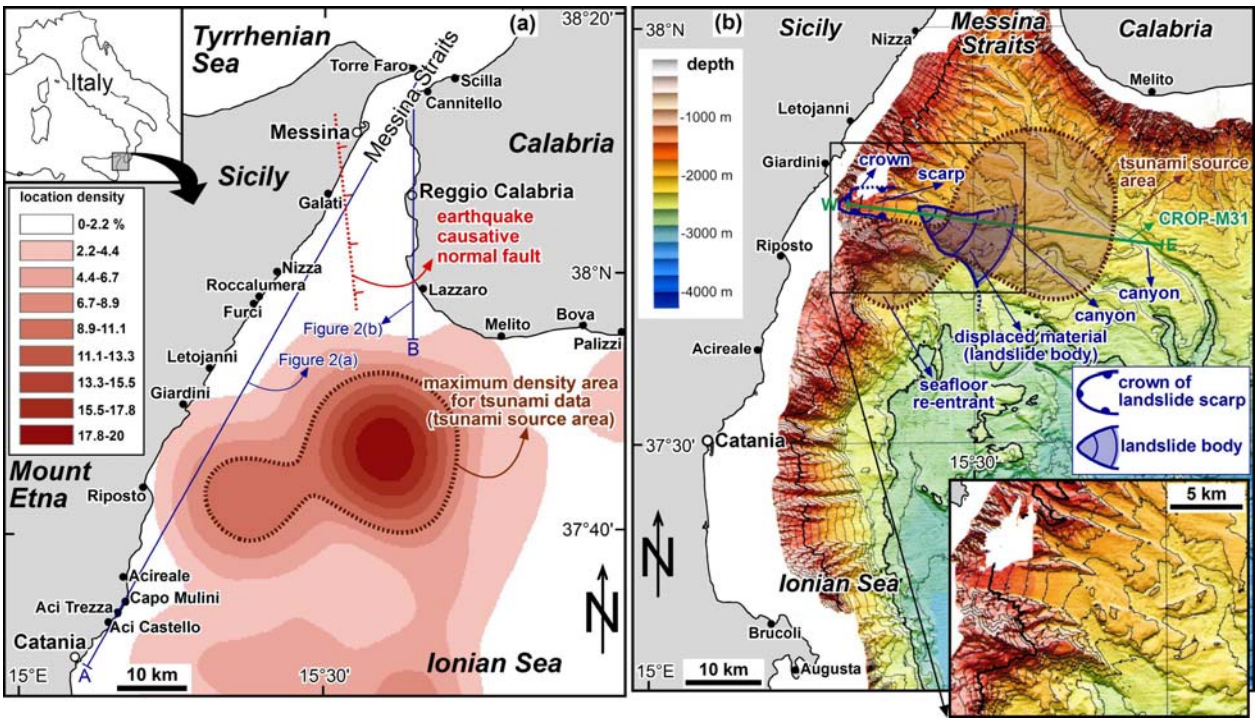

Figure 1 - (a) Map of Ionian Sea and adjacent areas, Southern Italy. Red-to-pink shadings are contours on the density distribution of backward ray-traced locations obtained by inverting travel-times of the 1908 Messina tsunami into distances. The complete ray-tracing analysis is shown in Figure S1. Tsunami travel-time data are listed in Table S1. Location coordinates are listed in Table S2. The region with a location density greater than 8.9 % is here considered the probable area of origin for the tsunami and is indicated with a brown dashed line. The hypothetical causative fault for the 1908 Messina earthquake is drawn after *Amoruso et al*. [2006]. (b) Bathymetric map of the Ionian seafloor (Figure S2) [*Marani et al*., 2004]. The probable area of origin for the 1908 Messina tsunami includes a submarine large landslide possibly slid along the Sicilian slope off Giardini, where a landslide scarp and crown are shown.

3. Methods and Results

Immediately after the 1908 Messina earthquake and tsunami, through surveys and numerous interviews and questionnaires distributed among the survivors, *Omori* [1909] and *Platania* [1909] reported the tsunami runup and the delay between the earthquake and tsunami arrivals for several cities and villages located along the Calabrian and Sicilian coasts. Afterward, *Baratta* [1910] conducted a new survey and then combined and compared his data with those from *Omori* [1909] and *Platania* [1909], thus producing a critically integrated data set of delays between the earthquake and tsunami arrivals. Here we use this data set to find the tsunami source area. For tsunami runup only, we use also the data from *Platania* [1909].

Assuming an approximately simultaneous (i.e. within a few seconds) generation of the earthquake and tsunami as for example *Okal et al*. [2003] did for the 1947 Aleutian tsunami, most of the reported delays between the earthquake and tsunami arrivals correspond to tsunami travel-times. For 9 out of a total of 32 sites, the reported tsunami travel-times are not relevant either because they are not sufficiently accurate (i.e. reported in the form such as "a few minutes") or because in these locations the tsunami runup was small and barely discernible (i.e. runup smaller than 1 m, Table S1).

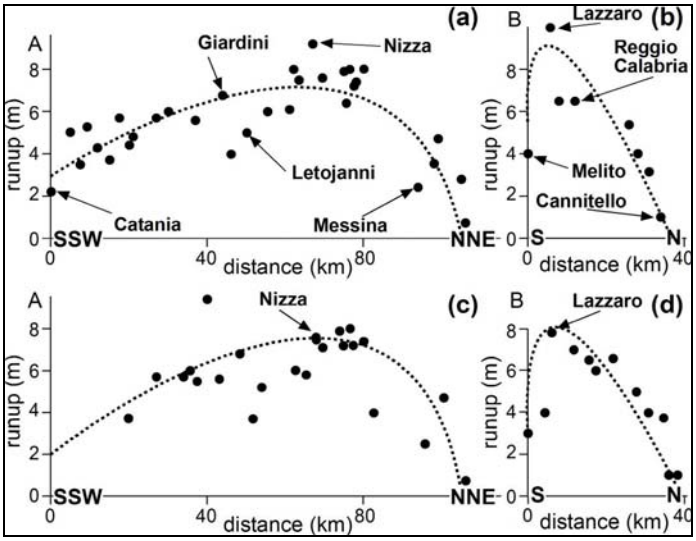

Figure 2 - Above, tsunami runup versus distance diagrams along the (a) Sicilian and (b) Calabrian coasts. Distances correspond to the A and B tracks in Figure 1(a). Dashed lines are indicative of data trend. Runup data are from *Baratta* [1910]. Below (c) and (d), same diagrams of (a) and (b) drawn by using runup data from *Platania* [1909] as reviewed by *Tinti* [2007].

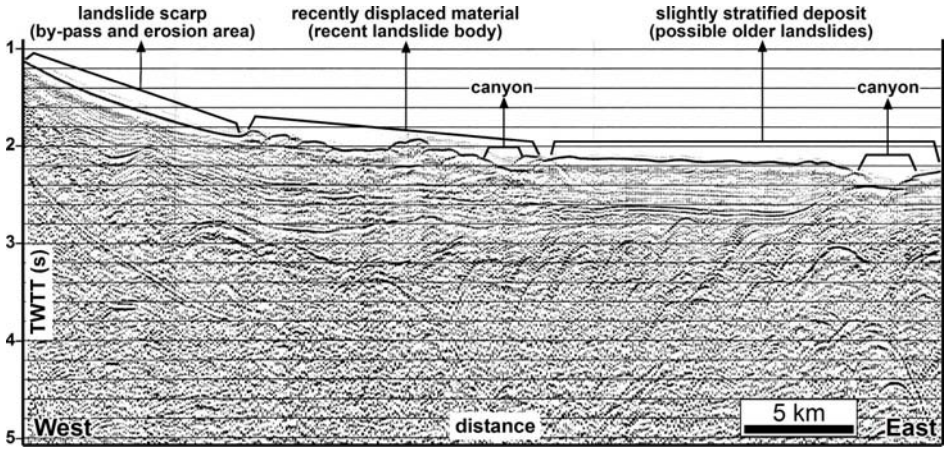

Figure 3 - CROP-M31 seismic reflection profile across the Ionian Sea [*Scrocca et al*., 2004]. Profile track is shown in Figure 1(b). TWTT is two-ways-travel-time.

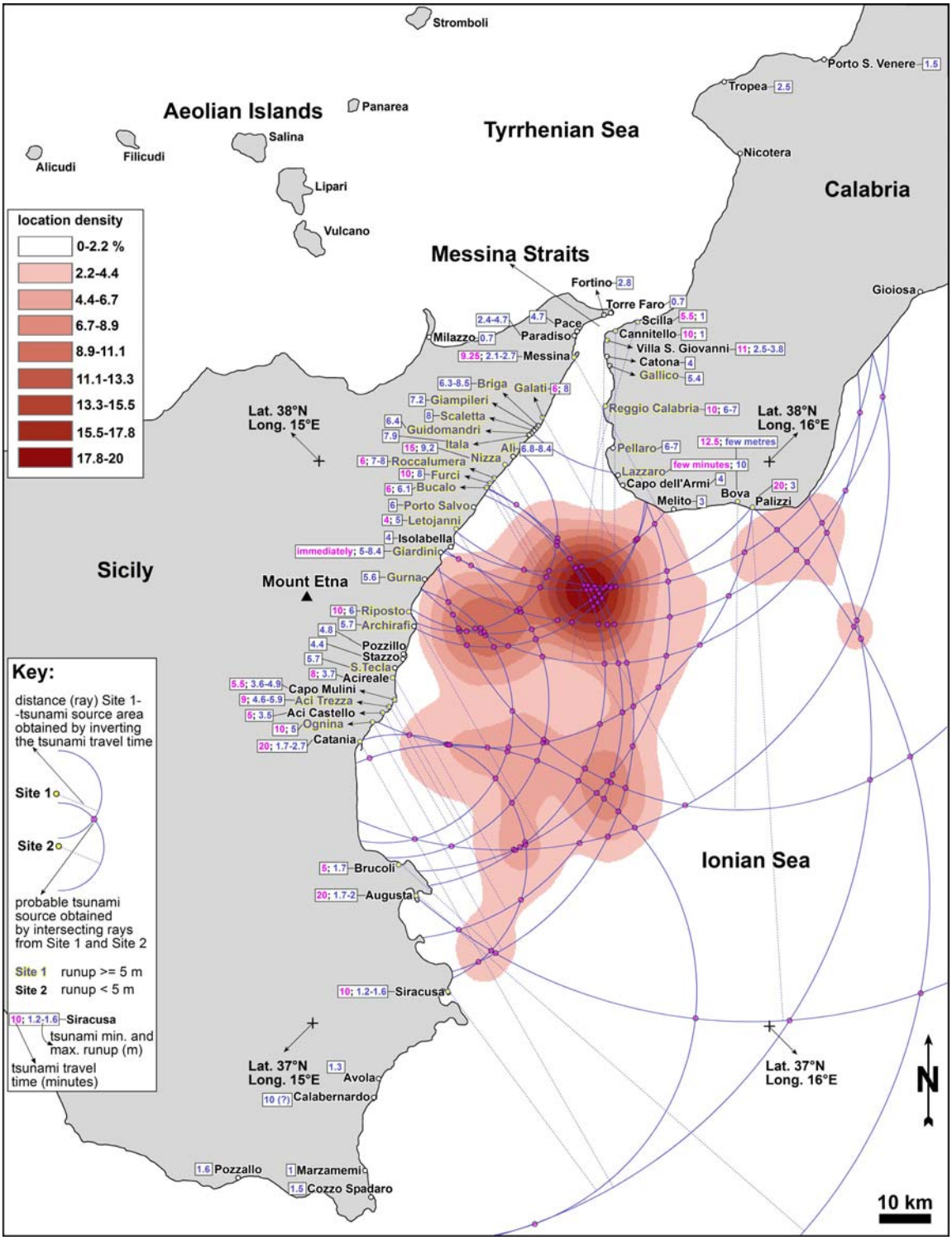

Figure 4 - Density map of the probable tsunami source area. The map is obtained by intersecting ray traces from each site (backward ray tracing method). For each localities are indicated tsunami runup and tsunami travel time.

Coastal localities	latitude N	longitude E	reported travel-time (minutes)	used travel-time (minutes)	reported runup height (m)	reason for data exclusion
Messina	38°11'30''	15°33'55''	8.50-10	9.25	2.1-2.7	
Paradiso	38°13'36''	15°34'06''	non-reported	non-used	2.4-3.7	unknow time
Pace	38°14'08''	15°34'22''	non-reported	non-used	4.7	unknow time
Fortino	38°15'55''	15°39'01''	non-reported	non-used	2.8	unknow time
Torre Faro	38°15'57''	15°38'23''	5-20	non-used	0.7	indefinite time
Milazzo	38°13'00"	15°14'57"	non-reported	non-used	0.7	unknow time
Galati	38°06'00''	15°30'18''	5-7	6	8	
Briga	38°04'37''	15°29'35''	non-reported	non-used	6.3-8.5	unknow time
Giampileri	38°03'39''	15°28'31''	non-reported	non-used	7.2	unknow time
Scaletta	38°02'23''	15°27'09''	non-reported	non-used	8	unknow time
Guidomandri	38°02'56''	15°28'08''	non-reported	non-used	6.4	unknow time
Itala	38°02'05''	15°27'04''	non-reported	non-used	7.9	unknow time
Alì	38°01'07''	15°26'26''	non-reported	non-used	6.8-8.4	unknow time
Nizza	37°59'34''	15°24'42''	15	15	9.2	
Roccalumera	37°58'26''	15°23'17''	6	6	7-8	
Furci	37°58'06''	15°23'03''	10	10	8	
Bucalo	37°57'18''	15°22'38''	6	6	6.1	
Porto Salvo	37°55'46''	15°21'16''	non-reported	non-used	6	unknow time
Letojanni	37°52'55''	15°18'09''	4	4	5	
Isolabella	37°51'08"	15°17'59"	non-reported	non-used	4	unknow time
Giardini	37°49'43"	15°16'04"	immediately	non-used	5-8.4	indefinite time
Gurna	37°47'05''	15°14'02''	non-reported	non-used	5.6	unknow time
Riposto	37°43'54"	15°12'16"	10	10	6	
Archirafi	37°42'32''	15°13'05''	non-reported	non-used	5.7	unknow time
Pozzillo	37°39'39''	15°11'46''	non-reported	non-used	4.8	unknow time
Stazzo	37°38'53''	15°11'27''	non-reported	non-used	4.4	unknow time
S. Tecla	37°38'01''	15°10'31''	non-reported	non-used	5.7	unknow time
Acireale	37°37'02''	15°10'10''	8	8	3.7	
Capo Mulini	37°34'36''	15°10'39''	5-6	5.5	3.6-4.9	
Aci Trezza	37°33'47''	15°09'45''	8-10	9	4.6-5.9	
Aci Castello	37°33'00''	15°08'59''	5	5	3.5	
Ognina	37°31'54''	15°06'55''	10	10	5	
Catania	37°29'58"	15°05'33"	20	20	1.7-2.7	
Brucoli	37°17'10''	15°11'10''	5	5	1.7	

Augusta	37°14'20''	15°13'14''	20	20	1.7-2	
Siracusa	37°03'53"	15°17'22"	10	10	1.2-1.6	
Avola	36°54'50''	15°09'06''	a few seconds	non-used	1.3	indefinite time
Calabernardo	36°52'22''	15°08'04''	30	non-used	10?	uncertain runup
Marzamemi	36°44'27''	15°06'44''	a few minutes	non-used	1	indefinite time
Cozzo Spadaro	36°41'12''	15°08'14''	non-reported	non-used	1.5	unknown time
Pozzallo	36°43'29''	14°50'32''	non-reported	non-used	1.6	unknown time
Reggio Calabria	38°06'45''	15°39'03''	10	10	6-7	
Gallico	38°09'51''	15°38'49''	non-reported	non-used	5.4	unknow time
Catona	38°11'01''	15°38'19''	non-reported	non-used	4	unknow time
Villa S. Giovanni	38°13'00"	15°38'00"	10-12	11	2.5-3.8	
Cannitello	38°13'53''	15°38'43''	10	10	1	
Scilla	38°15'18''	15°42'52''	5-6	5.5	1	
Nicotera	38°32'50''	15°56'02''	25	non-used	non-reported	unknown runup
Tropea	38°40'53"	15°54'08"	non-reported	non-used	2.5	unknow time
Porto S. Venere	38°42'54''	16°07'31''	non-reported	non-used	1.5	unknow time
Pellaro	38°01'19''	15°38'50''	a few minutes	non-used	6-7	indefinite time
Lazzaro	37°57'40''	15°40'22''	non-reported	non-used	10	unknow time
Capo dell'Armi	37°57'15''	15°40'44''	non-reported	non-used	4	unknow time
Melito	37°55'27''	15°47'09''	a few minutes	non-used	3	indefinite time
Bova	37°55'50''	15°55'30''	10-15	12.5	few metres	unknown runup
Palizzi	37°55'12''	15°59'33''	20	20	3	
Gioiosa	38°17'39''	16°19'31''	a few seconds	non-used	non-reported	indefinite time

Table 1 - Coastal localities of eastern Sicily and southern Calabria (Southern Italy), struck by the 1908 Messina tsunami. Tsunami reported travel-time and runup height data are from *Baratta* [1910]. Used travel-times (underlined localities) are the data used for the tsunami backward ray-tracing shown in Figure S1. Localities are listed by region (Messina to Pozzallo are in Sicily, whereas Reggio Calabria to Gioiosa are in Calabria) and from north to south.

The tsunami travel-times from the remaining 23 sites were processed by a backward ray-tracing method. Tsunami backward ray-tracing analyses based on historical accounts have been previously successful in locating the source area of several tsunamis older than the one here studied [e.g. *Baptista et al.*, 1998]. Unlike previous studies, we do not analyze historical accounts from untrained observers; rather, we analyze data collected and processed by scientists, who considered and mitigated possible biases by selecting and properly weighting the eyewitness accounts [*Omori*, 1909; *Platania*, 1909; *Baratta*, 1910]. For instance, accounts by railway station masters and officers of the watch, who were working at the time of events and for whom temporal

observations were important, were considered particularly accurate and formed the reference framework [*Baratta*, 1910]. To account for uncertainty, we present the results as contours on the density distribution of the backward ray-traced locations (Figure S1). If travel-times and assumptions used in the ray-tracing analysis are accurate, we would expect a concentration of ray traces in a tightly-defined source area (Figure 4).

The celerity of shallow water long waves in deep water is $c = (g\,d)^{0.5}$, where g is the gravity acceleration and d is the local seafloor depth. A preliminary analysis of tsunami data (i.e. site-by-site runup and travel-times of tsunami, Figure 4) allowed us to find an approximate location of the source area of the 1908 tsunami in the Ionian Sea off Giardini on the Sicily coast, and off Lazzaro on the Calabria coast (Figure 1a and Table S1). The tsunami maximum runup and shortest travel-times were in fact recorded near these locations. The approximate source area for the 1908 Messina tsunami lies at about 2000 m below the sea level and corresponds to the toe of steep slopes occurring along the Calabrian and Sicilian continental margins (Figure 1). By using a seafloor depth of 2000 m, we calculate the tsunami velocity in the source area to have been about 500 km/h (140.0 m/s). Assuming a decrease of the tsunami velocity with reduced seafloor depth toward the coasts, and assuming a tsunami minimum velocity (i.e. when hitting the coasts) of about 100 km/h (27.8 m/s), we estimate an average tsunami velocity of about 300 km/h (83.3 m/s). A velocity of about 100 km/h for the tsunami close to the coast is appropriate for steep coasts such as those surrounding the Ionian Sea. By using the average velocity of 300 km/h, we convert the tsunami travel-times (Table S1) for our 23 data points into distances from the tsunami source area. By using these distances as radii of circles centered on the sites to which the tsunami travel-times refer, we find 132 locations in the Ionian Sea marking the intersections between the 23 circles (Figure S1). The locations are concentrated in the sector above-defined as the approximate source area of the tsunami (i.e. off Letojanni and Lazzaro, Figure 1), thus validating the preliminary location of the tsunami source and confirming the general accuracy of the tsunami travel-time data [*Baratta*, 1910] and estimated average velocity (300 km/h). In this general area and in the adjacent ones, the presence of large debris bodies at the toe of the Calabrian and Sicilian continental slopes is inferred from the seafloor bathymetry (Figure 1b). In detail, the tsunami source area we identify includes a large landslide body with a headwall scarp lying offshore of Giardini on the Sicilian coast (Figure 1b). From the bathymetric map (Figure 1b), at least 20 km^3 of displaced material is estimated for this landslide. The Ionian bathymetric map does not show any other large landslide bodies with associated large scarps and crowns in this region. To the south of the landslide shown in Figure 1(b), in the large seafloor re-entrant located off Riposto, we find no evidence for a landslide and, therefore, this feature is not a collapse niche or at least not a recent one. It is possible that an older landslide body is masked by a cover of younger sediments.

The CROP-M31 seismic reflection profile across the Ionian Sea (Figure 2) cuts through the sector considered here as the candidate source area for the 1908 Messina tsunami (Figure 1b). In the seismic image, the area

interpreted as the landslide scarp on the seafloor bathymetry is displayed as a smooth and curved incline between the Sicilian coast and the Ionian bathyal plain, whereas the landslide body at the toe of the scarp is displayed as a chaotic accumulation of material with a very irregular upper surface (i.e. the seafloor), which is not covered by younger sediments. This evidence suggests a recent age for the collapse of this chaotic material along the Sicilian slope. A faintly layered body occurs close to the seafloor in the east of the recently displaced material lying at the toe of the Sicilian slope. The seafloor overlying this body is nearly planar and horizontal. We interpret this body as a debris cone [*Ryan and Heezen*, 1965] more compact and, therefore, older than the adjacent one toward the west. No major faults are imaged in the CROP-M31 profile beneath or across the above-depicted surficial bodies (Figure 2).

To determine whether the landslide is a possible cause of the tsunami, we spatially analyze the related runup reported by *Baratta* [1910]. In Figures 3(a) and 3(b), we observe maximum heights in the area of the landslide shown in Figure 1 and a rapid drop toward both the north and the south. We observe very similar patterns also by using runup data from *Platania* [1909] as reviewed by *Tinti* [2007] (Figures 3c and 3d). The observed spatial pattern of runup is typical of landslide-tsunamis rather than earthquake-tsunamis [*Synolakis et al*., 2002]. This is also shown by the ratio of maximum runup to the width of its distribution along the coast. This ratio is greater than 10^{-4} that is characteristic of landslide-tsunamis [*Okal and Synolakis*, 2004].

Baratta [1910] reports also on the tsunami leading waves along beaches [*Tadepalli and Synolakis*, 1994]. A significant leading depression was observed along all the Sicilian coast, particularly at Scaletta (~150 m), Letojanni (~100 m), Giardini (~200 m), Catania (~200 m), and Brucoli (~200 m). In contrast, along all the Calabrian coast, no significant leading depression was described except at Scilla (~30 m), Pellaro (~20 m), and Bova (a few meters) (see localities in Figures 1 and S1). In synthesis, these data indicate a significant leading wave depression in Sicily and suggest a leading wave elevation in Calabria.

To determine whether the causative fault of the 1908 Messina earthquake (Figure 1a) may have triggered the landslide shown in Figure 1(b), we estimate the Coulomb stress change produced by the earthquake. Source parameters of the causative fault are from the most recently published analyses [*Amoruso et al*., 2002, 2006]. The regional extensional stress is modeled assuming an intensity of 40 bar [*Jacques et al*., 2001] and a N115°E orientation of the minimum compressive stress [*Goes et al*., 2004]. Figure 4 shows that the Coulomb stress change in the area of the landslide is positive between about 0.1 and 0.4 bar. Such a stress change is compatible with an earthquake-landslide causal relationship [e.g. *Atakan and Ojeda*, 2005].

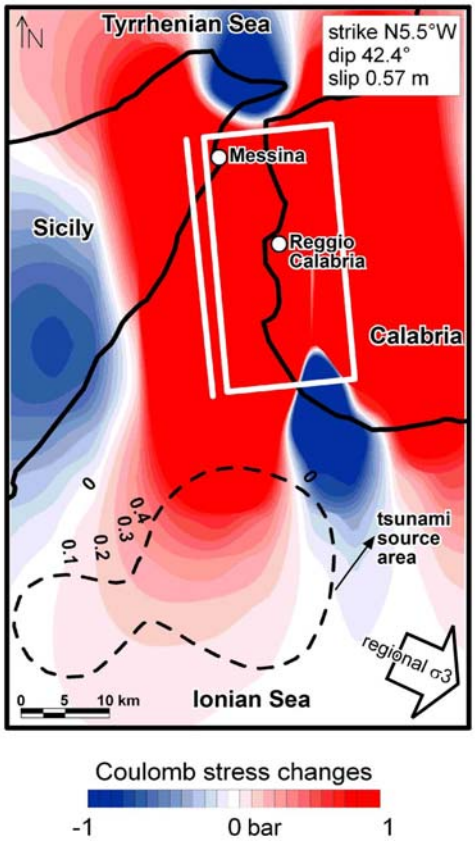

Figure 5 - Coulomb stress changes at 1.5 km depth produced by the 1908 Messina earthquake in presence of a regional stress (indicated by a white arrow). The white rectangle and line represent the surface projection of the seismogenic fault and the intersection of the fault plane with the surface, respectively. The black dashed line indicates the probable area of origin for the tsunami (Figure 1).

4. Discussion and Conclusions

Since the catastrophic events of December 1908, there is consensus on the hypothesis that the Messina earthquake epicenter was located in the northern Ionian region close to the narrowest section of the Messina Straits (i.e. close to the Messina city, Figure 1), and that the tsunami was concurrently generated by the seafloor displacement during coseismic rupture [*Tinti and Armigliato*, 2003]. Macroseismic, seismological, and geodetic data [*Baratta*, 1910; *Boschi et al*., 1989] show that the northern Ionian region close to the Messina Straits is beyond doubt the most suitable location for the causative fault of the 1908 Messina earthquake (Figure 1a), but an earthquake along this fault does not account for the reported tsunami travel-time and runup data (Figures 3 and S1). Although our tsunami ray-tracing analysis may be constrained by our assumptions concerning the tsunami velocity, the triangular shape of the Ionian Sea and the tsunami arrival data from the opposite coasts of the Ionian Sea (Figure 1, Table S1) allow us to locate unequivocally the tsunami source in the Ionian Sea off Giardini and Lazzaro (Figure 1). This location is at least 40 km in the south of the region where the earthquake maximum MCS intensity was recorded [*Baratta*, 1910; *Boschi et al*., 2000] and is clearly external to the source area of the earthquake (Figure 1a) [*Boschi et al*., 1989]. Recent earthquake

and tsunami modeling, based on the data collected soon after the events, has shown that finding a reliable tsunami source that matches both leveling data and tsunami runup is very difficult [*Tinti and Armigliato*, 2003]. This is because runup data are much better explained by a source significantly southward of the source location that accounts for the leveling data, which can be explained by a causative fault as drawn in Figure 1(a), or even further toward the north [*Boschi et al*., 1989]. The modeling work by *Tinti and Armigliato* [2003], together with the evidence presented in this paper indicates that the earthquake caused the surface depression but not necessarily the tsunami. *Omori* [1913] reached this same conclusion. By critically examining the hypothesis that the tsunami was generated by the seafloor displacement during coseismic rupture, the only suitable alternative to explain the generation of the tsunami is by a underwater landslide. Our results suggest that an important alternative candidate for the tsunami trigger is the recent submarine landslide located off Giardini (Figures 1 and 2). No further recent landslides are recognized in the studied portion of the Ionian Sea, thus the landslide off Giardini is the only possible cause for the 1908 Messina tsunami. The tsunami runup and leading waves as reported by *Baratta* [1910] are consistent with this landslide. The runup cannot be accounted for by the most likely earthquake rupture location in the north of the area [*Tinti and Armigliato*, 2003]. Even by ignoring the effect of the dynamic stress (i.e. the passage of the seismic waves), which is usually far greater than the Coulomb stress change, this latter alone is demonstrated as sufficiently effective at triggering the shown landslide (Figure 4).

Ryan and Hazeen [1965] concluded that, in the southeastern Ionian basin, at about 150 km from the landslide observed in Figure 1(b), the breakage of submarine telegraph cables immediately subsequent to the 1908 Messina earthquake is directly associated with a turbidity current, which originated from an underwater avalanche within the Messina Straits area. As supporting evidence, they found shallow turbiditic deposits in cores drilled in the region where the telegraph cables were broken.

We conclude that the source for the 1908 Messina tsunami was not the seafloor displacement during coseismic rupture, as thought previously. The source was a submarine landslide in the Ionian Sea. This study shows the importance of base research (post-tsunami field surveys in this case; e.g. *Synolakis and Kong* [2006]) consisting of accurate data that may result essential in the solution of complex problems even after a century from the data collection. Also, it improves the statistics of landslide-tsunamis, which have often been too simplistically interpreted as sourced by earthquakes [e.g. *Tappin et al*., 2001].

REFERENCES

Amoruso, A. et alii 2002, Source parameters of the 1908 Messina Straits, Italy, earthquake from geodetic and seismic data, *J. Geophys. Res*., *107*, doi:10.1029/2001JB000434.

Amoruso, A., L. et alii 2006, Spatial relation between the 1908 Messina Straits earthquake slip and recent earthquake distribution, *Geophys. Res. Lett*., *33*, doi:10.1029/2006GL027227.

Atakan, K., and A. Ojeda 2005, Stress transfer in the Storegga area, offshore mid-Norway, *Mar. Petrol. Geol.*, *22*, 161-170.

Baptista, M. A. et alii 1998, Constraints on the source of the 1755 Lisbon tsunami inferred from numerical modelling of historical data, *J. Geodyn.*, *25*, 159-174.

Baratta, M. 1910, La catastrofe sismica Calabro-Messinese (28 dicembre 1908), 496 pp., Società Geografica Italiana, Rome.

Boschi, E. et alii 1989, Modello di sorgente per il terremoto di Messina del 1908 ed evoluzione recente dell'area dello Stretto, Atti del Convegno GNGTS, pp. 245-258, CNR, Rome.

Boschi, E. et alii 2000, Catalogue of strong Italian earthquakes from 461 B.C. to 1997, *Ann. Geofis*., *43*, 609-868.

Goes, S. et alii 2004, A recent tectonic reorganization in the south-central Mediterranean, *Earth Planet. Sc. Lett.*, *226*, 335-345.

Jacques, E. et alii 2001, Faulting and earthquake triggering during the 1783 Calabria seismic sequence, *Geophys. J. Int.*, *147*, 499-516.

Marani, M. P. et alii (Eds.) 2004, Seafloor bathymetry of the Ionian Sea, 216 pp., APAT, Rome.

Okal, E. A., and C. E. Synolakis 2004, Source discriminants for near-field tsunamis, *Geophys. J. Int*., *158*, 899-912.

Okal, E. A. et alii 2003, Near-field survey of the 1946 Aleutian tsunami on Unimak and Sanak Islands, *B. Seismol. Soc. Am.*, *93*, 1226-1234.

Omori, F. 1909, Preliminary report on the Messina-Reggio earthquake of December 28, 1908, *Bull. Imp. Earthquake Invest. Comm.*, *3*, 37-46.

Omori, F. 1913, Note on the recent sea-level variation at the Italian and Austrian mareograph stations and on the cause of the Messina-Reggio earthquake, *Tokyo, Imp. Earthquake Inv. Comm. Bull*., *5*, 87-100.

Platania, G. 1909, Il maremoto dello Stretto di Messina del 28 dicembre 1908, *Boll. Soc. Sismol. It*., *13*, 369-458.

Ryan, W. B. F. and B. C. Heezen 1965, Ionian Sea submarine canyons and the 1908 Messina turbidity current, *Geol. Soc. Am. Bull*., *76*, 915-932.

Scrocca, D. et alii (Eds.) 2004, CROP Atlas, 197 pp., APAT, Rome.

Synolakis, C. E., and Kong, L. 2006, Runup measurements of the December 2004 Indian Ocean tsunami, *Earthquake Spectra*, *22*, S67-S91.

Synolakis, C. E. et alii 2002, The slump origin of the 1998 Papua New Guinea Tsunami, *P. Roy. Soc. Lond. A Mat*., *458*, 763-789.

Tadepalli, S. and C. E. Synolakis 1994, The Run-Up of N-Waves on Sloping Beaches, *P. Roy. Soc. Lond. A Mat*., *445*, 99-112.

Tappin, D. R. et alii 2001, The Sissano, Papua New Guinea tsunami of July 1998 - offshore evidence on the source mechanism. *Mar. Geol*., *175*, 1-23.

Tinti, S. 2007, I maremoti delle coste italiane, *Geoitalia*, *19*, 4-10.

Tinti, S., and A. Armigliato 2003, The use of scenarios to evaluate the tsunami impact in southern Italy, *Mar. Geol*., *199*, 221-243.

Introduction

Evolution of continental margin where salt layers are present has been well documented in offshore African (Angolan margin, Congo basin) and Brazil South Atlantic margin. Mediterranean regions, characterized by the occurrence of the thick salt deposits of Messinian age, are affected by several processes related to salt kinematics. Here we documented the case of the Crotone peninsula. We inferred the presence of a megalandslide (ML) moving on top of a weak, flat decollement localized in the Messinian evaporites from a study based on interpretation of seismic reflection profiles, well stratigraphy, adding to geological and bathymetric information. We clearly defined (thickness, age, kynematic) the offshore portion of the megalandslide and tried to interpreted the onshore prosecution by structural and geological evidences.

1. Geological setting

The Calabrian Arc formed by overthrusting of the Alpine and Tethys domain over the Mesozoic Apennine carbonate platform during the early Miocene (Fig. 1).

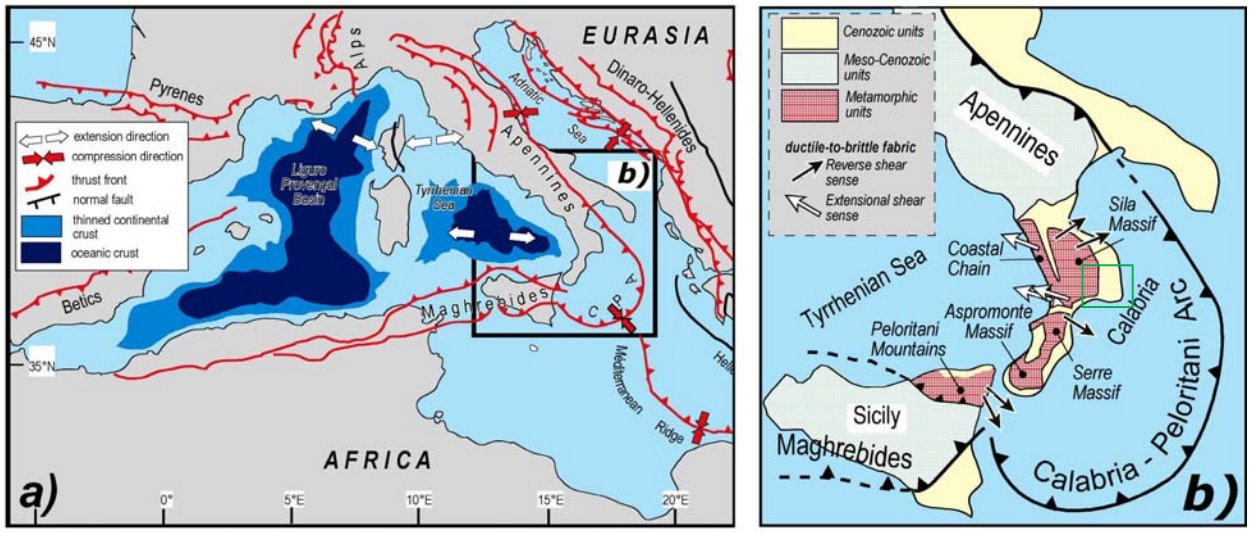

Figure 1 - (a) Synthetic tectonic map of the Tyrrhenian-Apennines system in the framework of the central Mediterranean region (modified after Jolivet *et al.*, 1998). (b) Geological sketch map of the Calabria-Peloritani Arc. The study area (Crotone peninsula) is included in the green box.

The southeastward migration of the Calabrian Arc related to the opening of the Tyrrhenian Basin from the Serravallian/Tortonian onwards (Mattei et al., 2002) led to passive subduction of the Ionian crust along an

inclined Benioff plane (Malinverno and Ryan, 1986; Moussat et al., 1986; Rehault et al., 1987; Patacca et al., 1990; Knott and Turco, 1991; Van Dijk and Scheepers, 1995).

During the Oligocene, the Calabrian Arc was affected by orogenic collapse through development of extensional shear zones in the inner sector of the accretionary complex (Rossetti et al. 2001; Rossetti et al. 2004), whereas the middle and late Miocene was characterized by overthrusting in the eastern domain (Ghisetti and Vezzani 1982a, 1982b; Malinverno and Ryan 1986; Rehault et al. 1986; Dewey et al. 1989; Roveri et al., 1992).

The eastern side of the Sila Massif, the main morphostructural high of the Ionian margin of northeastern Calabria, consists of pre-Mesozoic basement, made up of Hercynian metamorphics intruded by late Hercynian granitoids, covered by sedimentary upper Triassic – upper Liassic Longobucco group, unconformably overlie by Neogene to Quaternary dominantly clastic basinal successions.

The Rossano and Crotone basins (Ogniben 1962; Roda 1964), located on the northeastern margin of the Calabrian Arc at the northern and southeastern sectors, respectively, of the Sila Massif, are part of a larger Neogene basinal domain ranging as young as the early Messinian. The basinal domain also includes the Ciro` Basin (Roda 1964, 1967; Van Dijk et al. 2000), located in a position intermediate between the Rossano and Crotone basins, and characterized by lack of evaporitic sedimentation in the stratigraphic record during the early Messinian.

Rossano and Crotone basin represent two wedge-top basin (Barone et al., 2008) developed in the middle Miocene accretionary phase of the Calabrian Arc. During the Miocene the growing of the accretionary complex, due to Calabrian subduction, involved progressively in deformation the basement unit and the sedimentary series of the Crotone and Rossano basin.

The Messinian salinity crisis led to deposition on wide Mediterranean region of a massive salt formation. Salt thickness is around 500 m in the middle of the basin and wedge out both landward and seaward. From early Pliocene to the present day, post-salt sedimentation was entirely marine.

The recent Pliocene compressive phase, recognize onshore and in shallow water area, produces minor deformation in the Crotone area, and seems have been mainly affected by salt movements and large scale gravity tectonics (Roveri et al., 1992). On shore in the same time interval the Crotone basin was dominated by extensional faulting, controlling the geometry and thickness of sedimentary bodies, and later by strike-slip tectonics (Van Dijk, 2000; Zecchin et al., 2003).

Finally the Crotone basin underwent a phase of regional uplit started in the Middle-Late Pleistocene, as recorded by studies on the marine terraces (Roda, 1964; Ciaranfi et al., 1982; Massari et al., 2002; Zecchin et al., 2004).

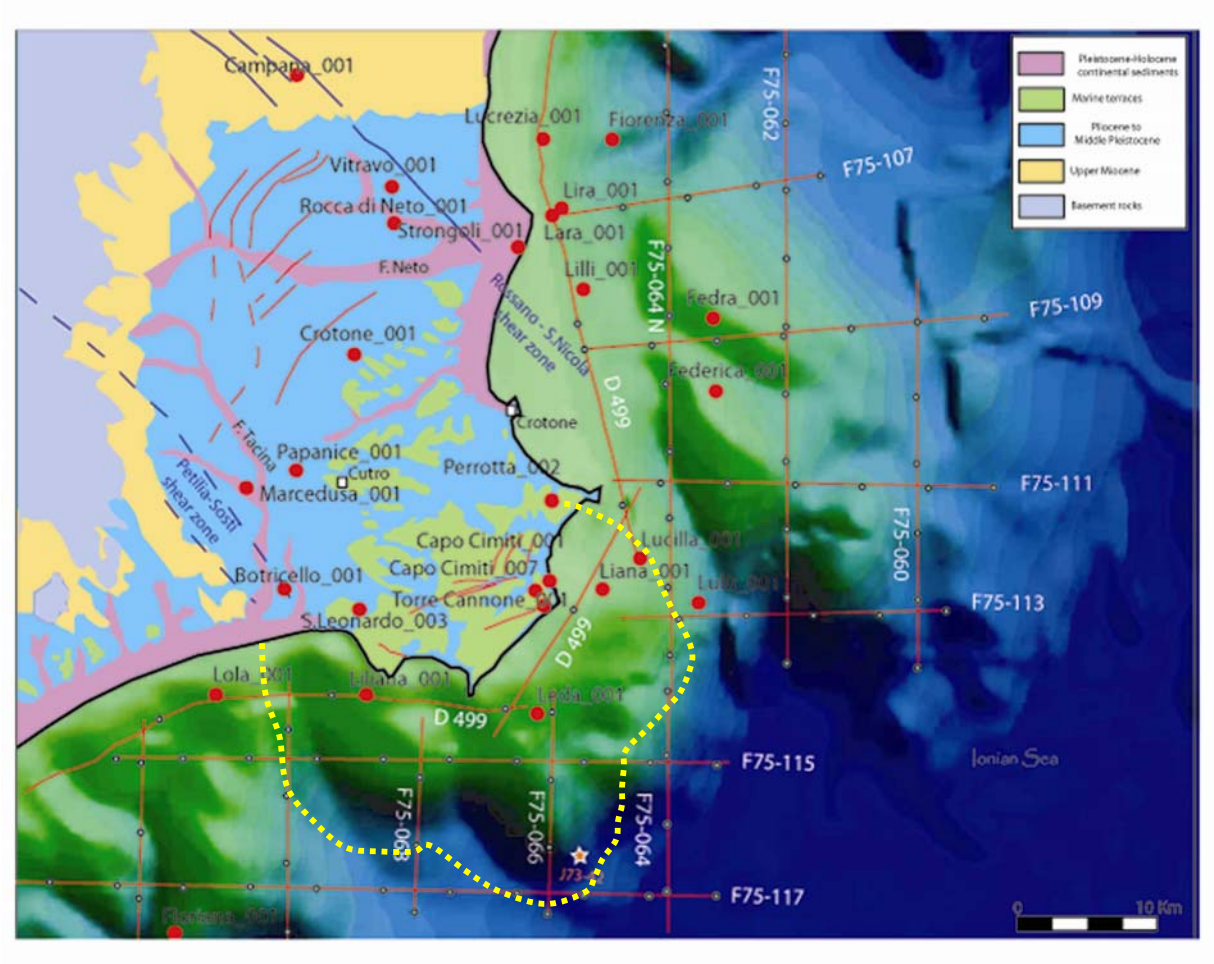

Figure 2 - Bathymetric data of the Ionian offshore and geological map of the Crotone peninsula (after Massari et al., 1999) whit main faults system. In map location of the seismic reflection profiles (Linee F) and available wells (red dots). White star indicate the dredge J73-42 (Rossi and Borsetti, 1974). In dotted yellow line the offshore extension of the megalandslide (ML).

2. Stratigraphic setting

Crotone basin represents the outcropping sector of a major basin, known as forearc Crotone-Spartivento basin (Rossi and Sartori, 1981), mainly located offshore, a type of thrust belt basin situated upon the internal slope of the Calabrian accretionary complex.

The Crotone Basin is bounded by two major NW trending left-lateral shear zones (Fig. 2), the Rossano–San Nicola shear zone (north) and the Petilia–Sosti shear zone (south) (Meulenkamp et al., 1986; Van Dijk, 1990, 1991; Van Dijk and Okkes, 1990, 1991). The stratigraphy of the Crotone Basin (Fig.3), showing several kilometers of Neogene deposits, was established by Ogniben (1955, 1962, 1973) and more extensively by Roda (1964, 1970, 1971), who recognized three major sedimentary cycles bounded by basin-wide unconformities

linked to structural basin reorganizations. The three units are: a Serravallian to Early Messinian unit, a Middle Messinian to Lower Pliocene unit, and a Middle Pliocene to Pleistocene unit.

More recent studies are those of Van Dijk (1990), Moretti (1993), Massari et al. (1999, 2002), and Zecchin et al. (2003, 2004).

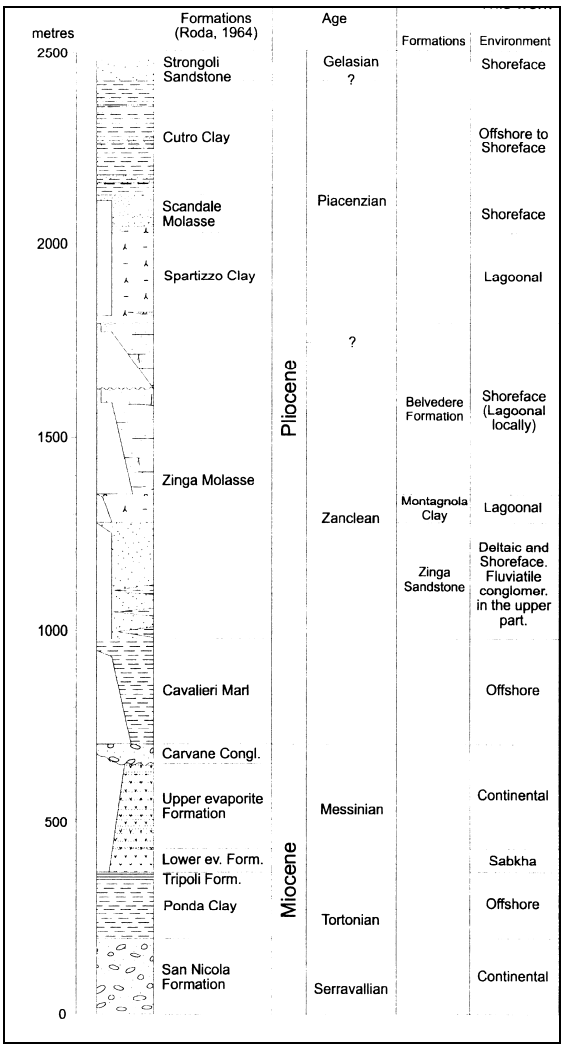

Figure 3 – Litostratigraphy scheme of the sedimentary succession in the northern Crotone basin following Roda, 1964 and Zecchin et al., 2003, 2004.

The first tectono-stratigraphic unit of Roda (1964) (Fig.3) starts with the Serravallian-Tortonian continental to shallow-marine San Nicola Formation, the offshore Ponda Clay, the diatomites of the lower Messinian Tripoli Formation and terminates with the first Messinian evaporitic cycle (Lower Evaporite Formation). The upper boundary of this first tectono-stratigraphic unit is an angular unconformity related to intra-Messinian tectonics (Roda, 1964a). This unconformity, recognizable throughout the Mediterranean region, possibly originated by the isostatic rebound of the Calabrian accretionary wedge after the drastic Messinian base level fall and consequent reduction of water load (De Celles and Cavazza, 1995; Cavazza and De Celles, 1998).

The second cycle, of Messinian to lower Pliocene age, began with deposition of the Messinian Upper Evaporite Formation and the fluvial Carvane Conglomerate. The basin was blanketed by the outer-shelf Cavalieri Marl, followed by the shallow-marine Zinga Molasse (Roda, 1964a). The latter unit was recently subdivided into three distinct formations called Zinga Sandstone, Montagnola Clay, and Belvedere Formation (Zecchin et al., 2003, 2004). A widespread angular unconformity marks the top of the second tectono-stratigraphic unit of Roda (1964a). The unconformity was probably induced by a generalized transpressional tectonic phase dated as late lower Pliocene–early middle Pliocene (Roda, 1964a; Van Dijk, 1990, 1991; Zecchin et al., 2004).

The third cycle encompasses the middle Pliocene to Pleistocene deposits. The basin recorded a long-term transgression (Spartizzo Clay and Scandale Molasse) and culminated with the complete blanketing of the basin by the offshore to slope Cutro Clay. The transgressive phase was then followed by a general regression, with deposition of the Pleistocene San Mauro Molasse in the central part of the Crotone Basin (Massari et al., 2002).

3. Well data

In order to better described the sedimentary sequences, and to calibrate the seismic reflection profiles we have choice to interpret six wells located inside the body of the megalandslide, four offshore (Liliana 1, Leda 1, Lulù 1 and Lucilla 1) and two onshore (Torre Cannone 1 and Botricello 1), and one well immediately out of the border of the slide (Lola 1). The wells have a total depth ranging from 1000 to 3000 m below sea level. The depths reported in fig. yy are related to height of rotary tables as indicated.

Summarizing the stratigraphic informations arising from the wells (Fig.4), and taking as reference the well Lola 1, out of the megalandslide, we found a stratigraphic succession made up of Serravallian (San Nicola) to Tortonian (Ponda) fining upward turbiditic sequences, resting on top of Limestone of Triassic-Jurassic age (equivalent of Longobucco group), followed by Messinian unit overlie by lower Pliocene clay (Argille di Crotone) up to Pleistocene.

In some wells (Liliana 1) the contact between Messinian and Pliocene is marked by an angular unconformity and in other case, mainly in the eastern side, the Messinian sequences are missing (Lucilla 1 and Lulù 1). In four wells inside the megalandslide on top of the Pliocene we find a repeated section of Messinian and Pliocene units. The contact is marked by a thrust that put older sediments above younger one. The main decollement is localized in the Messinian unit and moving upward in the section. In Torre Cannone 1 the tectonized domain localized in the Messinian sequence probably represents the decollement zone and, moving eastward, toward Lucilla 1 e Lulù 1 we can observe as the decollement localized itself in the Pliocene unit.

Velocity surveys and previous conversions found in AGIP reports have been very useful to make a conversion in depth of the time reflection profiles.

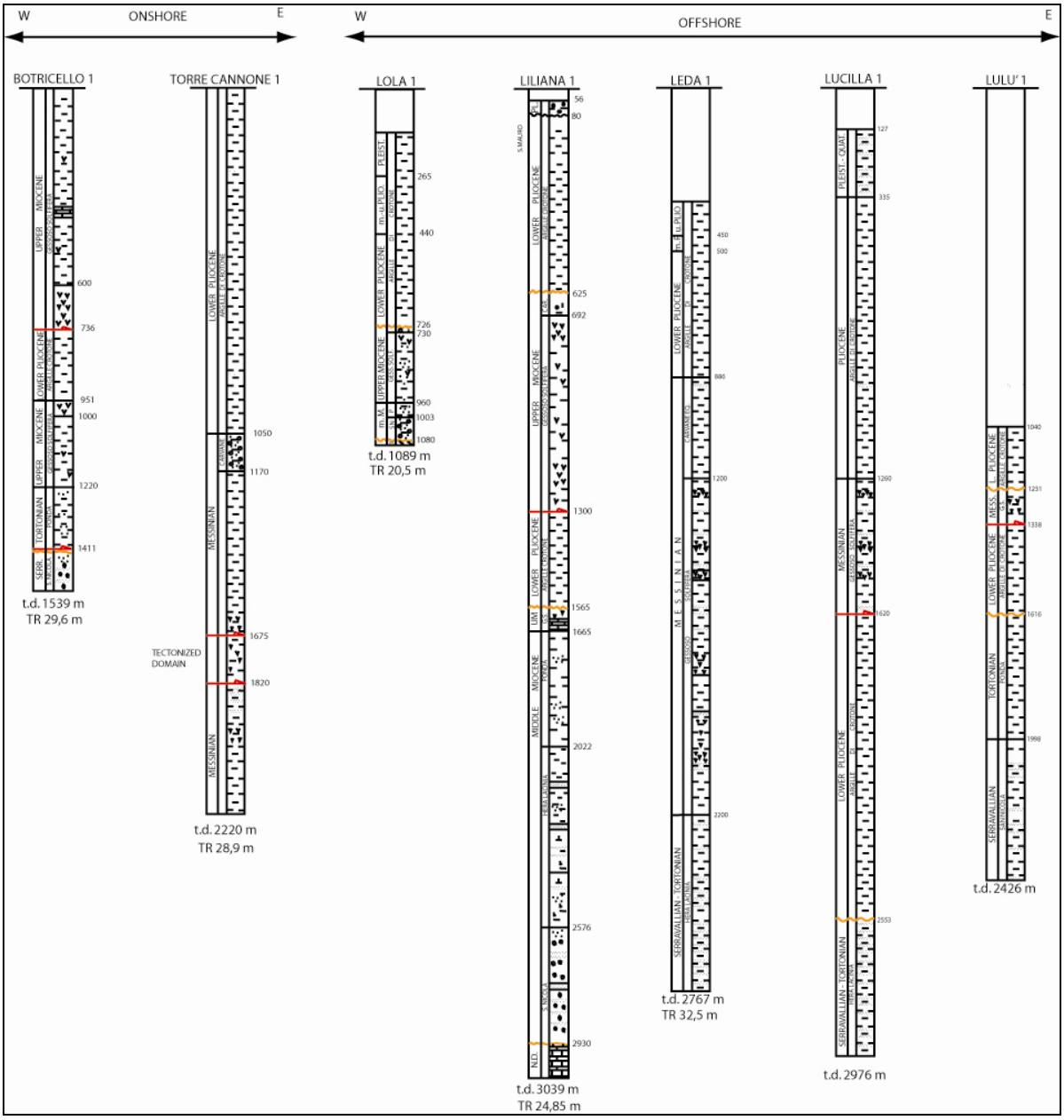

Figure 4 – Litostratigraphy columns of the wells used in this work. Depth indicated are referred to the height of the rotary table above sea level. The location of each wells in Fig. 2. In red the thrust and in orange the unconformity.

The decollement level of the megalandslide is situated around 1700 m below sea level near the coast, and it arrives at 1200 m near its frontal part. We find the most shallowest decollement in Botricello 1 (1000 m below s.l.) probably because the well is located near the border of the ML. In Leda 1 there is no evidence of detachment but the suspect thickness of Messinian sediments, not found in adjacent wells, probably implies a duplication in the Messinian sequence.

4. Seismic data

We have made the geological interpretation of the ENI (the Italian Ente Nazionale Idrocarburi)'s seismic data, acquired for hydrocarbon exploration in 1975, in order to investigate the evolution of this continental margin in a context of active geology (active subduction, regional uplift of the Sila massif and subsidence in the forearc basin). The seismic profiles (Linee commerciali zona F) are located in the Ionian offshore, in front of the Crotone peninsula.

The seismic sections, choice for this work, run NS and EW and cover the eastern and southern side of the Crotone peninsula (Fig.5). For better constrain the geological interpretation of the seismic profiles and calibrate them, we have used the hydrocarbon exploration boreholes available both onshore and offshore in the same area. Fig. 4 displays the lines-drawing of three parallel seismic sections, N-S oriented, located in the southern side of Crotone peninsula, in the Squillace Gulf, and two parallel profiles, E-W oriented, in the Ionian Sea. In all the five seismic profiles (Fig. 5) it is possible recognize a huge deformed body (ML), resting on top of a basement previously structured in different ways. The body of the megalandslide have chaotic seismic facies and evident deformations inside. The internal architecture of the slide seems to be composed of different thrust sheet stacking each onto other. Also the topographic profile, with ramp and flat geometry (Fig.5b) seems to be the result of the stacking and internal deformations in the body slide.

The Fig. 5 shows the volume of this huge gravity slide. The body have an average thickness of 1 s two-way traveltime. The contact with the unit below is very clear. The decollement layer of the ML seems very flat except at its tip where in some case steepens with classical geometry of ramp. According to well stratigraphy logs this gravity slide is made up of Messinian and Pliocene sequences covered by a thin layer (0,1-0,2 s twt) of Pleistocene sediments, deformed in some cases by the movement of the slide. The seismic facies and the well stratigraphy show that the basal decollement of the slide is represented by Messinian horizons. The tip of the slide coincides with the base of the Calabrian slope, as evident from bathymetric data. Geological constraints on the Calabrian slope arise from dredge taken by Rossi e Borsetti (1974) that yielded clay of Pliocene-Pleistocene age.

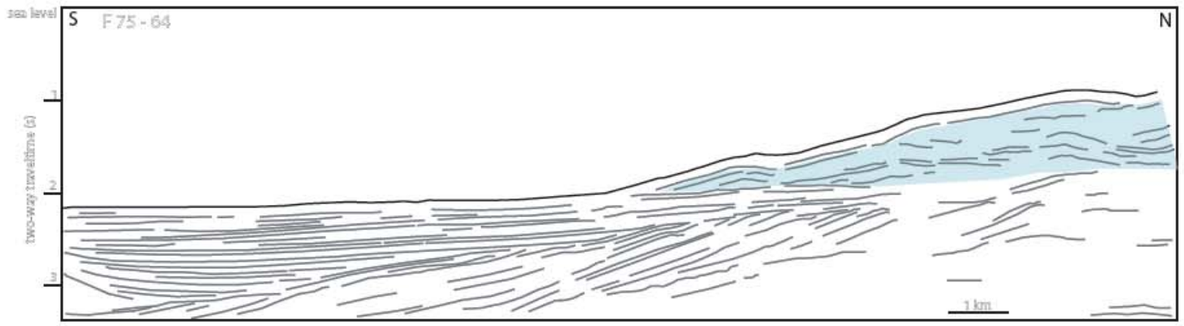

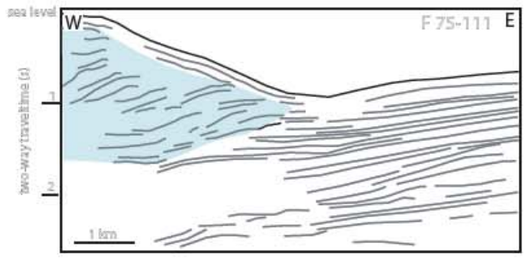

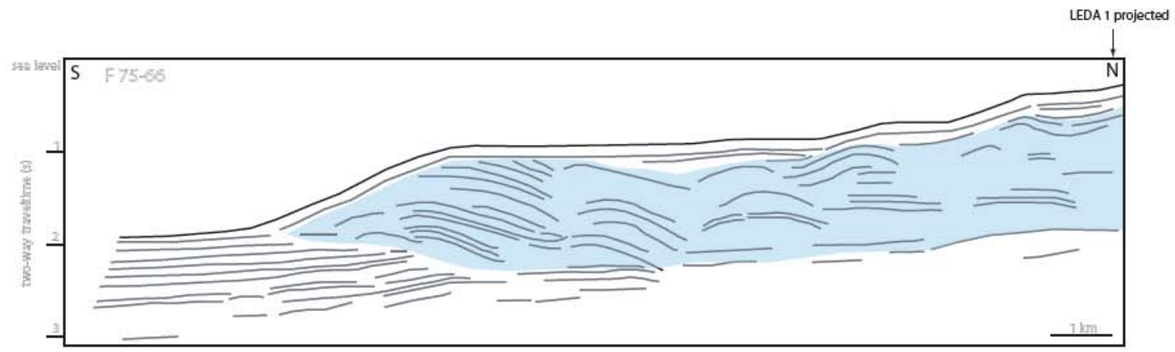

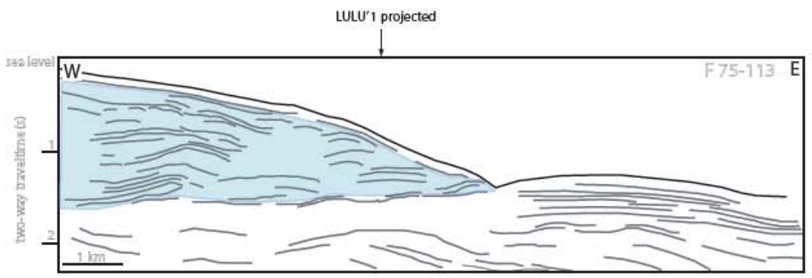

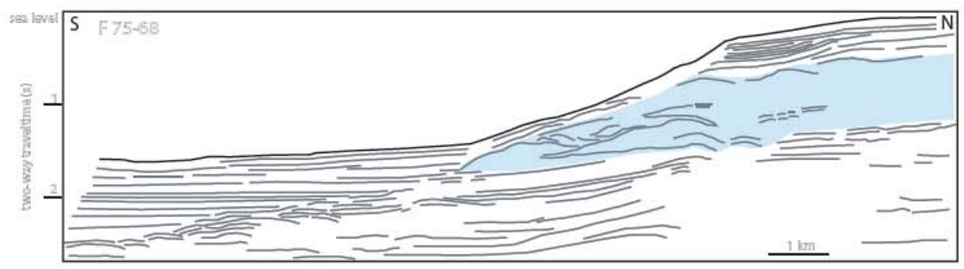

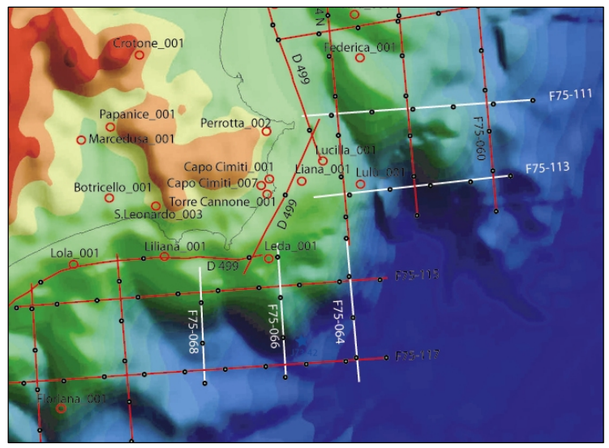

Figure 5 – Lines-drawing of the seismic reflection profiles cutting the megalandslide. (a), (b), and (c) are profiles oriented NS, (d) and (e) are oriented EW. The vertical scale is in second (two way travel time). Colored blue area represent the body of the ML; (f) location map of the seismic profiles and wells. White lines are the profiles shown in this figure.

In map the slide, have a circular shape with different lobes, as testified by the bathymetric chart (Fig. 2) and the movement is radial. Below the megalandslide body the upper Miocene sequences of the Crotone basin, San Nicola and Ponda units, outcropping in the eastern side of the Sila Massif, are present. In front of the tip of the slide, is quite evident that the Messinian unconformity cuts the variously tilted unit of upper Miocene, on top of which an horizontal Plio-Quaternary unit is deposed. The pre-Messinian unit are deformed by a Tortonian phase of deformation as previous seen by Roveri et al. (1992). The thickness of the Plio-Quaternary unit, on average, is about 1s two-way traveltime. The subhorizontally reflectors represent the present forearc basin, a subsident area located both on top of crystalline basement (Sila Massif) and the Calabrian accretionary wedge. Presumably, from the well stratigraphic informations, the age of the sediments is bracketed between Pliocene-Pleistocene. The Fig. 5 shows also as the tip of the megalandslide is located on top of the present forearc basin, suggesting a recent age of movement of the megalandslide. The architecture inside the slide suggest also a composite slow movement of the slide. This is confirmed from the non linear shape of the front of the slide.
On land the prosecution of the slide is more difficult to identify. Only using the wells stratigraphy and observing the structural feature of the Crotone basin it is possible to know its areal extension.

5. Discussion

According to seismic and well data we suggest a complex movement along a basal weak decollement, happens in different time as testified in the seismic profiles where we can observe different thrust sheet stacking seaward.
Similar cases are reported for the offshore South Atlantic basin where gravity spreading of the entirely sedimentary sections occurred above gently inclined salt layer. Several studies (Brun and Fort, 2004 and references therein) have been performed on the deformations associated to salt tectonics using both laboratory experiments and seismic interpretation.
At passive margins, gravity spreading above salt leads to the development of domains of upslope extension and downslope contraction (Wu et al., 1990; Demercian et al., 1993; Letouzey et al., 1995; Peel et al., 1995). The upslope domain is characterized by extensional structures: tilted blocks, grabens, rollovers and extensional diapir, while the downslope compressional domain is characterized by folding, thrusting and compressional diapirs (Fig.6).
These are the same structure that we can observe in the Crotone basin and offshore in the seismic reflection profiles.

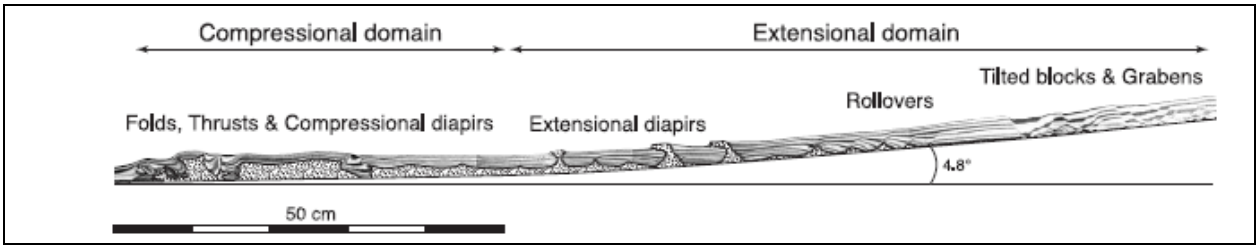

Figure 6 - Results of laboratory experiments. Cross section of a model showing the structural zonation induced by gravity spreading above salt layer (Brun and Fort, 2004).

The downslope compression is evident in the frontal thrust bounding the megalandslide that put older sediments on top of recent Plio-Quaternary sediments of the forearc basin.

It is possible to observe the upslope extensional domain (roll-over, graben and tilted blocks, diapirs) in the geology of the Crotone basin.

Geological survey in the Crotone basin, a tectonically active basin, have shown a complex stratigraphy related, by vary authors, to the interplay between tectonics, subsidence, eustatic sea-level changes and sediment supply (Van Dijk, 1990; Zecchin, 2002; Zecchin et al., 2003). Zecchin et al. (2003) recognize growth of NE-trending anticlines, characterized by steeply dipping axial planes and short wavelenght; also they found several imbricate listric normal faults northwestern dipping (Fig. 7). Tectonic movements are inferred to have started after the deposition of Messinian Carvane conglomerate. The occurrence of halite deposits of the Messinian Detrital Saline Formation (Roda, 1964) in the fold cores strongly suggests that anticlines were initiated by the emplacement of salt pillows. According to Zecchin et al. (2003) the salt tectonic was triggered by NE trending normal faults. We suggest indeed that the spreading of the basinal sequences over the salt layer gently inclined could have produce extensional (imbricate listric faults) and diapiric (anticlines) features and influenced the geometry deposition of the Plio-Pleistocene units in the Crotone basin.

Alternatively, the origin of NE trending folds may result from a compressional phase linked to the southeastward migration of Calabrian Arc (Van Dijk et al., 1998; Moretti, 1993).

The onshore domain of the Crotone basin is characterized by a series of salt diapirs that in the past had represent a resources for the salt and sulphur mines. Stratigraphy log of wells located on shore (Bronzini, 1959) also show thickness of Messinian clay or gyspsum or anydrite more than 1 Km. This is not the original thickness of the upper Miocene sediments but the results of duplications or salt movements.

The Cutro terraces, outcropping in the southeastern side of Crotone peninsula, is gently inclined souteastward and NNE-, ENE-, E-, and WNW-trending normal fault systems are present in this area. ENE trending faults took place after the formation of the oldest terraces but prior to the formation of the younger terraces (Zecchin et al., 2004). This fault pattern and the tilted terraces are compatible with the movement of the megalandslide toward the sea. The radial pattern mimics the shape of the ML, clear by bathymetric data.

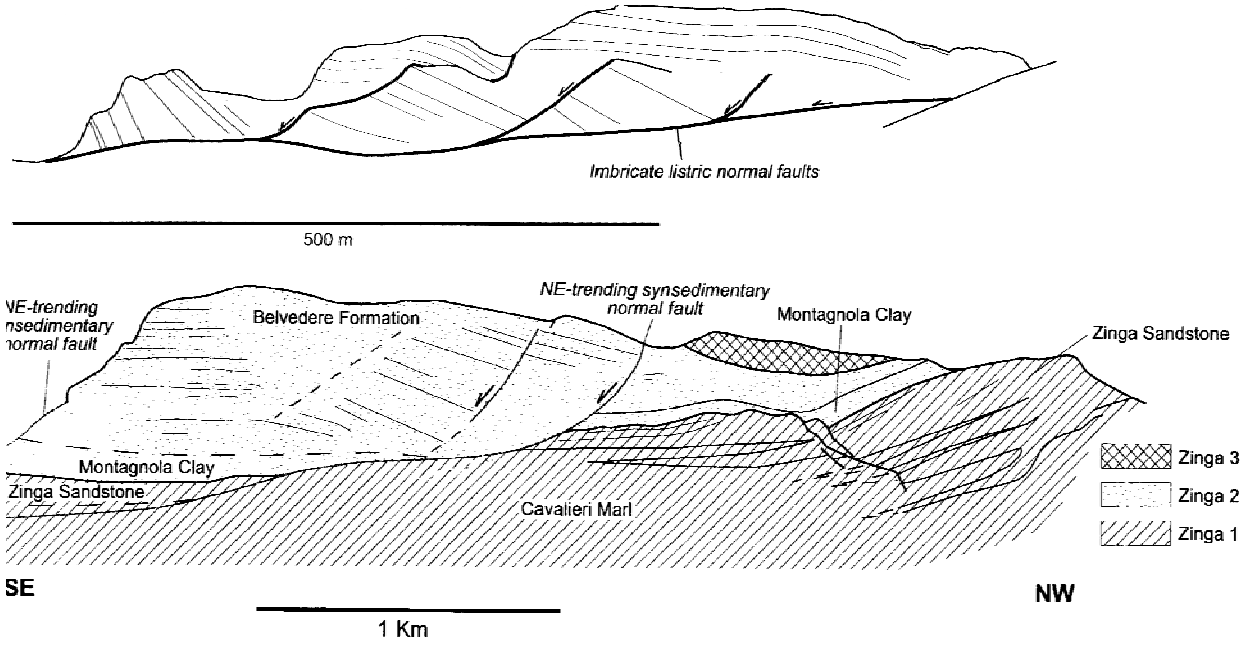

Figure 7 – Two examples of Lower Pliocene deformation that characterized the Crotone basin (rollovers, tilted blocks) near the eastern (a) and western(b) side of the Vitravo Valley (Zecchin et al., 2003).

The rejuvenation, moving from the northwestern sector of the basin to the southeastern, of the extensional faulting, Pliocene and Pleistocene respectively, could be related to the progressive movement of the megalandslide on top of the salt decollement.

The Crotone basin is moreover characterized by diapiric structure, extensional faulting and often graben and rollover (Mellere et al., 2006; Zecchin et al., 2004). These typical deformations has been attributed in the past to a tectonic transtensional setting related to the activity of the two main Rossano-S.Nicola and Petilia-Campana shear zones. We infer that a lot of structures observed on land can be related to a gravity spreading above a salt layer happens in recent time. Offshore also we observe a contractional downslope domain whit clear thrust and ramp (ML) and other kind of structure, like diapir and so on, yet discussed in the chapter on the accretionary complex.

One of the most probable triggering factor is represented by the original dip of the Messinian salt layer, being in an geologically active margin. Few grades of slope are necessary for trigger the movements of salt layers. An increase in recent movement could be related to the regional uplift of the Sila massif.

6. **Conclusion**

The present tectono-sedimentary setting of the Crotone basin, folding, extensional synsedimentary tectonics, diapirs, or little compressional events could be related to a spreading of a continental margin above a weak salt layer, acting as a decollement. The most clear feature due to this, is the megalandslide that involves the Plio-Quaternary sequences in the Crotone basin. The tip of the slope is located offshore in shallow water environment close to the Calabrian coast of Crotone peninsula. The landslide is clear evident by bathymetric data and seismic reflection profiles. Available stratigraphy well data, both on-shore and off-shore confirm this tectonic framework. Similar case are present in the Angolan margin and offshore Brazil. So we suggest that some of the geometry recognized in the field, oltre che for tectonic setting, can be related due to salt tectonics. The difference is on the primary role of salt movement that we identify in this geological context.

REFERENCES

Barone M., Dominici R., Muto F., Critelli S., 2008. Detrital modes in a late Miocene wedge-top basin, Northeastern Calabria, Italy: compositional record of wedge-top partitioning . Journal of Sedimentary Research, 78, DOI: 10.2110/jsr.2008.071.

Cavazza W, De Celles PG., 1998. Upper Messinian siliciclastic rocks in southeastern Calabria (southern Italy): palaeotectonic and eustatic implications for the evolution of the central Mediterranean region. Tectonophysics (Amst), 298, 223– 41.

De Celles PG, Cavazza W., 1995. Upper Messinian conglomerates in Calabria, southern Italy: response to orogenic wedge adjustment following Mediterranean sea-level changes. Geology, 23, 775–8.

Demercian, S., Szatmari, P., Cobbold, P.R., 1993. Style and pattern of salt diapirs due to thin-skinned gravitational gliding, Campos and Santos basins, offshore Brazil. Tectonophysics 228, 393– 433.

Dewey J.F., Helman M.L., Turco E., Hutton D.H.W., Knott S.D., 1989. Kinematics of the western Mediterranean. In Alpine Tectonic, edited by M. P. Coward and D. Dietrich. Geological Society London Special Publication, 45, 265-283.

Ghisetti, F., Vezzani, L., 1981. Contribution of structural analysis to understanding the geodynamic evolution of the Calabrian Arc (Southern Italy). J. Struct. Geol. 3, 371–381.

Ghisetti, F., Vezzani, L., 1982. The recent deformation mechanics of the Calabrian Arc. Structure evolution and present dynamics of the Calabrian, Mantovani, E., Sartori,(Eds.), Arc Earth Evol. Sci. 3, 197–206.

Knott SD, Turco E., 1991. Late Cenozoic kinematics of the Calabrian Arc, southern Italy. Tectonics , 10,1164–72.

Letouzey, J., Colletta, B., Vially, R., Chermette, J.C., 1995. Evolution of salt-related structures in compressional settings. In: Jakson, D.G.R.a.S.S.M.PA. (Ed.), Salt Tectonics, A Global Perspective. American Association of Petroleum Geologists Memoir, pp. 41–60.

Malinverno A. & Ryan W.B.F., 1986. Extension in the Tyrrhenian Sea and shortening in the Apennines as result of arc migration driven by sinking of the lithosphere. Tectonics, 5, 227-245.

Massari F, Sgavetti M, Rio D, D'Alessandro A, Prosser G., 1999. Composite sedimentary record of falling stages of Pleistocene glacio-eustatic cycles in a shelf setting (Crotone basin, south Italy). Sediment Geol., 1999, 127, 85– 110.

Massari F, Rio D, Sgavetti M, Prosser G, D'Alessandro A, Asioli A, et al., 2002. Interplay between tectonics and gladio-eustasy: Pleistocene succession of the Crotone basin Calabria (southern Italy). Geol. Soc. Amer. Bull.,114, 1183– 209.

Mattei M., Cipollari P., Cosentino D., Argentieri A., Rossetti F., Speranza F., 2002. The Miocene tectonic evolution of the southern Tyrrhenian Sea: Stratigraphy, structural and paleomagnetic data from the on-shore Amantea Basin (Calabrian arc, Italy). Basin Research, 14, 147-168.

Meulenkamp JE, Hilgen F, Voogt E., 1986. Late Cenozoic sedimentary–tectonic history of the Calabrian Arc. In: Boccaletti M, Gelati R, Ricci Lucchi F, editors. Paleogeography and Geodynamics of the Perityrrhenian Area. Gior Geol, 48, 345– 59.

Moretti A., 1993. Note sull'evoluzione tettono-stratigrafica del bacino crotonese dopo la fine del Miocene. Boll. Soc. Geol. Ital., 112, 845– 67.

Ogniben L., 1955. Le argille scagliose del crotonese. Mem. e note Ist. Geol. Appl. Napoli, 6, 1– 72.

Ogniben L., 1962, Le Argille Scagliose e i sedimenti messiniani a sinistra del Trionto (Rossano, Cosenza). Geologica Romana, 1, 255–282.

Ogniben L., 1973. Schema geologico della Calabria in base ai dati odierni. Geologica Romana, 12, 243-585.

Patacca E., Sartori R. Scandone P., 1990. Tyrrhenian basin and Apenninic arcs: kinematic relation since late Tortonian times. Memorie della Società Geologica Italiana, 45, 425-451.

Peel, F.J., Travis, C.J., Hossack, J.R., 1995. Genetic structural provinces and salt tectonics of the Cenozoic offshore U.S. Gulf of Mexico: a preliminary analysis. In: Jakson, D.G.R.a.S.S.M.PA. (Ed.), Salt Tectonics, A Global Perspective. American Association of Petroleum Geologists Memoir, pp. 153– 175.

Rehault, J.P., Moussat, E., Fabbri, A., 1986. Structural evolution of the Tyrrhenian back-arc basin. Mar. Geol. 74, 123–150.

Roda C., 1964. Distribuzione e facies dei sedimenti neogenici nel Bacino Crotonese. Geologica Romana, 3, 319-366.

Rossetti F., Faccenna C., Goffé B., Monié P., Argentieri A., Funiciello R. and Mattei M., 2001. Alpine structural and metamorphic signature of the Sila Piccola Massif nappe stack (Calabria, Italy): Insights for the tectonic evolution of the Calabrian Arc. Tectonics 20, 112-133.

Rossetti F., Goffé B., Monié P., Faccenna C., Vignaroli G., 2004. Alpine orogenic PTt deformation history of the Catena Costiera area and surrounding regions (Calabrian Arc, southern Italy): the nappe edifice of Northern Calabria revised with insights on the Tyrrhenian–Apennine system formation. Tectonics, 23, 1-26.

Rossi S., and Sartori R., 1981. A seismic reflection study of the external Calabrian Arc in the northern Ionian Sea (eastern Mediterranean). Mar. Geophys. Res., 4, 403 – 426.

Rossi, S., Borsetti, A.M., 1974. Dati preliminari di stratigrafia e di sismica del Mare Ionio settentrionale. Mem. Soc. Geol. Ital. 13, 251– 259.

Roveri M., Bernasconi A., Rossi M.E., Visentin C., 1992. Sedimentary evolution of the Luna Field Area, Calabria, Southern Italy. Generation, Accumulation, and Production of Europe's Hydrocarbons (Edited by Spencer A.M.), Europ. Assoc. Petrol. Geosci., Spec. Publ., 2, 217-224.

Van Dijk JP., 1990. Sequence stratigraphy, kinematics and dynamic geohistory of the Crotone Basin (Calabria Arc, Central Mediterranean): an integrated approach. Mem. Soc. Geol. Ital.. 44, 259–85.

Van Dijk J.P., Okkes F.W.M., 1990. The analysis of shear zones in Calabria; implications for the geodynamics of the Central Mediterranean. Riv. Ital. Paleontol. Stratigr. 96, 241–70.

Van Dijk JP, Okkes FWM., 1991. Neogene tectonostratigraphy and kinematics of Calabrian basins; implications for the geodynamics of the Central Mediterranean. Tectonophysics, 196, 23–60.

Van Dijk, J.P., Scheepers, P.J.J., 1995. Neogene rotations in the Calabrian Arc. Implications for a Pliocene–recent geodynamic scenario for the Central Mediterranean. Earth Sci. Rev. 39, 207–246.

Van Dijk J.P., Bello M., Brancaleoni G.P., Cantarella G., Costa V., Frixa A., Golfetto F., Merlini S., Riva M., Torricelli S., Toscano C., Zerilli A., 2000. A regional structural model for the northern sector of the Calabrian Arc (southern Italy). Tectonophysics, 324, 267-320.

Wu, S., Bally, A.W., Cramez, C., 1990. Allochtonous salt, structure and stratigraphy of the North Eastern Gulf of Mexico. Part II: structure. Marine and Petroleum. Geology 7, 334– 370.

Zecchin M., Massari F., Mellere D., Prosser G., 2003. Architectural styles of prograding wedges in a tectonically active setting, Crotone Basin, Southern Italy. J Geol Soc (Lond).160, 863– 80.

Zecchin M., Massari F., Mellere D., Prosser G., 2004. Anatomy and evolution of a Mediterranean-type fault bounded basin: the Lower Pliocene of the northern Crotone Basin (Southern Italy).Basin Res.. 16, 117–43.